Volume 68C
Number 1
Jan.–Mar. 1964

Engineering and Instrumentation

U.S. DEPARTMENT OF COMMERCE

SECTION C

JOURNAL OF RESEARCH

NATIONAL BUREAU OF STANDARDS

Journal of Research
of the
National Bureau of Standards

C. Engineering and Instrumentation

JAN.–MAR. • 1964

VOLUME • 68C

NUMBER • 1

Editor: Martin Greenspan

Associate Editors: G. F. Montgomery, R. B. Jacobs

Publication dates:
Feb. 15, May 15, Aug. 15, Nov. 15, 1964

JOURNAL OF RESEARCH

The National Bureau of Standards Journal of Research reports research and development in the fields of activity shown at right. Also included from time to time are survey articles on topics closely related to the Bureau's scientific and technical program.

The Journal is published in four separate sections as follows:

A. Physics and Chemistry

Contains papers of interest primarily to scientists working in these fields. Issued six times a year. Annual subscription: domestic, $4.00; foreign, $4.75.

B. Mathematics and Mathematical Physics

Presents studies and compilations designed mainly for the mathematician and the theoretical physicist. Issued quarterly. Annual subscription: domestic, $2.25; foreign, $2.75.

C. Engineering and Instrumentation

Reports research and development results of interest chiefly to the engineer and the applied scientist. Issued quarterly. Annual subscription: domestic, $2.25; foreign, $2.75.

D. Radio Science (formerly Radio Propagation)

Published in cooperation with U.S. National Committee of URSI. Presents papers in radio propagation, communications, and radio science generally. Issued monthly. Annual subscription: domestic, $9.00; foreign, $11.50.

Functions and Activities

The functions of the National Bureau of Standards are set forth in the Act of Congress, March 3, 1901, as amended. These include the development and maintenance of the national standards of measurement and the provision of means and methods for making measurements consistent with these standards; the determination of physical constants and properties of materials, the development of methods and instruments for testing materials devices, and structures; advisory services to government agencies on scientific and technical problems; invention and development of devices to serve special needs of the Government; and the development of standard practices codes, and specifications. The work includes basic and applied research development engineering, instrumentation, testing, evaluation, calibration services, and various consultation and information services. The Bureau also serves as the Federal technical research center in a number of specialized fields. The scope of activities of the National Bureau of Standards is suggested in the following listing of the divisions and sections engaged in technical work.

WASHINGTON, D.C.

Electricity. Resistance and Reactance. Electrochemistry. Electrical Instruments. Magnetic Measurements. Dielectrics. High Voltage. Absolute Electrical Measurements.

Metrology. Photometry and Colorimetry. Refractometry. Photographic Research. Length. Engineering Metrology. Mass and Volume.

Heat. Temperature Physics. Heat Measurements. Cryogenic Physics. Equation of State. Statistical Physics.

Radiation Physics. X-ray. Radioactivity. Radiation Theory. High Energy Radiation. Radiological Equipment. Nucleonic Instrumentation. Neutron Physics.

Analytical and Inorganic Chemistry. Pure Substances. Spectrochemistry. Solution Chemistry. Standard Reference Materials. Applied Analytical Research. Crystal Chemistry.

Mechanics. Sound. Pressure and Vacuum. Fluid Mechanics. Engineering Mechanics. Rheology. Combustion Controls.

Polymers. Macromolecules: Synthesis and Structure. Polymer Chemistry. Polymer Physics. Polymer Characterization. Polymer Evaluation and Testing. Applied Polymer Standards and Research. Dental Research.

Metallurgy. Engineering Metallurgy. Metal Reactions. Metal Physics. Electrolysis and Metal Deposition.

Inorganic Solids. Engineering Ceramics. Glass. Solid State Chemistry. Crystal Growth. Physical Properties. Crystallography.

Building Research. Structural Engineering. Fire Research. Mechanical Systems. Organic Building Materials. Codes and Safety Standards. Heat Transfer. Inorganic Building Materials. Metallic Building Materials.

Applied Mathematics. Numerical Analysis. Computation. Statistical Engineering. Mathematical Physics. Operations Research.

Data Processing Systems. Components and Techniques. Computer Technology. Measurements Automation. Engineering Applications. Systems Analysis.

Atomic Physics. Spectroscopy. Infrared Spectroscopy. Far Ultraviolet Physics. Solid State Physics. Electron Physics. Atomic Physics. Plasma Spectroscopy.

Instrumentation. Engineering Electronics. Electron Devices. Electronic Instrumentation. Mechanical Instruments. Basic Instrumentation.

Physical Chemistry. Thermochemistry. Surface Chemistry. Organic Chemistry. Molecular Spectroscopy. Elementary Processes. Mass Spectrometry. Photochemistry and Radiation Chemistry.

Office of Weights and Measures.

BOULDER, COLO.

Cryogenic Engineering Laboratory. Cryogenic Processes. Cryogenic Properties of Solids. Cryogenic Technical Services. Properties of Cryogenic Fluids.

CENTRAL RADIO PROPAGATION LABORATORY

Ionosphere Research and Propagation. Low Frequency and Very Low Frequency Research. Ionosphere Research. Prediction Services. Sun-Earth Relationships. Field Engineering. Radio Warning Services. Vertical Soundings Research.

(Continued on inside back cover)

JOURNAL OF RESEARCH of the National Bureau of Standards—C. Engineering and Instrumentation
Vol. 68C, No. 1, January–March 1964

A Fabry-Perot Spectrometer for High-Resolution Spectroscopy and Laser Work

Klaus D. Mielenz, Robert B. Stephens, and Karl F. Nefflen

A Fabry-Perot spectrometer with a piezoelectric spacer was constructed to record with a recorder, or display with an oscilloscope, the fine structure of the Haidinger fringes. The spectrometer is of the fixed spacer design, which provides great stability of adjustment. It was used to record the Zeeman splitting of the green line of Hg^{198}, as well as to exhibit, on the oscilloscope screen, the multimode output signal of a He-Ne gas laser.

1. Introduction

Modern advances in microwave techniques permit the detection and direct analysis of gigacycle frequencies. Optical frequencies, however, lie in the teracycle range and so, are still orders of magnitude beyond the state of that art. Optical methods, therefore, remain the most direct approach to analyze such frequencies as are encountered in laser work. Among them, of course, the Fabry-Perot interferometer or spectrometer is the foremost choice.

Essentially, a photoelectric Fabry-Perot spectrometer is a Fabry-Perot interferometer of variable optical plate separation nt, with a phototube viewing the center of the Haidinger ring pattern through a small circular diaphragm. As only the central portion of the ring pattern is used, it represents a linear frequency filter. With any change of nt, therefore, the phototube scans through the Airy intensity distribution. The phototube output thus obtained, and properly displayed as a function of nt on a chart recorder or oscilloscope screen, is a reproduction of the intensity structure within the interference rings.

2. The Jacquinot and Tolansky Spectrometers

The first photoelectric Fabry-Perot spectrometer was built by Jacquinot and Dufour [1].[1] They enclosed an etalon, of fixed physical plate separation t, in an air-tight chamber and obtained a continuous change of nt by varying the pressure p inside it. With p slowly varying linearly with time, a graph of intensity distribution versus frequency is obtained on a Y-axis recorder.

The Jacquinot spectrometer has been much used to record the fine and hyperfine structures of spectrum lines; compare, for instance, reference [2].

Another type of the spectrometer is due to Tolansky and Bradley [3]. They employed a Fabry-Perot interferometer in which one plate is oscillated through a distance of the order of $\lambda/2$ by means of a mechanical vibrator. The phototube output signal is fed into the Y-axis input of an oscilloscope and the horizontal sweep synchronized with the vibrator. A reproduction of the ring structure is then displayed on the screen.

Recently, Herriot [4] has used the Tolansky spectrometer, with confocal mirrors, and a permanent magnet and moving coil to oscillate one mirror, to detect laser modes.

In the Jacquinot spectrometer, high frequency noise is easily suppressed by limiting the frequency response of the recorder and recording at low speeds. Since the light source must remain stable within at least the recording period, unstable light sources cannot be analyzed. Adiabatic effects, on the other hand, prohibit a fast scan and, thus, the display of the signal with an oscilloscope.

The Tolansky spectrometer, as compared hereto, readily analyzes unstable light sources. However, a broader frequency pass-band is required to produce an undistorted pattern on the screen, and this will result in an undesirable display of noise. The mechanical vibrator does not lend itself easily to a sufficiently precise, slow continuous scan. The use of the same instrument with a recorder does not appear to be of merit, therefore.

In the design of conventional Fabry-Perot interferometers, a fixed spacer has long proved to be of great advantage [5]. A piece of fused quartz tubing, optically parallel at both ends and with the two mirrors optically contacted to it, has been found, in this laboratory, the most practical and simplest design. Such etalons have been shipped long distances without any need for readjustment at their point of destination. Jacquinot's instrument does use a fixed spacer. The oscillating spectrometers, as described, do not share this advantage, and are liable to have less stability.

The electrical control of the scan in Tolansky's spectrometer, on the other hand, is more convenient and versatile than a pressure control.

[1] Figures in brackets indicate the literature references at the end of this paper.

3. The New Fabry-Perot Spectrometer

The new spectrometer to be described here combines the advantages of the Jacquinot and Tolansky designs, and is simpler in construction and handling than either. It can readily be used with either a recorder or an oscilloscope, is of the fixed spacer design, and is controlled entirely electrically by the simplest of means.

The etalon used (fig. 1) essentially consists of a piece of lead zirconate-titanate (Clevite piezoelectric ceramic PZT–4) tubing of 2.0 in. outside and 1.6 in. inside diameter, with the mirrors contacted to its ends. The tube is silver-plated on its inside and outside. The voltages required to provide length changes are applied through wires soldered to the inside and outside of the ceramic tube.

The ceramic used yielded a linear expansion of about 0.5 mμ per volt per inch. The voltage required to scan the etalon through its range without overlap, for visible light and a 3-in. tube, is of the order of 100 v. Since the ceramic is primarily a capacitive circuit element, the only current drawn is a changing current. A d-c voltage to provide a continuous linear expansion or contraction can, therefore, be obtained with a simple filtered power supply or with batteries. An a-c voltage to provide oscillations can be taken from the 60-cycle power line with a variable transformer. These characteristics make the ceramic easy to use.

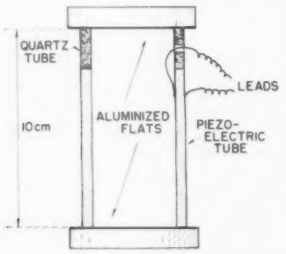

FIGURE 1. *10-cm etalon with piezoelectric spacer.*

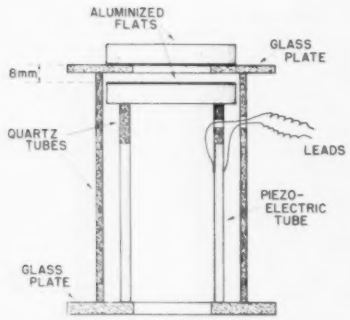

FIGURE 2. *8-mm etalon with piezoelectric spacer.*

Another design, which was used to achieve a shorter plate separation with the 3-in. tube at hand, is shown in figure 2. It might also prove advantageous when, for small spacings or long wavelengths, the higher voltages required by the other design tend to be impracticable. In both cases, flat mirrors were used, but it is planned to also use confocal plates for further experiments.

Although both etalons were used in an exploratory manner only, with the components held together by wax, and with aluminum mirrors of not more than 75 percent reflectance, the results obtained were very promising. The etalons were easy to adjust and maintained their adjustment. With d-c and a-c voltages high enough to provide a scan through five fringes, the expansion of the ceramic was found to be linear and reproducible. It did not affect the parallelism of the etalon at any time.

The etalons were employed in an upright manner, with a pentaprism at each end to deflect the light by 90°, figure 3. A collimating lens of 199 mm focal length was used in front of, and a telescope lens of 275 mm focal length behind the etalon. The aperture of the diaphragm at the center of the ring pattern varies with the length of the etalon and was in each case chosen to yield optimum resolution.

With the Hg^{198} lamp, as employed in some of the experiments described below, a combination of Wratten filters was used to isolate the green line.

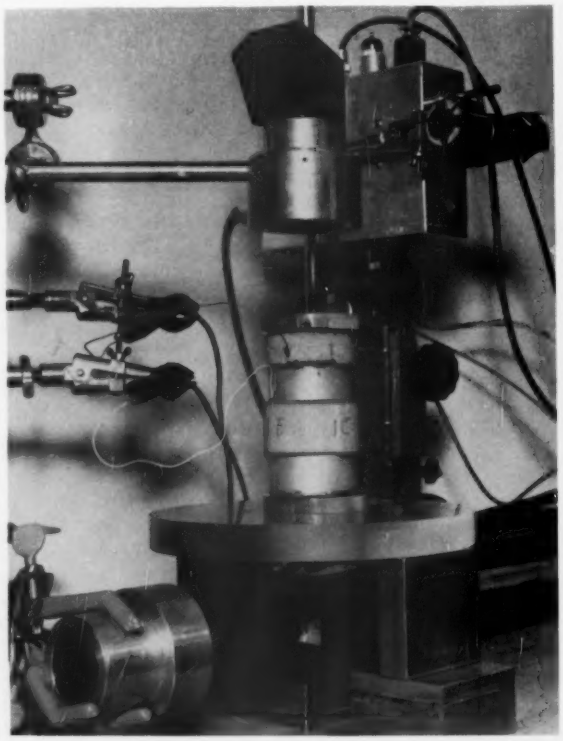

FIGURE 3. *10-cm etalon with lenses, pentaprisms, diaphragm, photomultipler, and cathode follower.*

A Fabry-Perot interferometer with continuous piezoelectric scanning was already described by Dupeyrat [6]. Being altogether different in design, it did not show much promise at the time.

4. Experimental Results

The new Fabry-Perot Spectrometer was employed in two ways, in a setup schematically shown in figure 4.

4.1. Recording Spectrometer

With a slowly linearly increasing or decreasing d-c voltage at the ceramic, the instrument represents the analog of the Jacquinot spectrometer. The voltage was supplied by a filtered full-wave power supply whose output of 410 v was applied across a 10-turn precision 300 kΩ potentiometer driven by a 32 v d-c, ⅓ rpm motor. The resulting variations in the output signal of the RCA 1P21 photomultiplier were recorded versus time on a potentiometer-type recorder. Recording time was about 10 min per interference fringe.

The record reproduced in figure 5 shows the transverse, normal Zeeman splitting of the 5461 Å Hg^{198} line. It was obtained with a magnetron magnet of approximately 2200 oersteds applied to a water-cooled Hg^{198} lamp excited by a microwave oscillator. The 8 mm etalon of figure 2 was used.

Figure 5a shows two rings with no magnetic field applied. In figure 5b, the line is broadened due to the field, and one can vaguely see the beginning resolution of a triplet. In figure 5c, the π-component of the triplet is isolated by insertion of a Polaroid filter. Figure 5d shows the σ-components obtained after rotating the Polaroid by 90°.

The advantage of the recorder method lies, as mentioned, in the removal of noise. This is illustrated by contrasting figure 5a with figure 6, in which the unsplit Hg^{198} line is shown as obtained on the oscilloscope screen by the method described below.

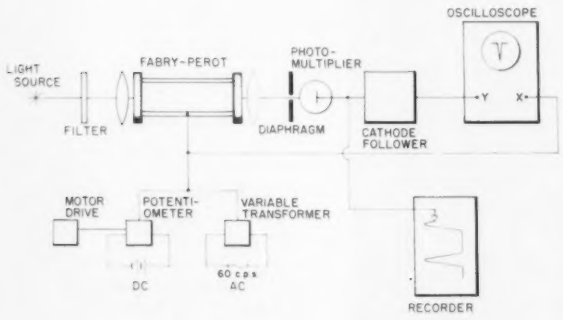

FIGURE 4. *Block diagram of spectrometer with recorder and oscilloscope.*

Due to a low signal-to-noise ratio, the oscilloscope pattern in figure 6 exhibits a strong photomultiplier noise which, however, is largely eliminated in the recorded pattern of figure 5a.

4.2. Oscillating Spectrometer

With a 60-cycle a-c voltage at the ceramic and at the X-axis input of the oscilloscope, and the photo-

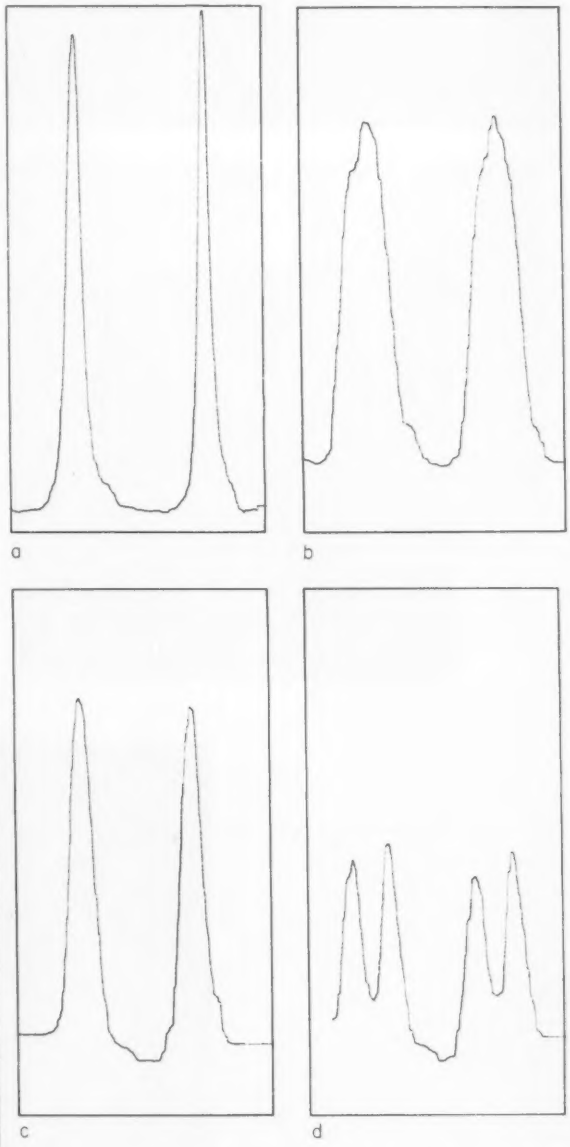

FIGURE 5. *Normal Zeeman effect of green line of* Hg^{198}. (a) Without field; (b, c, d) with field, (b) all components, (c) π-component, (d) σ-components. 8-mm etalon.

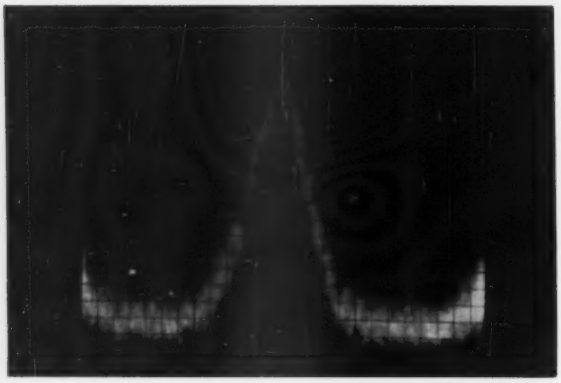

FIGURE 6. *Oscilloscope pattern of green line of* Hg^{198}, *obtained at low signal-to-noise ratio.*

tube output fed into the *Y*-axis input, the instrument corresponds to Tolansky's spectrometer and reproduces the Airy pattern on the scope screen.

The number of interference rings displayed on the screen increases as the a-c voltage is increased (fig. 7). A d-c voltage is superimposed to conveniently center the pattern about a dark or bright ring, as desired (fig. 8). Any need for mechanical positioning of the etalon is thus eliminated.

The a-c voltage was taken from the 60-cycle power line, and was varied with a Variac transformer. The d-c voltage was supplied by the 410 v power supply, or batteries, and was varied with potentiometers. A cathode follower was used between the 1P21 photomultiplier tube and the oscilloscope to provide an impedance match.

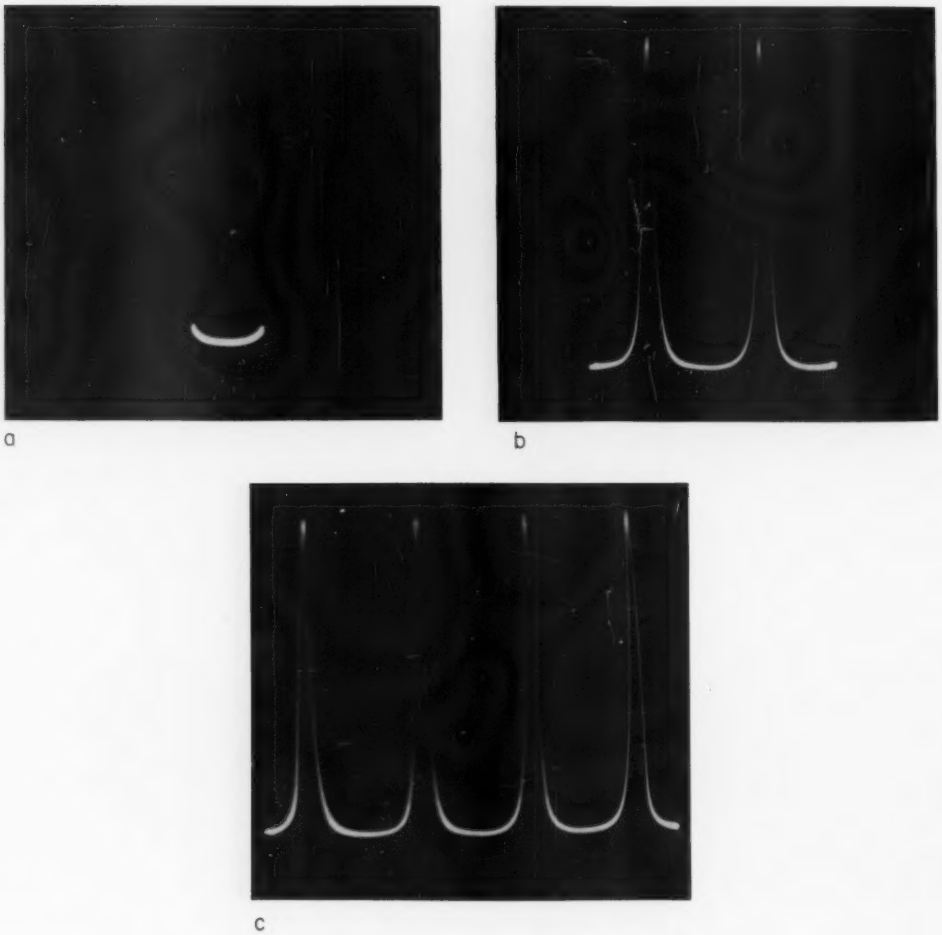

FIGURE 7. *Effects of a-c voltage on scope pattern.*
(a) 50 volts, (b) 150 volts, (c) 250 volts rms.

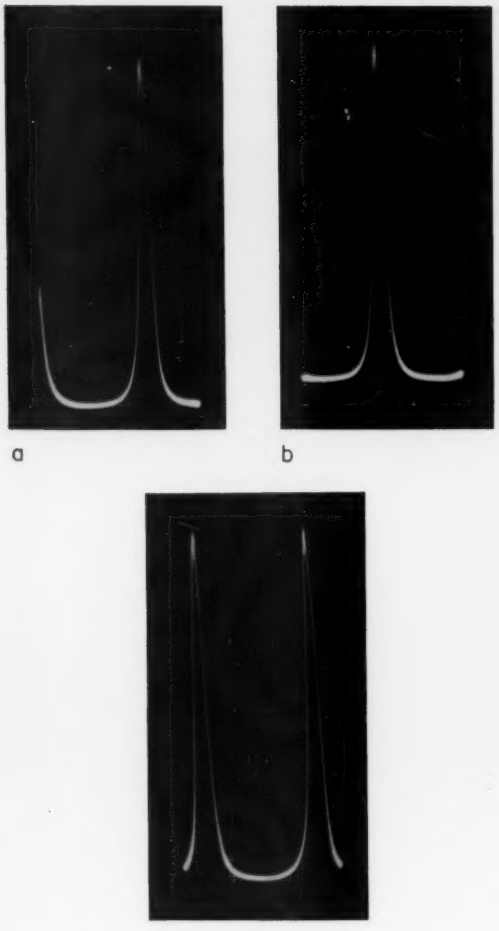

FIGURE 8. *Effect of d-c voltage on scope pattern.*
(a) 0 volts, (b) 40 volts, (c) 130 volts.

The oscillograms shown in figures 7 and 8 were obtained with the 8-mm etalon, illuminated with a Spectra-Physics Model 115 He-Ne laser operating at 6328 Å. The resolving power of the etalon was not sufficient to resolve the laser modes.

With the 10-cm etalon, however, the patterns shown in figure 9 were obtained in which the modes are clearly resolved. As the laser used was not designed for frequency stability, the oscilloscope displayed a continuously changing pattern. The series of pictures in figure 9 were selected at random to show this effect. It is almost impossible, though, to reproduce in print this very striking demonstration of how, in such a laser, energy continuously shifts back and forth between modes.

Only an oscilloscope can display such rapid changes, and here, then, lies the advantage of the oscillating Fabry-Perot spectrometer as compared to the recording one.

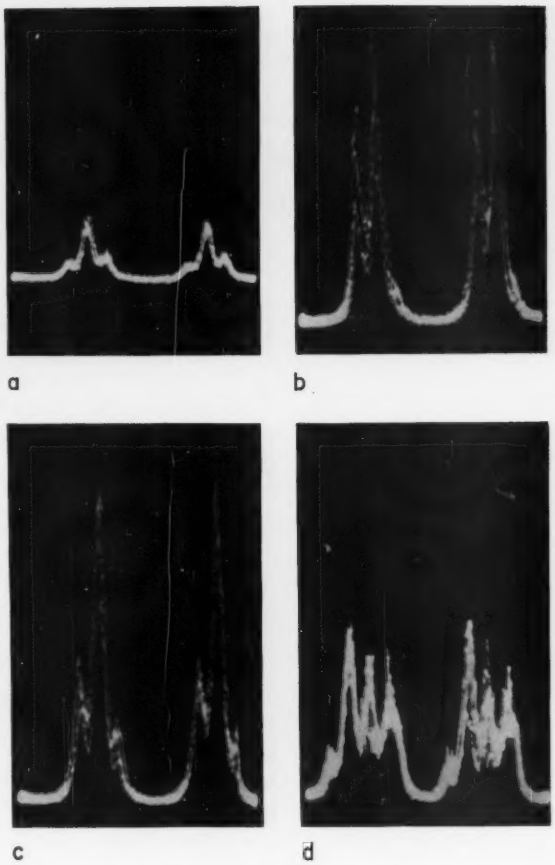

FIGURE 9. *Varying frequency output of* He-Ne *laser at 6328* Å
10-cm etalon.

5. Conclusion

A preliminary setup only, with much room for improvement, was used for the above described experiments. Yet, a simple Fabry-Perot spectrometer with a "fixed" piezoelectric spacer has proved to be a most adaptable and useful spectrum analyzer for high-resolution spectroscopy and laser work. It is planned to use such spectrometers, in an improved, permanent design, for the analysis of the frequency output of infrared and visible lasers. For this purpose, greater spacings than the ones used here will be required to provide better resolution.

The use of piezoelectric spacers to tune laser cavities has also been realized in this laboratory.

K. E. Gillilland and T. Morokuma, of this laboratory, provided valuable ideas and skillful assistance throughout the work described. H. D. Cooke and

J. J. Spijkerman, both at NBS, made helpful suggestions. The loan of the gas laser by R. L. Mortensen, of Spectra-Physics, is greatly appreciated.

6. References

[1] P. Jacquinot and C. Dufour, J. Rech. Centre Nat. Rech. Sci. **2,** 91 (1948).

[2] A. Steudel, Naturwiss. **44,** 249 (1957).

[3] S. Tolansky and D. J. Bradley, Nat. Phys. Lab. Symp. 11., Interferometry, Her Majesty's Stationary Office, p. 375 (London, 1960).

[4] D. R. Herriot, Appl. Opt. **2,** 865 (1963).

[5] C. Candler, Modern Interferometers, Hilger & Watts, p. 213 (London, 1951).

[6] R. Dupeyrat, Colloq. Intern. Centre Nat. Rech. Sci. LXXX, p. 106 (Pans, 1958).

(Paper 68C1–147)

JOURNAL OF RESEARCH of the National Bureau of Standards—C. Engineering and Instrumentation
Vol. 68C, No. 1, January–March 1964

A Variable Impedance Power Meter, and Adjustable Reflection Coefficient Standard

Glenn F. Engen

(October 10, 1963)

Most microwave power meters, such as those of the bolometric and calorimetric types, completely absorb the power which they indicate. The use of these meters is thus usually accompanied by the requirement to either (1) determine the power at another place in the microwave circuit from the meter reading, or (2) determine the power which will be delivered to a different load which is to be substituted for the meter.

The evaluation of these relationships plays an important role in the power measurements art.

These problems are alleviated by the power measuring device to be described. This instrument, which is based on reflectometer techniques, may be used either as a feed-through power meter which indicates the power delivered to loads of arbitrary impedance, or as a terminating power meter whose input impedance can be adjusted to arbitrary values without requiring recalibration.

In a slightly modified form the instrument also gives an indication of the reflection coefficient magnitude to which it has been adjusted.

A comprehensive error analysis permits the accuracy to be determined under general operating conditions.

1. Background

Power meters, for the high, ultrahigh, and microwave frequency spectrum, may usually be classed as either "feed-through" or "terminating" types. The former includes a section of appropriate waveguide and contains provision for measuring the power flow, while absorbing as little energy as possible. The second type of meter terminates the waveguide and, ideally, absorbs all of the incident power. That is, the power meter terminates the waveguide by its characteristic impedance. At microwave frequencies, most power meters belong to this second category.

In the use of these power meters, comparison theory and techniques play an important role. This theory deals with predicting the power delivered to a load of arbitrary characteristics when the power absorbed by a different load is known (usually a terminating power meter). In the laboratory, this problem may take the form of calibrating one terminating power meter in terms of a second and similar type meter. In the field it may be required to determine the power delivered to an antenna by the use of a meter of this type. With few exceptions, the use of a terminating type power meter is motivated by the desire to predict the power which will be delivered by a particular signal source to another load whose impedance differs from that of the power meter. Unfortunately, the associated problems are not as widely appreciated as they should be. It is probably safe to say that in many cases the accuracy realized in the current art is to a substantial degree limited by the failure to apply this comparison theory.

The variable impedance power meter, which is the subject of this paper, provides a potential simplification in this comparison theory and procedure because its impedance may be adjusted to equal that of the second meter or load with which it is being compared. In a slightly modified form, this device also provides the magnitude of the reflection coefficient to which it has been adjusted. Because of the strong interdependence between these applications, they will be developed simultaneously, but with major emphasis on the power meter theory. The adjustable reflection coefficient standard will be included as a modification of the power meter application.

2. Introduction

If two loads are connected in turn to a constant voltage, arbitrary impedance, signal source as indicated in figure 1, it can be shown that the ratio of the two powers is given by: [1] [1]

$$\frac{P_A}{P_B}=\frac{|1-\Gamma_g\Gamma_B|^2}{|1-\Gamma_g\Gamma_A|^2}\frac{1-|\Gamma_A|^2}{1-|\Gamma_B|^2} \tag{1}$$

where P_A and P_B are the powers absorbed by the loads of reflection coefficient Γ_A and Γ_B, respectively, and Γ_g is the reflection coefficient of the signal source. A major portion of the comparison theory and techniques, referred to earlier, is devoted to various methods of coping with the relationships and measurement problems implicit in this equation.

The existing techniques for dealing with this problem include the following.

(1) Measurements of Γ_g, Γ_A, and Γ_B, and substitution of their values in eq (1). This approach is seldom, if ever, used. Note that both the magnitudes and phase angles of the reflection coefficients are required. Although a slotted line is capable of providing both pieces of information, the procedures associated with the phase angle determination are somewhat awkward and the overall accuracy leaves something to be desired. The reflectometer provides a more accurate measurement of the reflection coefficient magnitude, but does not, in its usual form, provide any phase information.

(2) Adjust $\Gamma_g=0$ and measure $|\Gamma_A|$ and $|\Gamma_B|$. This is a useful technique when one is interested in comparing two power meters. The techniques for matching a generator include the use of attenuators and load isolators such that the equivalent generator impedance at the terminal surface of interest tends to become independent of the actual source of energy. An alternative equivalent to a matched generator is provided by the use of a directional coupler and associated techniques [2, 3].

(3) Use of a "reflectometer type" transfer instrument [4]. The cited reference [4] describes an alternative technique for comparing power meters which utilizes a four-arm waveguide junction together with appropriate power detectors and calibration procedures. This device may be regarded as a feed-through type wattmeter. For example, if a reflectometer is employed as the four-arm junction, it can be shown that the instrument performs the operations required in item 2 implicitly. It should be noted, however, that a reflectometer is only a special case of a more general class of four-arm junctions which satisfy the criteria outlined in [4].

(4) Adjust one of the impedances so that $\Gamma_A=\Gamma_B$. In this case, the ratio P_A/P_B reduces to unity. Of the methods described, this one is potentially the most accurate, at least in

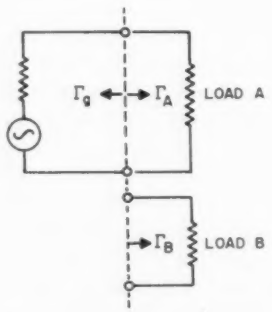

FIGURE 1. *Basic circuit for power measurements by comparison.*

[1] Figures in brackets indicate the literature references at the end of this paper.

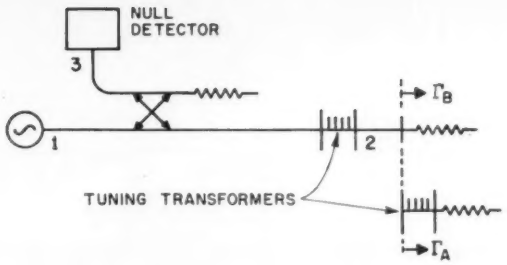

FIGURE 2. *Circuit for recognizing the equality of two impedances.*

reducing the uncertainty in the ratio P_A/P_B. In addition, while the measurement of ultrahigh frequency and microwave impedance is an exacting art, the techniques for recognizing the equality of two impedances are comparatively simple.

This may be done as indicated in figure 2. For definiteness, it will be assumed that Γ_A is variable while Γ_B is fixed in value. The procedure consists of terminating arm 2 of the coupler by Γ_B and adjusting the transformer for a detector null. Load B is then replaced by load A. If Γ_A is now adjusted so that a detector null is again realized, $\Gamma_A = \Gamma_B$ as required.

In the discussion to follow, it will be assumed that load A is a terminating type power meter of reflection coefficient Γ_A and which has been calibrated by some means such that it indicates the absorbed power. It will frequently be referred to as the "standard." Load B, for which the power is required, may be another power meter or other termination such as an antenna.

The technique outlined above of making $\Gamma_A = \Gamma_B$ has found but little use because of the implicit requirement for a tuning transformer, and the uncertainty it can introduce. For example, if this transformer is added ahead of or included as part of the standard, an uncertainty is introduced into its calibration unless the transformer loss is known. Alternatively if the transformer is introduced in conjunction with load B, it must either become part of this load or a similar error will be introduced. Although the attenuation in a typical waveguide transformer is probably not large, the uncertainty in this loss usually precludes the use of transformers in this manner. This technique of adjusting for $\Gamma_A = \Gamma_B$ has found, however, a limited use at the Boulder Laboratories of the National Bureau of Standards. Here the impedance of a bolometer mount of special design is adjusted, before calibration, to equal that of the load of interest. The design of the NBS bolometer mount permits its calibration in the microcalorimeter [5] and this calibration procedure is independent of the bolometer mount impedance.

The proposed power meter, which is the primary subject of this paper, is of the terminating type and includes a means of adjusting its input impedance without requiring recalibration. In common with other terminating meters, it indicates the net power absorbed. However, the problem of transformer losses is avoided and, within certain limits, this meter may be regarded as the equivalent of a conventional terminating type power meter preceded by a *lossless* and adjustable tuning transformer.

This device is in appearance, a tuned reflectometer, and in fact an alternative use for the "power transfer instrument" described in [4]. For a simplified explanation, consider figure 3. By use of tuners T_x and T_y it is possible to compensate for imperfect coupler directivity, etc., so that the powers indicated by detectors 3 and 4 are respectively proportional to the powers associated with the incident and emergent waves on arm 2. These proportionality factors may be determined by a suitable calibration.

If arm 1 is connected to the signal source, the device may be regarded as a feed-through wattmeter since the net power leaving arm 2 is the difference between the emergent and incident powers. Alternatively, with arm 2 connected to the signal source, and arm 1 ter-

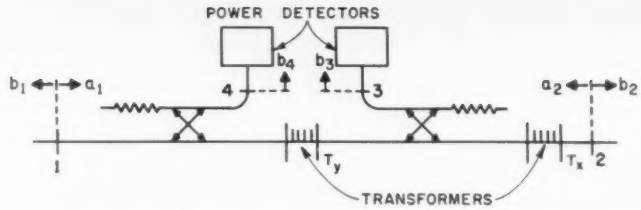

FIGURE 3. *Basic four arm junction used in power and impedance measuring applications.*

minated by a passive load, the device becomes a terminating power meter with the net power delivered to arm 2 given by the difference between the incident and emergent powers.[2]

The impedance observed at arm 2 under these conditions depends, to some extent, upon the impedance terminating arm 1. On the other hand, the proportionality factors (between the incident or emergent waves at arm 2 and the detectors on arms 3 and 4) are independent of the impedance which terminates arm 1. This makes possible the described operation. In the sections to follow the pertinent theory will be developed. For the sake of completeness, and in order to bring out those features which are pertinent to the present applications, the earlier theory [3, 4, 6] will be reviewed in some detail.

3. Review of Prior Art

Consider first a four arm waveguide junction assembled from a pair of directional couplers and tuning transformers as shown in figure 3. Arms 3 and 4 are terminated by constant impedance power detectors. Since the subsequent operation does not require access to the terminal surfaces between the junctions and these detectors, it is not required that the terminal surfaces employed in the analysis coincide with those of the mating waveguide flanges. This permits a substantial simplification in the treatment by use of the following artifice. For convenience it will be assumed that the power detectors are of the bolometric type. In general the bolometer mount reflects a certain fraction of the incident energy and absorbs another portion. The remainder is delivered to the bolometer or power sensing element. It is thus possible to construct an equivalent circuit of the bolometer mount as shown in figure 4. This circuit consists of a lossless transformer, a matched attenuator, and an "ideal" detector connected in tandem as shown. The characteristics of the transformer and attenuator are adjusted as required to duplicate the power reflected and absorbed [3] by the actual bolometer mount. The "ideal" detector by definition includes a matched and lossless waveguide structure which delivers all of the incident power to the bolometer element. The power detectors shown in figure 3 are now replaced by these equivalents and the terminal surfaces between the four arm junction and detector chosen as indicated in figure 5. This procedure, in effect, shifts the nonideal behavior of the detectors to the junction, and incorporates it as part of the junction behavior. This stratagem permits an analysis of the general behavior of the device

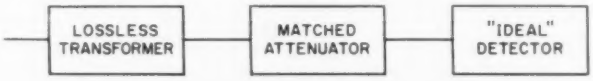

FIGURE 4. *Equivalent circuit of bolometer mount (power detector).*

[2] The reader may wonder if the power input at *arm 1* could also be obtained from the readings on arms 3 and 4. In order to achieve this result the junction would have to satisfy certain additional conditions, the realization of which would prove difficult in the existing art.

[3] Strictly speaking the attenuator is adjusted so that its *efficiency* equals the *effective efficiency* of the bolometer mount. These concepts are explained in [5].

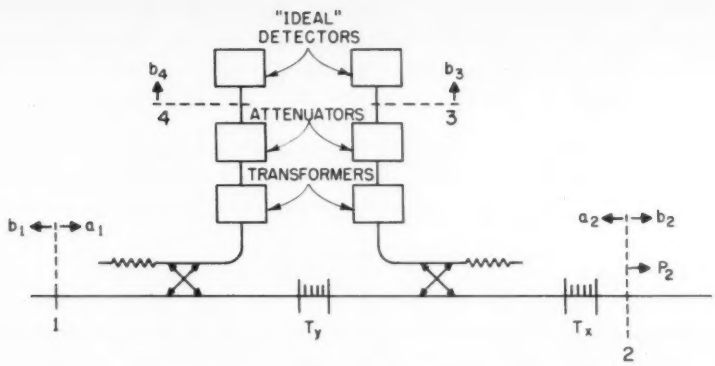

FIGURE 5. *Illustrating the choice of terminal surface employed in the analysis.*

under the simplifying assumption of matched and ideal detectors on arms 3 and 4. It must be remembered, however, that the new terminal surfaces 3 and 4 are, in general, not available for supplementary observations. In addition, certain of the detector characteristics have been absorbed within the junction. These must be taken into account in any attempt to construct the junction behavior from the characteristics of its individual components.

The system behavior will be described in terms of appropriately normalized incident and emergent "voltage" wave amplitudes at the different terminal surfaces. These will be designated by a_m and b_m respectively, where the subscripts take the values 1 . . . 4 corresponding to the different terminals of interest.

The powers, P_3 and P_4, delivered to detectors 3 and 4 are given by $\frac{|b_3|^2}{Z_0}$ and $\frac{|b_4|^2}{Z_0}$ respectively. (Note that the a's and b's are in general complex.) The *net* power emerging from arm 2 is given by:

$$P_2=\frac{1}{Z_0}\left[|b_2|^2-|a_2|^2\right]. \tag{2}$$

In accordance with frequently used microwave practice, the normalization is made in such a way that the characteristic impedance, Z_0, reduces to unity. Thus, this factor does not appear in the equations which follow.

The relationships imposed by the junction on the a's and b's are given by:

$$\begin{aligned} b_2&=S_{21}a_1+S_{22}a_2 \\ b_3&=S_{31}a_1+S_{32}a_2 \\ b_4&=S_{41}a_1+S_{42}a_2 \end{aligned} \tag{3}$$

where the $S_{m,n}$ are the scattering coefficients of the four arm junction (a fourth equation involving b_1 could be written but is not required in the analysis). The advantage of the choice of reference planes outlined earlier is now evident. Ordinarily eqs (3) would include terms in a_3 and a_4. Six terms have been eliminated by choosing the terminal surfaces so that a_3 and a_4 vanish.

Solving eqs (3) for a_2 and b_2 in terms of b_3 and b_4 yields:

$$\begin{aligned} a_2&=\frac{Db_3-Bb_4}{\Delta} \\ b_2&=\frac{Ab_4-Cb_3}{\Delta} \end{aligned} \tag{4}$$

where

$$A=S_{21}S_{32}-S_{31}S_{22}$$
$$B=S_{31}$$
$$C=S_{21}S_{42}-S_{41}S_{22}$$
$$D=S_{41}$$
$$\Delta=S_{41}S_{32}-S_{31}S_{42}.$$

Substituting eqs (4) into eq (2) gives:

$$P_2=\frac{|A|^2-|B|^2}{|\Delta|^2}|b_4|^2-\frac{|D|^2-|C|^2}{|\Delta|^2}|b_3|^2+\frac{1}{|\Delta|^2}[(BD^*-AC^*)b_3^*b_4+(B^*D-A^*C)b_3b_4^*] \tag{5}$$

where (*) denotes the complex conjugate. Equation (5) gives the *net* power *emerging* from arm 2 in terms of b_3, b_4 and the parameters of the junction.

For reflectometer applications it is desirable to express b_3/b_4 as a function of a_2 and b_2. Equations (4) may be rearranged to yield·

$$\frac{b_3}{b_4}=\frac{A\dfrac{a_2}{b_2}+B}{C\dfrac{a_2}{b_2}+D}. \tag{6}$$

If arm 2 is terminated by a passive load, of reflection coefficient Γ_l, this becomes:

$$\frac{b_3}{b_4}=\frac{A\Gamma_l+B}{C\Gamma_l+D} \tag{7}$$

since, under the specified conditions, $a_2/b_2=\Gamma_l$.

Thus far the only explicit assumption concerning the four arm junction is that its behavior is described by eqs (3). (This involves a number of implicit assumptions such as linearity, etc.). By use of the tuners T_x and T_y it is possible to impose a variety of conditions on the constants A . . . D. For example, in the reflectometer application, it is required that B and C be made negligibly small as compared with A and D, respectively. This may be achieved by the adjustment of T_x and T_y as described by Engen and Beatty [6].

Note that if both B and C vanish, b_3/b_4 is proportional to Γ_l. In addition,

$$|a_2|^2=\left|\frac{D}{\Delta}\right|^2|b_3|^2, \qquad |b_2|^2=\left|\frac{A}{\Delta}\right|^2|b_4|^2, \tag{8}$$

$$P_2=|b_2|^2-|a_2|^2=\left|\frac{A}{\Delta}\right|^2|b_4|^2-\left|\frac{D}{\Delta}\right|^2|b_3|^2, \tag{9}$$

and the powers observed by detectors 3 and 4 are respectively proportional to the powers associated with the incident and emergent waves in arm 2.

Another condition of interest is that in which BD^*-AC^* is made to vanish. (Note that this is satisfied if $B=C=0$.) In general this may be achieved by the adjustment of T_y [4, 6] only. In this case eq (5) becomes

$$P_2=k_1|b_4|^2-k_2|b_3|^2=k_1P_4-k_2P_3 \tag{10}$$

where

$$k_1=\frac{|A|^2-|B|^2}{|\Delta|^2}$$

$$k_2=\frac{|D|^2-|C|^2}{|\Delta|^2}.$$

Although eqs (9) and (10) are similar in form, there is an important difference. In the right side of eq (9) the power represented by the two terms may be associated with the incident

and emergent waves in arm 2. In eq (10), the *net* power leaving the junction is similarly given by the difference between two terms, but these terms no longer bear a simple relationship to the incident and emergent waves. That is, as a consequence of satisfying only the condition $BD^*-AC^*=0$ instead of $B=C=0$, it is no longer possible to resolve the "incident" and "emergent" powers at arm 2.

The fact that the net emergent power can be written in the form of eq (10) is important, however, since this provides the basis for proving that the operation is (ideally) independent of impedance discontinuities at terminal surface 2 [4].

4. General Theory

In the foregoing section, four arm junction theory has been reviewed and adjustments described which are useful in reflectometer and power measuring applications. The associated calibration procedures have been omitted, but will be described in the following section.

The foregoing analysis has been based on the assumption—implicit or explicit—that the junction will be energized via arm 1 and a passive load connected to arm 2. When used in conjunction with appropriate calibration procedures, to be described, the given techniques permit a determination of the power delivered to a load on arm 2 and/or the magnitude of its reflection coefficient.

However, with the exception of eq (7) the relationships expressed by eqs (2 through 10) are valid for excitation applied via either arm 1 or 2 (or both). The termination of arm 1 by a passive but adjustable load, as shown in figure 6, permits the same junction to be used in several additional applications, in which the excitation is supplied via arm 2.

Consider first eq (10). Since k_1 and k_2 are functions *only* of the junction parameters, their values will be independent of the adjustment of transformer T_t (fig. 6) which is part of the load terminating arm 1. On the other hand, the impedance "looking into" arm 2 will, in general, depend on this adjustment. Assuming the constants k_1 and k_2 have been determined, the measurement of P_3 and P_4 thus yields the net input power (at arm 2) for arbitrary values of input impedance. (Note that P_2, eq (10) will now be *negative* since P_2 is, by definition, the net *emerging* power.)

The entire assembly shown in figure 6 may thus be regarded as a terminating type power meter. In the area of power measurement additional applications include:

(1) A variable impedance terminating type power meter. The utility of such an instrument will be evident from the discussion found in the introduction.

(2) A means for measuring the maximum available power from a signal source.

In this latter application the load impedance is adjusted until the maximum power is indicated,[4] as given by eq (10). Theoretically, the input impedance of the power meter will now be the complex conjugate of the source impedance. In principle, this also provides a means of measuring the impedance of an active source by adjusting for maximum power transfer and then measuring the impedance at arm 2 of the junction. As a practical measure,

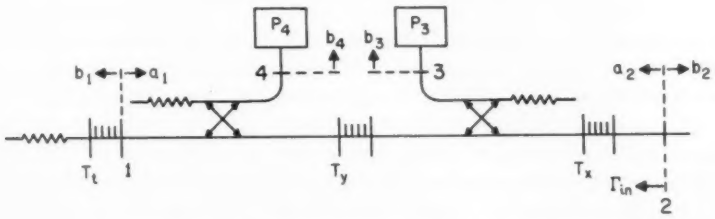

FIGURE 6. *Addition of passive and adjustable load to provide further applications.*

[4] The practical utilization of this idea would probably require accessory instrumentation to perform the operations indicated in eq (10).

unfortunately, it cannot be necessarily anticipated that this technique will yield a high degree of accuracy because the dependence of power transfer upon load impedance vanishes as the maximum is approached.

For these two applications it is only necessary that the junction satisfy the condition $BD^*-AC^*=0$.

In impedance measuring applications it is desirable that both B and C vanish. Subject to this latter condition, the reciprocal of eq (6) becomes:

$$\frac{b_4}{b_3}=\frac{D}{A}\Gamma_{in} \tag{11}$$

where $\Gamma_{in}=\frac{b_2}{a_2}$ is the reflection coefficient "looking into" arm 2.

Because the indicated detection techniques respond only to the magnitudes of b_3 and b_4 it is appropriate to write this equation in the form:

$$\left|\frac{b_4}{b_3}\right|=\left|\frac{D}{A}\right||\Gamma_{in}|. \tag{12}$$

Subject to the determination of $\left|\frac{D}{A}\right|$, the measurement of the ratio of $|b_3|$ to $|b_4|$ thus determines the magnitude of the input reflection coefficient at arm 2.

There are a number of possible applications for such a device in the field of impedance measurement. Perhaps the most attractive is that of providing a variable impedance for evaluating a lower order accuracy instrument—such as a slotted line.

For completeness, it may be noted that the device could also be used as (1) an impedance transfer standard and (2) to measure unknown reflection coefficient magnitudes. In the latter case, for example, the impedance is first adjusted to equal that of the unknown (by means of the technique described in conjunction with fig. 2), and the reflection coefficient magnitude determined from the indications on arms 3 and 4. In general, however, these two measurement requirements are more readily satisfied by existing techniques.

Finally, the impedance and power measuring applications may be combined in an application such as measuring the power output of a signal source as a function of load impedance, e.g., a Rieke diagram. For this application, if the phase information is required, certain modifications and extensions of the system are desirable. These details, however, are not within the scope of the present paper.

It should be emphasized that the tuning procedures required for these applications are identical to those employed in the prior art. Thus the cited applications may be regarded as further uses for the existing techniques. For example, the "variable impedance terminating type power meter" is nothing more than the "power transfer instrument" of [4], with an adjustable impedance connected to arm 1. Thus, with appropriate adjustment and calibration, the same device may be employed as either a feed-through or terminating type power meter.

5. Calibration Procedures

The tuning procedures required in the foregoing techniques are described in [6] and need not be repeated here. A similar observation applies to much of the calibration procedure. However, because certain modifications are indicated by these newer applications, this section will also include a review of some of the prior art.

For power measurement applications, the values of k_1 and k_2 (eq (10)) are required. As outlined in [4] these may be determined by the following procedure which includes two steps.

(1) Arm 2 is terminated by a standard [5] power meter, arm 1 is connected to a suitable generator and the values of P_2, P_3, and P_4 are noted.

---

[5] I.e., a terminating type power meter whose characteristics have been determined in some manner such that an accurate determination of P_2 is possible. See reference [5], for example.

(2) The standard power meter is then replaced by a short circuit ($P_2=0$) and the corresponding values of P_3 and P_4 again noted. Substitution of the appropriate values in eq (10) yields a pair of equations which can be solved for k_1 and k_2.

This procedure is based on the fact that eq (10) must hold for all operating conditions. Thus the observation of P_3 and P_4 for two known values of P_2 is, in general, sufficient to determine k_1 and k_2.

A third step, which could be employed in place of either of the other two is as follows:

(3) Arm 1 is terminated by a load such that the impedance observed at arm 2 is equal to that of the standard power meter. Arm 2 of the assembly is then connected to a suitable generator and the values of P_3 and P_4 noted. The power absorbed by the junction under this condition is determined by connecting the standard meter to the same source. (Note that P_2 is now negative.)

Thus a third set of values for P_2, P_3, P_4 is obtained which may be substituted into eq (10). This latter step is somewhat more complicated than the other two, thus it is appropriate to investigate the relative merits of the different procedures. This question can perhaps be most easily answered by inspection of eq (5).

Equation (5) may be written in the following form,

$$P_2=k_1P_4-k_2P_3+2\epsilon\sqrt{P_3P_4}\cos\theta \tag{13}$$

where

$$\epsilon=\frac{|BD^*-AC^*|}{|\Delta|^2},$$

$$\theta=\arg\,[(BD^*-AC^*)b_3^*b_4],$$

and the other quantities have been previously defined.

Because the indicated instrumentation measures magnitudes only, θ must be regarded as a random variable. In order to secure the desired operation, it is therefore necessary to make ϵ vanish. In theory this can be done by using a sliding short to terminate arm 2 and adjusting the appropriate transformer until a constant ratio of P_3/P_4 is obtained. This procedure is described in greater detail in the references.

As a practical measure, however, there is a limit to how closely the desired condition may be achieved. In the existing art this is determined primarily by limitations in the ability to recognize the desired condition. Other potential limitations include the tuner resolution and ability of the system to retain the desired adjustment.

The inability to make ϵ completely vanish affects both the calibration and subsequent use of the device. During the calibration procedure this effect is the equivalent of an uncertainty in the value of P_2 by the amount $\pm 2\epsilon\sqrt{P_3P_4}$. This, in turn, will be reflected as an uncertainty in the calculated values of k_1 and k_2. In operation as either a feed-through or terminating type power meter, the value of P_2 will again be indeterminate by the amount $\pm 2\epsilon\sqrt{P_3P_4}$. This is in addition to the uncertainty introduced into the values of k_1 and k_2 during the calibration procedure.

A general statement as to the relative merits of the different calibration procedures can now be given. From an inspection of eq (13) it is evident that the error due to a nonzero value of ϵ, in determining k_1 and k_2 respectively, can be minimized if the junction is energized in such a way that the conditions, $k_2P_3 \ll k_1P_4$ and $k_1P_4 \ll k_2P_3$ are satisfied, in turn, during the calibration. In practice these criteria are nominally satisfied by steps 1 and 3.

On the other hand, the relative importance of k_1 and k_2 depends upon the subsequent use which is made of the device. In a terminating power meter application, k_2 is of prime importance while in the feed-through power meter (power transfer standard) the important constant is k_1.

Thus if only feed-through applications are anticipated, the use of step 1 and either step 2 or 3 is indicated. If "terminating" applications are planned the calibration should include step 3 and either step 1 or 2. Where both applications are envisaged, steps 1 and 3 should be

employed. In those applications where impedance measurements are included, it is the ratio of k_1 to k_2 which is important, and this is provided by step 2. Finally, the use of all three steps provides a useful check on the system performance. Thus the choice of calibration procedure depends primarily upon the intended applications. These considerations may be summarized by noting that, for optimum results, the calibration procedure should include those steps which approximate the intended use. Certain aspects of these procedures will be further developed in the section on error analysis.

6. Practical Considerations

The degree of flexibility inherent in these techniques is such as to provide for a wide variety of applications. This can perhaps be best illustrated by considering a number of specific examples. For convenience it will be assumed that the detectors terminating arms 3 and 4 are of the bolometric type and operated in conjunction with a bridge type power meter such that the bolometer resistance is maintained at a constant value.

First, consider the junction illustrated in figures 3 and 6. This is a useful configuration in applications where the power to be measured exceeds, by 10 db or more, the level at which the bolometric detectors operate. In this configuration the values of k_1 and k_2 are approximately equal to the coupling ratios in the first and second couplers (numbered from left to right) respectively. For example, if both coupling ratios are 10 db, k_1 and k_2 will approximately equal 10. For a 20 db ratio, these values will nominally equal 100 etc. The value of coupling ratio also determines over what limits the input VSWR may be adjusted in the terminating power meter application. This is primarily determined by the attenuation which exists between arms 1 and 2. For 10 db coupling, the upper limits for the VSWR is approximately 9.

If the power to be measured is of the level at which the bolometric detectors operate (nominally 0.01–10 mw), smaller values of k_1 and k_2 are desirable. These are provided by the alternative configuration, as shown in figure 7, where the main arm of the first coupler feeds the side arm of the second. If the coupling ratios are equal, and have a value of 10 db or more, the values of k_1 and k_2 are approximately unity. This is a useful configuration for intercomparing and calibrating power meters of the bolometric type.

As a feed-through wattmeter, this configuration suffers from a fairly high insertion loss —10 db or more in the cited example. Thus the practical applications are limited to those in which power loss is a secondary consideration. In a terminating power meter application, the 10 db coupling limits the input VSWR to values of 1.2 and less. As a general rule, a limited VSWR range is associated with an instrument which provides the smaller values of k_1 and k_2.

It is also possible to use single coupler arrangements, as shown in figure 8. In the existing art it is more difficult to implement this form of the instrument, both because of the limited availability of suitable components and because the tuning procedure is more difficult. On the

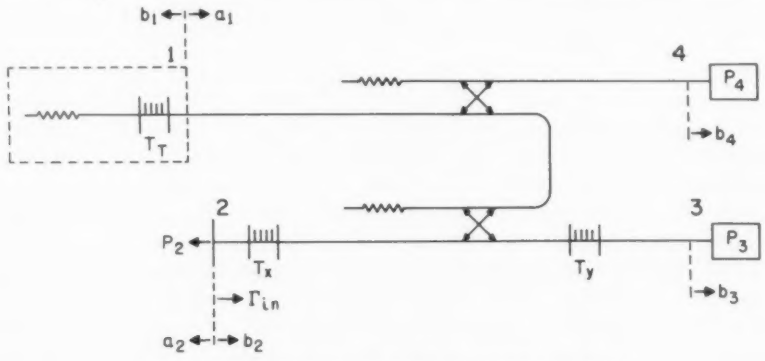

FIGURE 7. *Alternative form of terminating or feed-through wattmeter.*

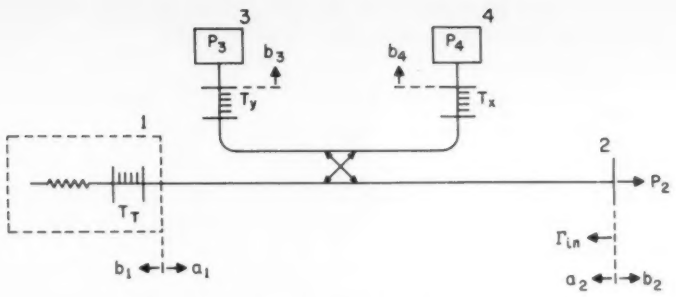

FIGURE 8. *Single coupler form of power meter.*

other hand, if a 3 db coupler is employed, this configuration will provide values of 1 and 2 for k_1 and k_2 respectively with only 3 db of attenuation, and will permit VSWR's as large as 3 in the terminating application. The single coupler arrangement thus provides a lower combination of values, for k_1, k_2, and insertion loss, than is possible with the two-coupler instruments.

Although bolometric power meters have been specified for arms 3 and 4, it is evident that any type of constant impedance power detector may be employed. Indeed, absolute power detectors are not actually required. Since only power ratios are involved, these detectors could in principle take the form of a calibrated attenuator followed by a detector which is capable of recognizing when the signal level is at an arbitrary reference value.

In an earlier section it has been noted that, for power measurement applications, it is sufficient that the junction satisfy the condition $BD^*-AC^*=0$ instead of the condition $B=C=0$ which is required in impedance measuring applications. However, as a practical measure, improved accuracy results if either of the conditions, $k_1P_4<<k_2P_3$ or $k_2P_3<<k_1P_4$ is satisfied *both* during the calibration and subsequent operation.

In practical terms this usually means that, when used as a feed-through wattmeter, the VSWR's of the terminating loads (including power meter used for calibration), are limited to values below 1.5. This limit also applies to the input VSWR when employed as a terminating power meter. In addition, the directivity of the second coupler (including tuner T_x if present) should be 20 db or more. In the existing art, these criteria are satisfied by nearly all of the anticipated applications. It is possible, however, to violate the foregoing criteria, and still satisfy the $k_1P_4<<k_2P_3$ or $k_2P_3<<k_1P_4$ conditions. For example, assume two terminating type power meters are to be compared, and that their impedances, while approximately equal, differ substantially from that required for an impedance match. In this case tuner T_x would be adjusted so that P_3 vanishes when arm 2 is terminated by one of the meters. (This must be done *before* the adjustment of tuner T_y.) The condition $k_2P_3<<k_1P_4$ is then satisfied.

The preceding paragraphs may be summarized by noting that while the technique provides the means for accurately comparing the power in loads of different impedance, some deterioration in accuracy results if this difference in impedance is large.

7. Error Analysis

In the analysis which follows, a number of approximations will be introduced, most of which are based upon the impedance and directivity criteria outlined in the immediately preceding paragraphs. Although, in many instances, the ultimate conclusions are substantially independent of these criteria, in careful work it would be desirable to check the validity of these approximations in an application where there is a marked departure from the stated conditions.

Equation (13) gives the net power flow, P_2, across the terminal surface of arm 2 (figs. 3, 6, 7, 8), in terms of the powers P_3, P_4, and the junction parameters k_1, k_2, ϵ, and θ. In general, the error in P_2 will include a contribution from the uncertainty in each of these quantities.

Let the uncertainty in P_3 be denoted by δP_3, etc. Then the limit of error due to the uncertainty in P_3, P_4, k_1, k_2 and from neglecting ϵ is given by:

$$\left|\frac{\delta P_2}{P_2}\right| = \frac{k_1 P_4\left(\left|\frac{\delta k_1}{k_1}\right| + \left|\frac{\delta P_4}{P_4}\right|\right) + k_2 P_3\left(\left|\frac{\delta k_2}{k_2}\right| + \left|\frac{\delta P_3}{P_3}\right|\right) + 2\epsilon\sqrt{P_3 P_4}}{|k_1 P_4 - k_2 P_3|}. \tag{14}$$

Note that in order to determine the maximum error θ has been chosen so that $|\cos\theta| = 1$. The error determination thus reduces to an evaluation of ϵ, $\delta k_1/k_1$, $\delta k_2/k_2$, $\delta P_3/P_3$, $\delta P_4/P_4$. These will be discussed in the order listed.

7.1. Evaluation of ϵ

As already noted, it is an objective of the tuning procedure to make ϵ vanish. In theory this can be accomplished by the use of tuner T_v. The tuning procedure consists of terminating arm 2 by a sliding short and adjusting for a constant ratio, P_3/P_4, for all positions of the short. It is possible to relate the value of ϵ to the inability to completely realize this condition through the following argument.

The operation of the sliding short may be described by the equation $\Gamma_2 = e^{i\phi}$ where the value of ϕ is determined by the short position. Substitution into eq (7) yields:

$$\frac{b_3}{b_4} = \frac{Ae^{i\phi} + B}{Ce^{i\phi} + D}. \tag{15}$$

It can be shown[6] that the locus of b_3/b_4, which is generated by varying ϕ, is a circle of radius

$$R = \frac{|AD - BC|}{|D|^2 - |C|^2}.$$

The distance from the origin to the center of this circle is given by

$$R_c = \frac{|BD^* - AC^*|}{|D|^2 - |C|^2}.$$

As ϕ varies, the ratio $|b_3/b_4|$ will, in general, take on different values with the maximum and minimum values given by:

$$\left|\frac{b_3}{b_4}\right|_{\max} = R + R_c$$

$$\left|\frac{b_3}{b_4}\right|_{\min} = R - R_c.$$

This is illustrated in figure 9.

By performing the indicated operations one obtains the result:

$$\frac{\left|\frac{b_3}{b_4}\right|_{\max} - \left|\frac{b_3}{b_4}\right|_{\min}}{\left|\frac{b_3}{b_4}\right|_{\max} + \left|\frac{b_3}{b_4}\right|_{\min}} = \frac{R_c}{R} = \frac{|BD^* - AC^*|}{|AD - BC|}. \tag{16}$$

In practice, however, it is

$$\left|\frac{b_3}{b_4}\right|^2 = \frac{P_3}{P_4}$$

[6] See a text on complex variable theory.

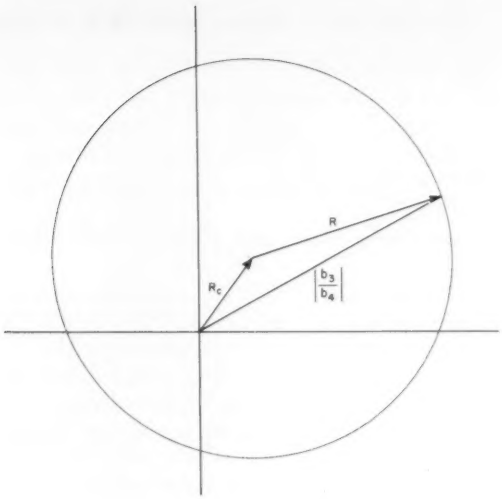

FIGURE 9. *Diagram giving relationship between* R, R_c, *and* $\left|\frac{b_3}{b_4}\right|$.

which is observed. If the maximum and minimum values are approximately equal it can be easily shown that:

$$\frac{\left(\frac{P_3}{P_4}\right)_{max}-\left(\frac{P_3}{P_4}\right)_{min}}{4\left(\frac{P_3}{P_4}\right)_{av}}\approx\frac{\left|\frac{b_3}{b_4}\right|_{max}-\left|\frac{b_3}{b_4}\right|_{min}}{\left|\frac{b_3}{b_4}\right|_{max}+\left|\frac{b_3}{b_4}\right|_{min}}.$$

Let

$$\rho=\frac{\left(\frac{P_3}{P_4}\right)_{max}-\left(\frac{P_3}{P_4}\right)_{min}}{\left(\frac{P_3}{P_4}\right)_{av}}, \tag{17}$$

then

$$\frac{|BD^*-AC^*|}{|AD-BC|}=\frac{|BD^*-AC^*|}{|AD|\cdot\left|1-\frac{BC}{AD}\right|}=\frac{\rho}{4}. \tag{18}$$

Now, by definition,

$$\frac{\epsilon}{\sqrt{k_1k_2}}=\frac{|BD^*-AC^*|}{|AD|\left(1-\left|\frac{B}{A}\right|^2\right)^{1/2}\left(1-\left|\frac{C}{D}\right|^2\right)^{1/2}} \tag{19}$$

and by hypothesis $|BD^*-AC^*|$ is small so that $\frac{B}{A}\approx\frac{C^*}{D^*}$. Therefore,

$$\left|\frac{B}{A}\right|^2\approx\frac{BC}{AD}\approx\left|\frac{C}{D}\right|^2. \tag{20}$$

Substitution of eq (20) into eqs (18) and (19) yields:

$$\epsilon\approx\frac{\sqrt{k_1k_2}}{4}\rho. \tag{21}$$

Equation (21) thus gives ϵ in terms of the measurable quantities ρ, k_1, and k_2.

7.2. Evaluation of Error Limits for k_1 and k_2

The experimental error, in determining k_1 and k_2, may be divided into contributions from two sources: (1) the error due to a nonzero ϵ, and (2) the error which accrues from the uncertainty in the associated values of P_2, P_3, and P_4. The error in k_1 and k_2 will also depend, to a considerable degree, upon which two of the three possible calibration procedures are employed.

In order to include the various possibilities, it is useful to outline the investigation in the following manner.

The two steps employed in the calibration procedure will be designated as "step a" and "step b."

Step a may be either of steps 1 and 2 as listed in section 5, but not step 3.

Step b may be either of steps 2 and 3 but not step 1.

Steps a and b may not represent step 2 simultaneously.

It should be noted that the introduction of these definitions involves no loss in generality. In the equations which follow, the subscripts "a" and "b" will be employed. For example, P_{3b} represents the power absorbed by the detector on arm 3 during step b of the calibration procedure—etc.

a. Error in k_1 Due to ϵ

Subject to these definitions, the following equation is obtained for k_1:

$$k_1=\frac{P_{2b}P_{3a}-P_{2a}P_{3b}+2\epsilon(\sqrt{P_{3a}P_{4a}}P_{3b}\cos\theta_a-\sqrt{P_{3b}P_{4b}}P_{3a}\cos\theta_b)}{P_{3a}P_{4b}-P_{3b}P_{4a}}. \tag{22}$$

The limit of error, $E_{1\epsilon}$, due to ϵ is thus given by:

$$E_{1\epsilon}=\frac{2\epsilon[\sqrt{P_{3a}P_{4a}}P_{3b}+\sqrt{P_{3b}P_{4b}}P_{3a}]}{P_{2a}P_{3b}-P_{2b}P_{3a}}. \tag{23}$$

Use of the approximations,

$$\begin{aligned} P_{2a}&\approx k_1P_{4a}-k_2P_{3a}\\ P_{2b}&\approx k_1P_{4b}-k_2P_{3b} \end{aligned} \tag{24}$$

and rearranging yields:

$$E_{1\epsilon}\approx\frac{2\epsilon}{k_1}\sqrt{\frac{P_{3a}}{P_{4a}}}\frac{1+\sqrt{\dfrac{P_{3a}P_{4b}}{P_{4a}P_{3b}}}}{1-\dfrac{P_{3a}P_{4b}}{P_{4a}P_{3b}}}$$

$$E_{1\epsilon}\approx\frac{\rho}{2}\sqrt{\frac{k_2P_{3a}}{k_1P_{4a}}}\left(1+\sqrt{\frac{P_{3a}P_{4b}}{P_{4a}P_{3b}}}\right), \tag{25}$$

since in general,

$$\frac{P_{3a}P_{4b}}{P_{4a}P_{3b}}<<1.$$

b. Error in k_1 Due to P_2, P_3, P_4

If the terms in ϵ are ignored, eq (22) may be written:

$$k_1=\frac{\dfrac{P_{2a}}{P_{4a}}-\dfrac{P_{3a}P_{2b}}{P_{4a}P_{3b}}}{1-\dfrac{P_{3a}P_{4b}}{P_{4a}P_{3b}}}. \tag{26}$$

When step 2 is included in the calibration procedure, one of the numerator terms must, ideally, vanish since either $P_{2a}=0$ or $P_{2b}=0$. Then, because the denominator is essentially equal to

unity, the experimental error in k_1 is primarily that in the remaining numerator term.

If the calibration is effected by means of steps 1 and 3, the conditions

$$k_2 P_{3a} << k_1 P_{4a}$$

$$k_1 P_{4b} << k_2 P_{3b}$$

are usually satisfied. In this case it can be easily shown that

$$\frac{P_{2a}}{P_{4a}} >> \frac{P_{3a} P_{2b}}{P_{4a} P_{3b}}$$

and the error in k_1 is essentially that in P_{2a}/P_{4a}.

The limit of error in P_{2a}/P_{4a} will be the sum of the errors in the individual terms. The term P_{2a} is usually determined by a "standard" power meter and the errors will be of both random and systematic types such as those due to instability and uncertainty in calibration. Conversely, the errors in P_{4a} will be only of the random type, since any systematic error may be included in the definition of k_1. Thus when k_1 is determined by step 1 and either of steps 2 or 3 the limiting uncertainty, E_p in k_1 (due to errors in P_2, P_3, P_4), may be written:

$$E_{1p} = \frac{|\delta P_{2a}|}{P_{2a}} + \frac{|\delta P_{4a}|}{P_{4a}}. \tag{27}$$

In the case where k_1 is to be determined by the use of steps 2 and 3, k_1 is given by the equation:

$$k_1 = \frac{-\frac{P_{3a} P_{2b}}{P_{4a} P_{3b}}}{1 - \frac{P_{3a} P_{4b}}{P_{4a} P_{3b}}}. \tag{28}$$

Again, the error is determined primarily by the numerator. But now there are three terms which are subject to random error, and one, P_{2b}, in which the errors are both random and systematic. This expression is also subject to another type of error because the condition, $P_{2a}=0$, which leads to its use, is never completely satisfied.[7] This is due to the inability to construct a perfectly reflecting short. For the sake of brevity, an intuitive rather than analytical treatment of this error will be given.

Consider eq (26). The value of this expression must remain invariant when the perfect "short" is replaced by an imperfect one. Thus the change from a zero to nonzero value for the first numerator term must be reflected by a corresponding, and very nearly equal, change in the second term. This change will occur in, and only in, the factors P_{3a} and P_{4a} since the factors P_{2b}, P_{3b} pertain to the other part of the calibration procedure. Now the ratio P_{3a}/P_{4a} is approximately [8] proportional to $|\Gamma_s|^2$, where Γ_s is the reflection coefficient of the short. Thus it is appropriate to replace eq (28) by:

$$k_1 = \frac{-\frac{1}{|\Gamma_s|^2} \frac{P_{3a} P_{2b}}{P_{4a} P_{3b}}}{1 - \frac{P_{3a} P_{4b}}{P_{4a} P_{3b}}}. \tag{29}$$

The limit of error in k_1 for this case is thus:

$$E_{1p} = \left|\frac{\delta P_{2b}}{P_{2b}}\right| + \frac{|\delta P_{3b}|}{P_{3b}} + \frac{|\delta P_{3a}|}{P_{3a}} + \frac{|\delta P_{4a}|}{P_{4a}} + \frac{|\delta |\Gamma_s|^2|}{|\Gamma_s|^2}. \tag{30}$$

---

[7] The inability to satisfy this condition also results in an error when step 1 is included in the calibration procedure. In this case, however, the contribution from this source is negligible.

[8] This relationship is exact if $B=C=0$.

Comparison with eq (27) indicates that the expected error in a determination of k_1, using steps 2 and 3, is considerably in excess of that which results when step 1 is included in the procedure. This bears out the earlier statement concerning the desirability of including in the calibration procedure those steps which correspond to the intended usage. (Note that if only terminating applications are planned, the lower accuracy in k_1 is not too important because $k_1 P_4$ is typically no more than a few percent of $k_2 P_3$.)

In summary, the uncertainty in k_1, $|\delta k_1|/k_1$, is given by:

$$\frac{|\delta k_1|}{k_1} = E_{1\epsilon} + E_{1p} \tag{31}$$

where

$$E_{1\epsilon} = \frac{\rho}{2}\sqrt{\frac{k_2 P_{3a}}{k_1 P_{4a}}}\left(1 + \sqrt{\frac{P_{3a}P_{4b}}{P_{4a}P_{3b}}} + \text{higher order terms in } \sqrt{\frac{P_{3a}P_{4b}}{P_{4a}P_{3b}}}\right) \tag{32}$$

$$E_{1p} = \frac{|\delta P_{2a}|}{P_{2a}} + \frac{|\delta P_{4a}|}{P_{4a}} \tag{27}$$

using steps 1 and 2 or steps 1 and 3;

$$E_{1p} = \left|\frac{\delta P_{2b}}{P_{2b}}\right| + \frac{|\delta P_{3b}|}{P_{3b}} + \frac{|\delta P_{3a}|}{P_{3a}} + \frac{|\delta P_{4a}|}{P_{4a}} + \frac{|\delta|\Gamma_s|^2|}{|\Gamma_s|^2} \tag{30}$$

using steps 2 and 3; and

$$\rho = \frac{\left(\frac{P_3}{P_4}\right)_{\max} - \left(\frac{P_3}{P_4}\right)_{\min}}{\left(\frac{P_3}{P_4}\right)_{\text{av}}}. \tag{17}$$

In an entirely analogous manner it can be shown that the maximum error in k_2, $|\delta k_2|/k_2$, is given by:

$$\frac{|\delta k_2|}{k_2} = E_{2\epsilon} + E_{2p} \tag{33}$$

where

$$E_{2\epsilon} = \frac{\rho}{2}\sqrt{\frac{k_1 P_{4b}}{k_2 P_{3b}}}\left(1 + \sqrt{\frac{P_{3a}P_{4b}}{P_{4a}P_{3b}}} + \text{higher order terms in} \sqrt{\frac{P_{3a}P_{4b}}{P_{4a}P_{3b}}}\right) \tag{34}$$

$$E_{2p} = \left|\frac{\delta P_{2b}}{P_{2b}}\right| + \frac{|\delta P_{3b}|}{P_{3b}} \tag{35}$$

using steps 1 and 3 or steps 2 and 3; and

$$E_{2p} = \frac{|\delta P_{2a}|}{P_{2a}} + \frac{|\delta P_{4a}|}{P_{4a}} + \frac{|\delta P_{4b}|}{P_{4b}} + \frac{|\delta P_{3b}|}{P_{3b}} + \frac{|\delta|\Gamma_s|^2|}{|\Gamma_s|^2} \tag{36}$$

using steps 1 and 2.

7.3. Evaluation of $\frac{|\delta P_3|}{P_3}$ and $\frac{|\delta P_4|}{P_4}$

The terms $|\delta P_3|/P_3$ and $|\delta P_4|/P_4$ (eq (14)) represent the random errors in P_3, P_4 during the measurement procedure. These errors will in general be equal, but in addition to, the errors $|\delta P_{3a}|/P_{3a}$ etc., observed during the the calibration.

7.4. Summary of Errors

By use of the preceding theory it is thus possible to set limits to the error terms introduced in eq (14). The necessary relations are summarized in the preceding paragraph and by eqs (17), (21), (27), (30), (31), (32), (33), (34), (35), and (36).

Finally, if the recommendations as to choice of calibration procedures are followed, and the conditions $|B| \approx |C| \approx 0$ are satisfied, these relations for both applications may be summarized by the approximate formula:

$$\frac{|\delta P_2|}{P_2} \approx \frac{\rho}{2}(|\Gamma_c| + |\Gamma_m|) + \frac{|\delta P_{2s}|}{P_{2s}} + \frac{|\delta P_c|}{P_c} + \frac{|\delta P_m|}{P_m} \tag{37}$$

where the following definitions apply:

Γ_c = reflection coefficient of power standard employed in calibration procedure,

Γ_m = reflection coefficient of load in feed-through application, or input reflection coefficient of device in terminating application,

$\frac{|\delta P_{2s}|}{P_{2s}}$ = error in "standard" power meter employed for calibration,

$\frac{|\delta P_c|}{P_c}$ = random error in detector P_4 in feed-through application, or P_3 in terminating application, during calibration procedure,

$\frac{|\delta P_m|}{P_m}$ = as above except during measurement procedure.

In many cases the errors

$$\frac{|\delta P_c|}{P_c} \text{ and } \frac{|\delta P_m|}{P_m}$$

will be nominally equal. However, if the application calls for a significant difference in power levels during the calibration and measurement procedures, there may be some difference in these terms.

Equation (37) is a convenient "rule of thumb" for many of the anticipated applications. However, where more precise limits of error are required, the more exact equations should be employed.

This error analysis has been limited to the power measurement application. A similar analysis for the adjustable reflection coefficient application is beyond the scope of this paper although it may be anticipated that this would be a comparatively simple extension of the "conventional" reflectometer error analysis. [6, 7]

8. Summary

The preceeding sections have given the theoretical and practical details for an instrument which, when properly adjusted and calibrated, can be used as either a feed-through, or variable impedance terminating type power meter. As a feed-through device, the net power to a load of arbitrary impedance is obtained. In the terminating application, the net power absorbed is indicated and this is independent of the input impedance value to which it has been adjusted.

Impedance measurements and mismatch error corrections represent a burdensome and annoying aspect of the current power measurements art. As noted earlier, it is reasonably safe to say that the failure to apply, or ignorance of, these corrections represents a major source of error.

The techniques presented and developed in this paper contain the potential for a significant improvement: both in terms of simplifying the measurement procedure and providing improved accuracy.

In the existing art, however, there are a number of practical problems associated with the implementations of these ideas, such as the time consuming nature of the tuner adjustments. Thus there is room for a considerable amount of developmental work in the reduction of these ideas to practice—both in the areas of microwave hardware and associated instrumentation. The important point is that it is now possible (in principle) to construct a microwave power meter which all but eliminates the need for these awkward mismatch error measurements and corrections.

9. References

[1] R. W. Beatty and A. C. Macpherson, Mismatch errors in microwave power measurements, Proc. IRE **41,** 1112–19 (Sept. 1953).

[2] G. F. Engen, Amplitude stabilization of a microwave signal source, IRE Trans. MTT, **MTT–6,** 202–06 (April 1958).

[3] G. F. Engen, Recent developments in the field of microwave power measurements at the NBS, IRE Trans. Instr. **I–7,** 304–06 (Dec. 1958).

[4] G. F. Engen, A transfer instrument for the intercomparison of microwave power meters, IRE Trans. Instr. **I–9,** 202–08 (Sept. 1960).

[5] G. F. Engen, A refined X-band microwave microcalorimeter, J. Res. NBS, **63C** (Engr. and Instr.) No. 1, 77–82 (July–Sept. 1959).

[6] G. F. Engen and R. W. Beatty, Microwave reflectometer techniques, IRE Trans. on Microwave Theory and Techniques, **MTT–7,** 351–55 (July 1959).

[7] W. J. Anson, A guide to the use of the modified reflectometer technique of VSWR measurement, J. Res. NBS, **65C** (Engr. and Instr.) No. 4, 217–223 (Oct.–Dec. 1961).

(Paper 68C1–148)

JOURNAL OF RESEARCH of the National Bureau of Standards—C. Engineering and Instrumentation
Vol. 68C, No. 1, January–March 1964

A Laser With a Multihole Diaphragm

Tadashi Morokuma*

(October 21, 1963)

The properties of a laser with a multihole diaphragm were both theoretically and experimentally examined. This laser may be called a multibeam laser. Laser action was observed in the optical paths which were defined by the position of the holes and the cavity configuration. Interference fringes were observed on one of the cavity mirrors. A wavelength dependent interaction among the beams was observed. It is believed that the wavelength of a beam can be stabilized by the intensities of the other beams. A possible method will be proposed for the stabilization.

1. Introduction

In order to use continuous wave lasers for interferometric length measurement, their wavelengths should be stable enough to secure the required accuracy. The stability of a helium-neon laser has been intensively studied by Javan et al., [1, 2].[1] They have obtained short-term stability to better than two parts in 10^{13} by isolating their lasers from mechanical vibration, and, they were able to reset the wavelength with an accuracy of one part in 10^9. Gould [3] proposed to use the pulling effect for stabilization. A different approach has been pursued in this laboratory by placing a multihole diaphragm inside the confocal cavity of a laser.

The interesting phenomena found in the beams of the laser and also a possible method for stabilization will be described. The laser is provided with a diaphragm containing five circular holes; four of them are symmetrically located around a central one. The diaphragm is placed inside the cavity and in front of the one of the cavity mirrors. It is possible to obtain laser action so that one beam travels back and forth through the central hole on the axis of the cavity. The other two beams travel diagonally through the top and bottom holes, and the two side holes, respectively. Five bright round spots have been observed on the mirror that is covered with the diaphragm and a larger spot with interference fringes on the other mirror.

This laser essentially consists of three sublasers with common cavity mirrors. Their wavelengths are determined by the effective cavity spacings corresponding to the optical paths for one transit of each beam in the cavity. According to the resonance condition of a confocal cavity [4], it is possible for the oscillation in each beam to take place at several discrete wavelengths separated by a mode spacing of the cavity. Fabry-Perot rings, however, show interaction among the beams so that the oscillation at certain wavelengths is suppressed. Therefore, the wavelength relation is more complicated than expected.

It was possible for the laser to satisfy the necessary conditions for the wavelength stabilization by the use of a suitable diaphragm, and by the adjustment of its position and the excitation power.

2. Modes of Oscillation

The 1-m laser used in this laboratory is composed of an 80-cm discharge tube and a multihole diaphragm that is located close to one of the cavity mirrors. The discharge tube contains a mixture of 1 mm Hg of helium and 0.1 mm Hg of neon. The maximum gain of the tube is about 5 percent per pass at 1.152 μ.

The schematic diagram of the laser and a photograph of the diaphragm are shown in figures 1a and b. The beam is elliptical in shape, approximately 10 mm along one axis and 8 mm along the other. This distortion is due to an aberration in the Brewster's angle windows. The central hole was purposely made smaller than the outer holes so that the larger diffraction loss due to the smaller opening would compensate for the larger gain of the central beam. Thus, each of the three beams can be operated in a single mode with the intensities almost equal to each other. The diameter of the holes and spacings should be determined by several factors, such as the gain, the diameter of a discharge tube, the aberration of windows or mirrors, etc. The modes of oscillations are shown schematically in figure 2. The frequencies of the beams are given by

$$f_o = \frac{cN_o}{2d_o} \tag{1}$$

for beam 1

$$f_1 = \frac{cN_1}{4d_1} \tag{2}$$

*Guest worker—National Bureau of Standards, present address: Olympus Optical Company Ltd., Tokyo, Japan.

[1] Figures in brackets indicate the literature references at the end of this paper.

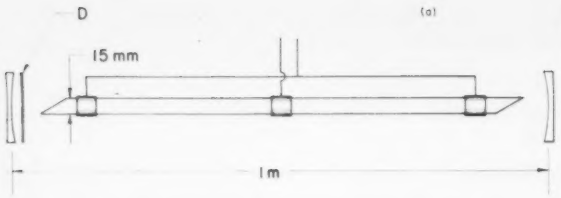

FIGURE 1a. *Schematic diagram of a laser with a multihole diaphragm, D.*

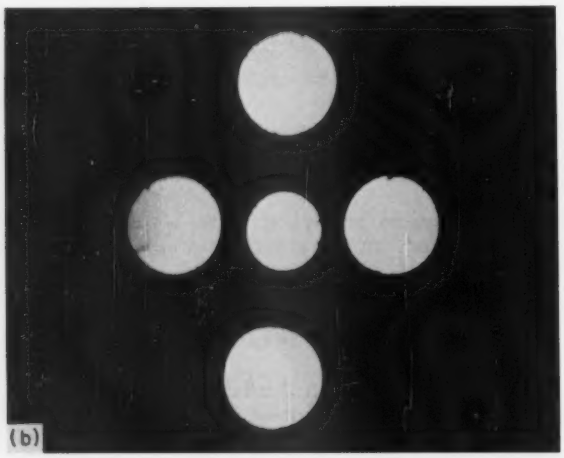

FIGURE 1b. *Photograph of the diaphragm.*

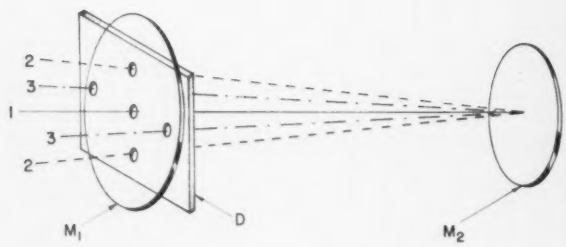

M_1, M_2 MIRRORS
D DIAPHRAGM
1. —— CENTRAL BEAM
2. - - - TOP & BOTTOM BEAM
3. — — SIDE BEAM

FIGURE 2. *Modes of oscillation.*

for beam 2

$$f_2=\frac{cN_2}{4d_2} \tag{3}$$

for beam 3

where N_c, N_1, and N_2 are order numbers (integers), d_0, d_1, and d_2 are optical paths between the cavity mirrors, and c is the velocity of light.

The modes of outer beams 2 and 3 will be called even modes when N_1 and N_2 are even and odd modes when they are odd. In case of an ideal confocal cavity, the optical paths d_0, d_1, and d_2 are all the same so that f_1 and f_2 are equal and the frequencies of the even modes of the outer beams are equal to those of the central beam. If there is an aberration within the cavity, however, the three frequencies may be slightly different from each other. This will play an important role in the discussion of the wavelength relation, as is described later.

3. Mode Pattern

Since a diaphragm is placed in front of only one of the cavity mirrors, symmetrical intensity distribution, as described in Fox and Li's theory, [5] cannot be expected. In other words, five bright spots are observed on the same mirror, and a large spot with interference patterns is observed on the other mirror. The five spots are shown in figure 3. The interference patterns are shown in figures 6, 7, and 8.

3.1. Central Beam

Figure 4 shows the beam on mirror M_2 when the outer holes are blocked. This photograph was taken with a low excitation power so that higher order

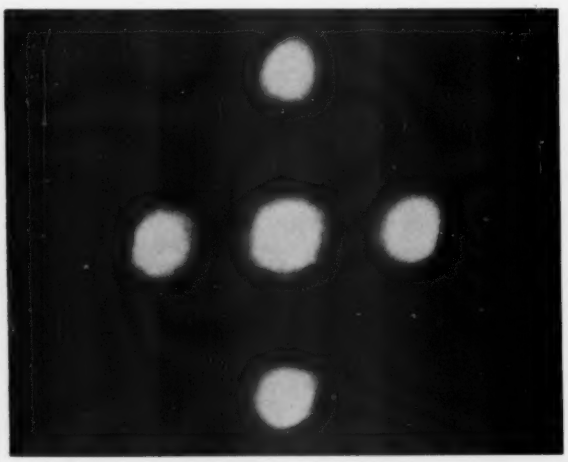

FIGURE 3. *Cross section of the beams on mirror M_1, with diaphragm as shown in figure 2.*

[2] The patterns which are seen in the photograph are produced in the image converter used in this experiment. They are not inherent in the beam.

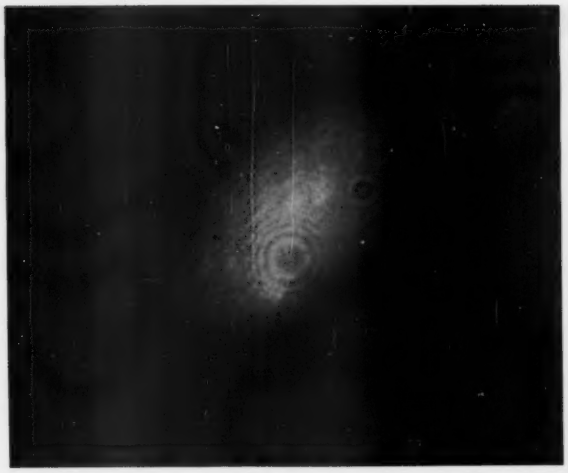

FIGURE 4. *Cross section of the central beam on mirror M_2, with diaphragm as shown in figure 5.*

modes did not appear. The cross section of the elliptical beam is about 4.8 mm along one axis and 2.9 mm along the other. This cross section is much larger than that of the central beam in figure 3, which measures 0.9 mm in diameter. In figure 4, of course, no fringe pattern is observed.[2]

These spot sizes can be calculated with a theory similar to Fox and Li's [5].

3.2. Outer Beams

Consideration will be given first to the case of two holes and then to the case of four holes. The observed fringe patterns can be explained as the result of interference between two or four spherical wave fronts.

a. Two Holes

When the central and the two side holes are blocked, two beams are observed coming out of the laser in different directions, as shown in figure 5. Figure 6 shows interference fringes observed on M_2 when the excitation power is decreased until single mode operation is achieved. The spacing, s, of the fringes is given by $s=d\lambda/a$, where a is the distance between the holes, d the mirror separation and λ the wavelength. In the case $d=1m$, $\lambda=1.15\mu$, and $a=3.1$ mm, the spacing is 0.37 mm. This agrees with the spacing measured on figure 6. It is to be noted that a bright fringe is observed on the axis of the cavity for an even mode and a dark fringe for an odd mode. Since the phase difference between the two beams is πN_1 on mirror M_2 from eq (2), it becomes $2n\pi$ radians for an even mode (N_1=even) and $(2n+1)\ \pi$ radians for an odd mode (N_1=odd). In this case n is an integer. These two fringe patterns intermesh with each other. Consequently, no fringes will be observed when even and odd modes are coexistent and their intensities are exactly equal. Figure 7 shows the intermeshed fringe patterns observed in the case of multimode operation.

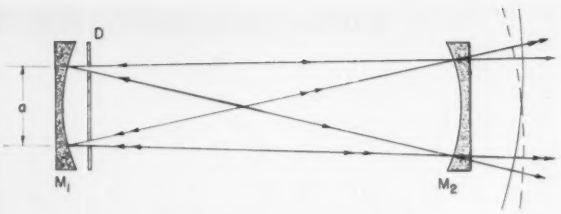

FIGURE 5. *Optics of a two-beam laser.*

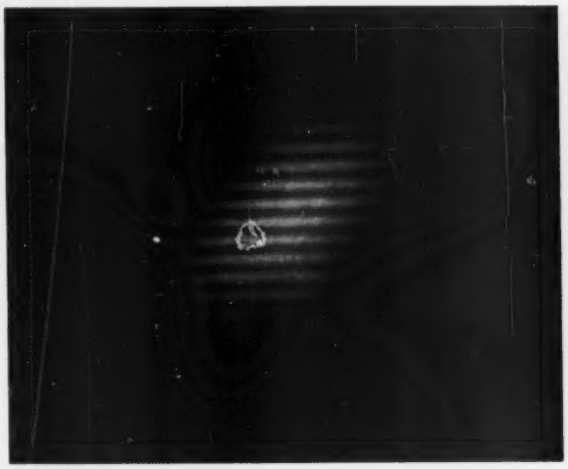

FIGURE 6. *Fringes observed on mirror M_2, with diaphragm as shown in figure 5.*

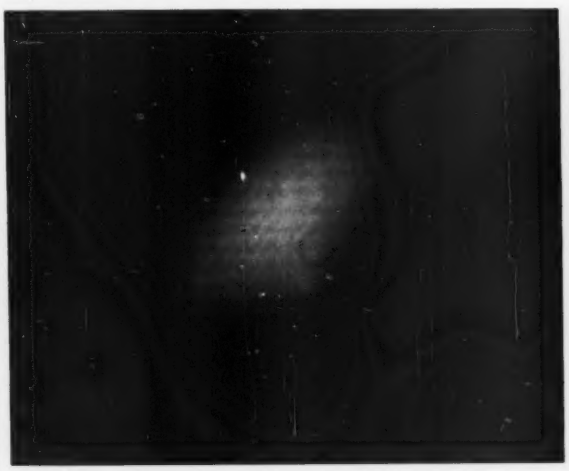

FIGURE 7. *Intermeshed fringe patterns.*

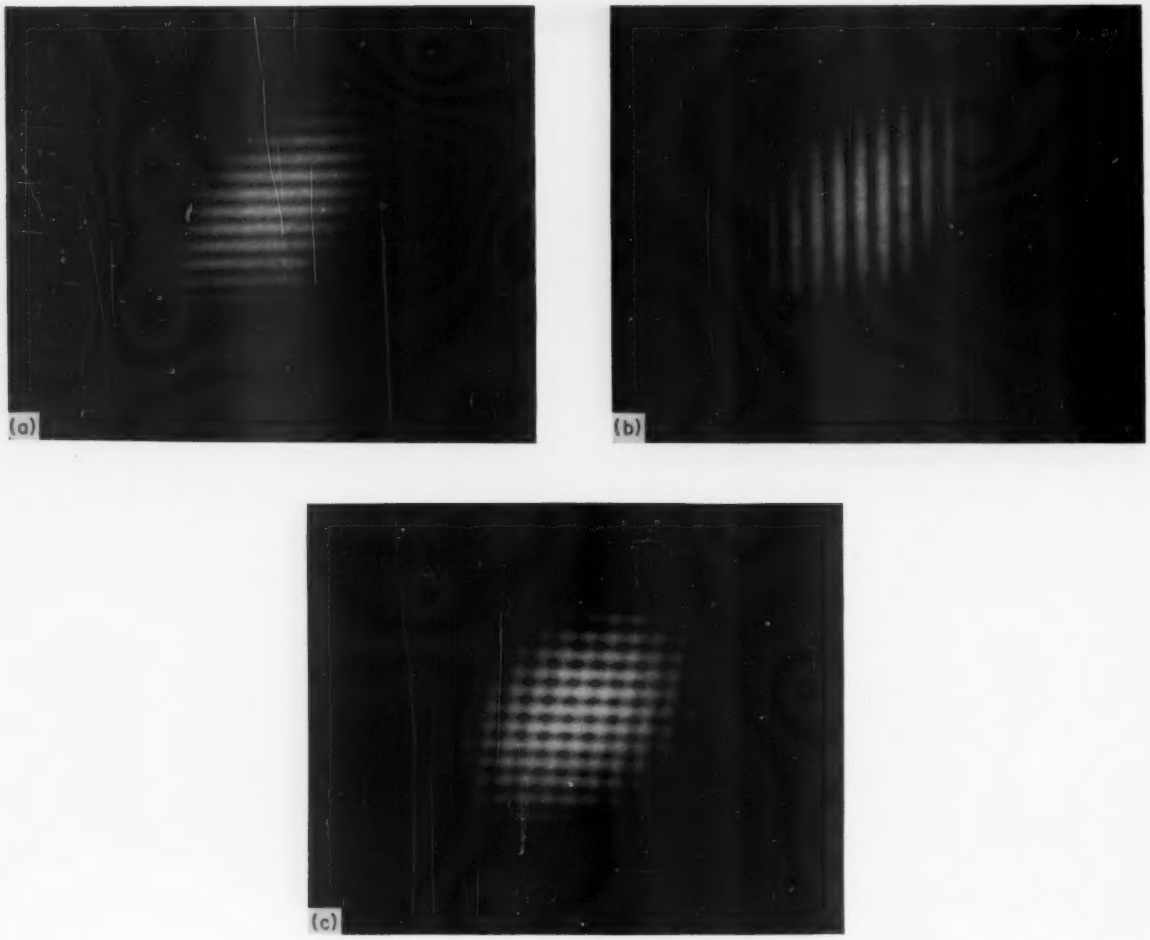

FIGURE 8. *Fringes observed on mirror M_2, with diaphragm as shown in figure 9.*
(a) Fringes between beams 1 and 2,
(b) fringes between beams 3 and 4,
(c) superposition of (a) upon (b).

b. Four Holes—The Superposition and the Interference of Two Sets of Fringes

One of the interference patterns is shown in figure 8c. It is obtained by superimposing the fringe pattern of figure 8a on the one of figure 8b. The pattern in figure 8a is the same as that in figure 6. Another pattern that has been observed is composed of bright spots. This pattern is very unstable and remains stationary for only a few seconds. (See the discussion pertaining to figure 11.) The intensity distribution of these patterns can be easily explained by assuming that the wave fronts of the four beams are replaced by plane wave fronts propagating in the directions connecting the center of curvature of mirror M_1 and the centers of the holes, as shown in figure 9. In the x-y plane, which is tangential to mirror M_2, with the origin of the coordinates on the optical axis, the four beams can be represented in the following forms:

$$A_1 = \exp i(\omega_1 t - k_1 ax/2d_1) \quad \text{for beam 1.}$$

$$A_2 = \exp i(\omega_1 t + k_1 ax/2d_1 + \alpha) \quad \text{for beam 2.}$$

$$A_3 = C \exp i(\omega_2 t - k_2 by/2d_2 + \gamma) \quad \text{for beam 3.}$$

$$A_4 = C \exp i(\omega_2 t + k_2 by/2d_2 + \gamma + \beta) \quad \text{for beam 4.}$$

Here k_1 and k_2 are given by $k_1 = 2\pi/\lambda_1$ and $k_2 = 2\pi/\lambda_2$ where λ_1 and λ_2 are wavelengths; ω_1 and ω_2 are angular frequencies; a and b, the spacings between holes; α and β, the phase differences between beams 1 and 2, and beams 3 and 4, respectively. C is the amplitude ratio between A_1 and A_3. The origin of time, t, is

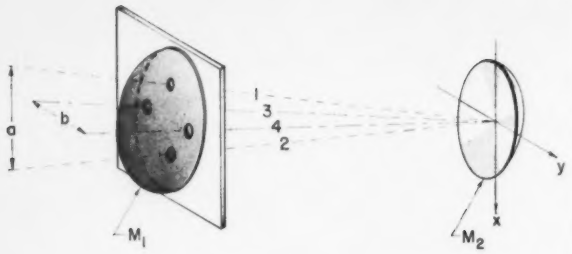

FIGURE 9. *Optics of a four-beam laser.*

chosen so that the phase angle of beam 1 is equal to zero at $x=0$. The initial phase angle of beam 3 is then given by γ at $y=0$. It is to be noted that α and β should be $2n\pi$ or $(2n+1)\ \pi$ radians, as previously described, corresponding to even or odd modes. The intensity distribution is

$$I(x,y)\propto\{\cos^2\ (k_1ax/2d_1+\alpha/2) + C^2\ \cos^2\ (k_2by/2d_2+\beta/2)\}$$

when $\lambda_1\neq\lambda_2$, and

$$I(x,y)\propto\{\cos^2\ (kax/2d_1+\alpha/2) + C^2\ \cos^2\ (kby/2d_2+\beta/2) + 2C\ \cos\ (kax/2d_1+\alpha/2)\ \cos\ (kby/2d_2 + \beta/2)\ \cos\ (\alpha/2-\beta/2-\gamma)\}$$

when $\lambda_1=\lambda_2=\lambda$, and $k=2\pi/\lambda$. Spacings d_1 and d_2 are almost equal to the spacing d_0 on the axis and the difference is less than $\lambda/2$. Therefore, they can be replaced by d_0 in the above equations. Then

$$I(x,y)\propto\{\cos^2\ (k_1ax/2d_0+\alpha/2) + C^2\ \cos^2\ (k_2by/2d_0+\beta/2)\} \quad (4)$$

when $\lambda_1\neq\lambda_2$ and

$$I(x,y)\propto\{\cos^2\ (kax/2d_0+\alpha/2) + C^2\ \cos^2\ (kby/2d_0+\beta/2) + 2C\ \cos\ (kax/2d_0+\alpha/2)\ \cos\ (kby/2d_0 + \beta/2)\ \cos\ (\alpha/2-\beta/2-\gamma)\} \quad (5)$$

when $\lambda_1=\lambda_2=\lambda$. Figure 10 shows the intensity distribution calculated from eq (4) for $\lambda=1.152\ \mu$, $d=1$ m, $a=3.1$ mm, $b=4.1$ mm, and $C=1$. The maximum intensity is normalized to 1.0 in the drawing. This is the case where the two patterns are simply overlapped without interference between them.

When λ_1 is exactly equal to λ_2, two kinds of patterns have been observed. One pattern has the same distribution as shown in figure 10 and is given by eq (5) when $\cos\ (\alpha/2-\beta/2-\gamma)=0$. The theoretical distribution of another pattern is shown in figure 11. This pattern is composed of bright spots and dark lines. They are obtained when $\cos\ (\alpha/2-\beta/2-\gamma)=\pm1$ in eq (5).

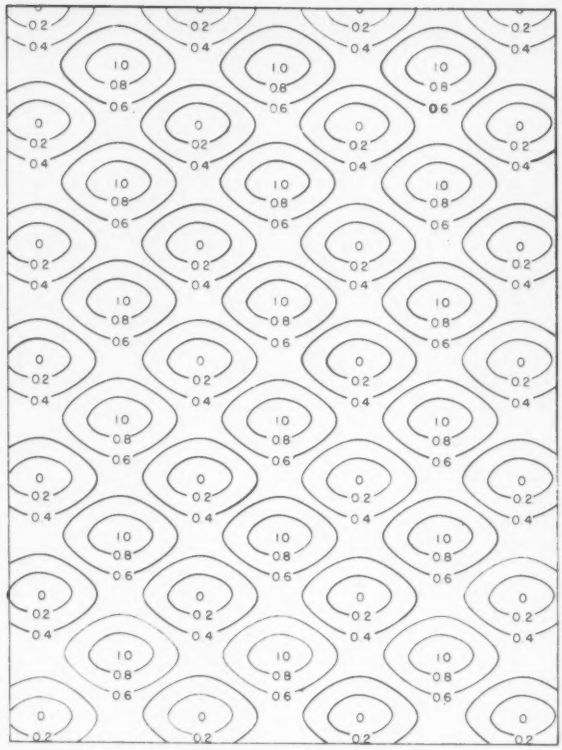

FIGURE 10. *Theoretical intensity distribution of fringes when* $\lambda_1\neq\lambda_2$ *or cos* $(\alpha/2-\beta/2-\gamma)=0$ *at* $\lambda_1=\lambda_2$.

A possible explanation for this is as follows: In the volume that beams occupy in common, they interact with each other. In other words, the photon in one pair of beams stimulate the laser oscillation in another pair of beams. Therefore, the phase difference would be zero, on the assumption that stimulated radiation is in phase with the incident radiation. When both pairs of beams are either in even or in odd modes, the cosine term is equal to unity; that is, $\cos\ (\alpha/2-\beta/2-\gamma)=\pm1$. If one pair of beams is in an even mode and another pair in an odd mode, the term vanishes; that is, $\cos\ (\alpha/2-\beta/2-\gamma)=0$ The experimental results are not sufficient to prove the validity of the above statements and further investigation is necessary.

4. Wavelength Relation

A wavelength dependent interaction of one beam on the others has been found by means of a Fabry-Perot etalon. Although the diameter of the central hole was purposely made smaller than the outer holes, the central beam is more intense than the other beams. The even modes of the outer beams

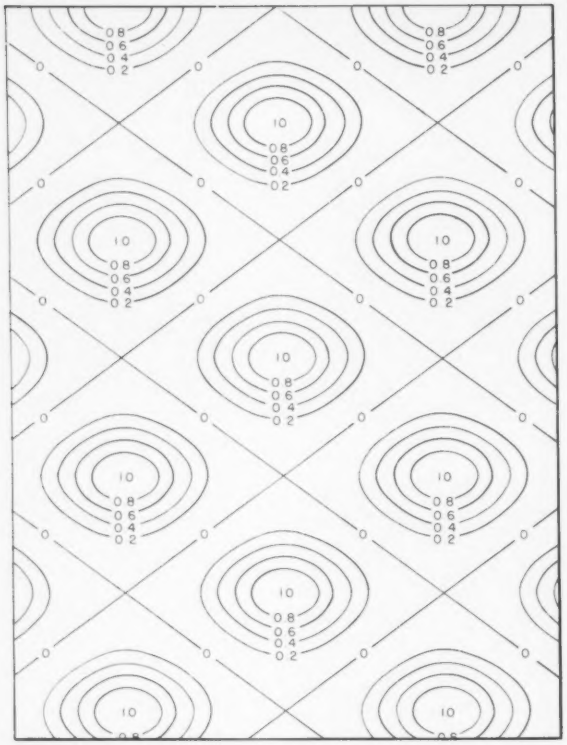

FIGURE 11. *Theoretical intensity distribution of fringes when* $\lambda_1=\lambda_2$ *and cos* $(\alpha/2-\beta/2-\gamma)=1$.

could not be observed at low excitation power. Since every beam passes a common space at one end of the cavity, the gain for the modes becomes lower than the threshold due to the high density of photons in the central beam. Hence at low excitation level, it is possible for outer beams to have only odd modes separated by 150 Mc/s for a 1-m confocal cavity. Also interaction between outer beams results in the suppression of some odd modes in one beam by another.

4.1. Experimental Arrangement

In order to study the wavelength relation among the beams, Fabry-Perot etalons are used as shown in figure 12. The first lens L_1, is focused on mirror M_2. A spherical wave front from a point source on M_2 becomes a plane wave front, passing through either a 1-m or a 50-cm Fabry-Perot etalon, then through the second lens, L_2. Haidinger fringes are formed on its focal plane, and the surface of mirror M_2 is also imaged on the same plane. Therefore, the Haidinger fringes are modulated by the image of a pattern on M_2. A given set of fringes identifies the location of the beams, either by a visual or a photographic method. For example, if a set of fringes is composed of continuous rings with even

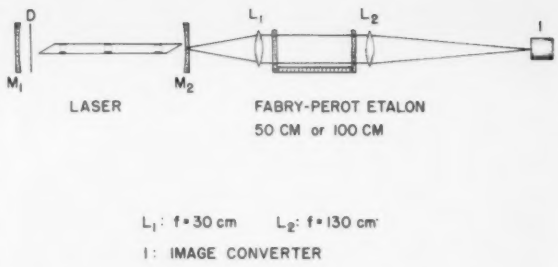

FIGURE 12. *Optical arrangement to study the wavelength relation.*

distribution of intensity, these fringes are formed by the central beam. If fringes are broken vertically with dark parallel lines equally spaced, these fringes are formed by the side beams.

No attempt was made to eliminate the feedback of photons from the etalon to the laser.

4.2. Experimental Results

When a 1-m Fabry-Perot etalon is used, the Haidinger fringes of all the even modes, having approximately the same diameters, appear to be superimposed on each other. Those of the odd modes are similarly superimposed with their bright fringes between the bright fringes of the even modes.

a. Interaction

When the laser tube is excited with low energy, the central beam can suppress oscillation in the even modes of the outer beams, as previously described. Figure 13a shows fringes obtained when only the top and bottom holes are open. Both even and odd modes are clearly seen in figure 13a, which shows the phase shift equal to π radians between them.

If the central hole is opened, without changing other conditions, one set of the broken fringes of even modes changes into a set of continuous fringes but another set remains broken as shown in figure 13b. This result shows the suppression of oscillation in the even modes of the outer beams by the central beam. In other words, the gain for these modes reduces below the threshold because neon atoms are partly used to emit the photons of the central beam. Interaction between the two pairs of outer beams is not so distinct as is that between the central beam and the outer beam. It may be useful to evalute the intensity of the beams in order to understand the interaction. In case of a single beam laser, intensity is approximately proportional to the value $G-g$[6]. Here G and g are the gain per pass before and after laser action. Therefore, gain g can be written in the form $g=G-hI$, where h is a constant and I the intensity of the beam inside the cavity. In case of a three-beam laser, the following assumption may be made for a si nple treatment.

In portion A, of the tube in figure 14, the three be ams have common volume and interaction takes place. Beams 2 and 3 are degenerate in frequency and intensity. In portion B, they take different paths, therefore no interaction occurs.

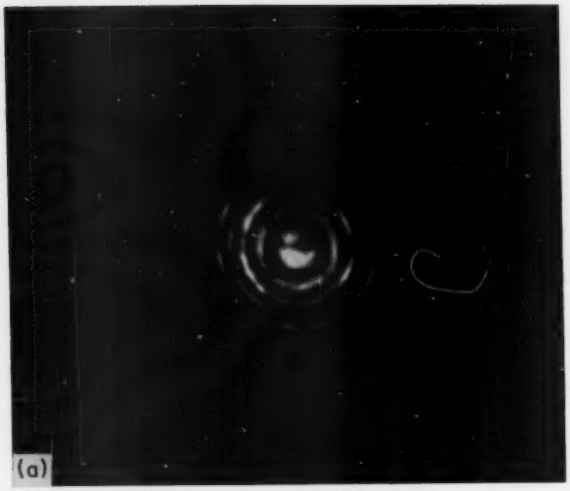

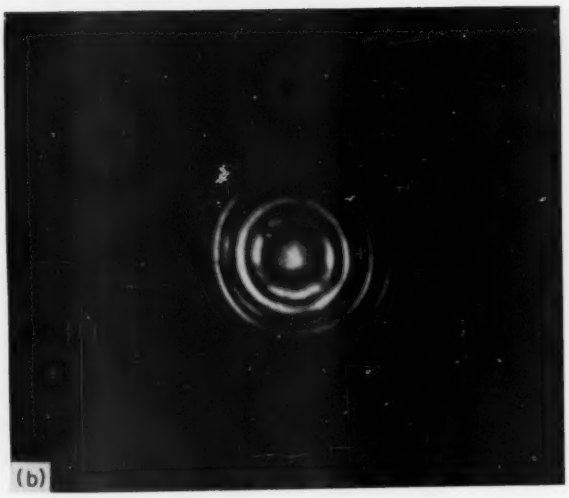

FIGURE 13. *Haidinger fringes with a 1-m Fabry-Perot etalon.* In (a), the top and bottom holes are open and in (b), the central hole is also open.

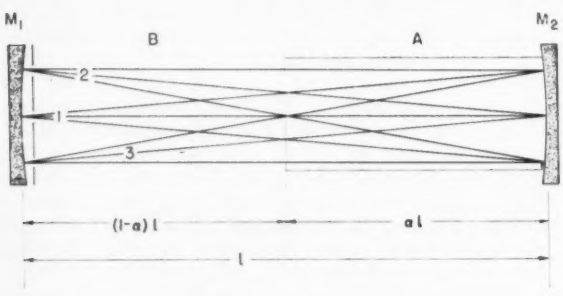

FIGURE 14. *Volumes* A *and* B, *with and without interaction of beams, in a three-beam laser.*

If the lengths of portions A and B are given by αl and $(1-\alpha)l$, respectively, l being the total length of the tube, the gain for beam 1 is given by

$$g_1=(1-\alpha)(G-hI_1)+\alpha\{G-h(I_1+2I_2)\}$$
$$=G-hI_1-2\alpha hI_2.$$

Here α will be called a coupling constant. Subscript 1 denotes the central beam; subscript 2 denotes the outer beams.

For beams 2 and 3, the gain is given by

$$g_2=G-\alpha hI_1-(1+\alpha)hI_2.$$

Now assume that laser oscillation takes place in all of the beams. Gains g_1 and g_2 will decrease as intensities I_1 and I_2 increase. They will become equal to the total energy losses L_1 and L_2 respectively, after the oscillation reaches equilibrium, that is

$$L_1=G-hI_1-2\alpha hI_2 \qquad \text{for beam 1}$$
$$L_2=G-\alpha hI_1-(1+\alpha)hI_2 \qquad \text{for beams 2 and 3.}$$

Solving the above equations, intensities I_1 and I_2 are given by

$$I_1=\{(1+\alpha)J_1-2\alpha J_2\}/(1-\alpha)(1+2\alpha)$$
$$I_2=(J_2-\alpha J_1)/(1-\alpha)(1+2\alpha)$$

where $J_1=(G-L_1)/h$, and $J_2=(G-L_2)/h$. Since intensity is positive, the following relation should be held

$$1/\alpha>J_1/J_2>2\alpha/(1+\alpha)$$

or

$$1/\alpha>(G-L_1)/(G-L_2)>2\alpha/(1+\alpha).$$

When $(G-L_1)/(G-L_2)\geq 1/\alpha$, the laser action takes place only in the central beam, with the intensity given by

$$I_1=(G-L_1)/h.$$

On the other hand, the action takes place in outer beams 2 and 3, with the intensity given by

$$I_2=(G-L_2)/(1+\alpha)h$$

when $(G-L_1)/(G-L_2)\leq 2\alpha/(1+\alpha)$. Figure 15 shows the criteria given by the above inequalities. Oscillation takes place only in the central beam when J_1/J_2 falls in region (a). It takes place in all the beams when J_1/J_2 falls in region (b), and in beams 2 and 3 when J_1/J_2 falls in region (c).

The value of α is approximately 0.6 for the laser used in this experiment. Therefore, $(G-L_1)/(G-L_2)$ should be larger than 1.67 in order to make J_1/J_2 fall in region (a) and thus suppress oscillation in the outer beams by the central beam. In the case of a five beam laser, similar treatment may be applied by using different values of α for each pair of beams, also by using different values of J. If the coupling constants are all the same, the intensities

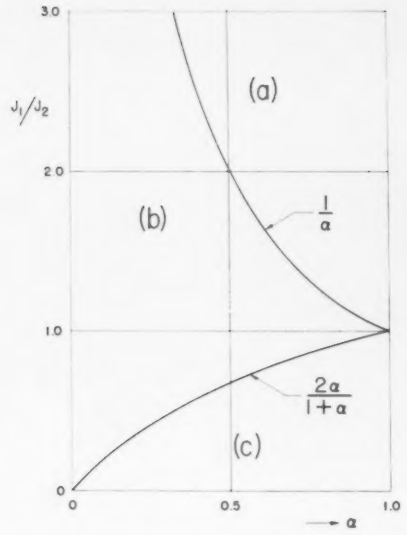

FIGURE 15. *Range of J_1/J_2 versus coupling constant α.*
In the region (a) only the central beam exists; in (b) the central and all outer beams exist; and in (c) only the outer beams exist.

of the beams are given by

$$I_1 = \{(1+3\alpha)J_1 - 2\alpha J_2 - 2\alpha J_3\}/(1-\alpha)(1+4\alpha)$$
$$I_2 = \{(2\alpha+1)J_2 - 2\alpha J_3 - \alpha J_1\}/(1-\alpha)(1+4\alpha)$$
$$I_3 = \{(2\alpha+1)J_3 - 2\alpha J_2 - \alpha J_1\}/(1-\alpha)(1+4\alpha).$$

Here, the subscripts 2 and 3 represent the top and bottom beams and the side beams respectively. From the above equations, the following condition is necessary to suppress the oscillation in the outer beams:

$$1/\alpha \leq 2J_1/(J_2+J_3).$$

b. Wavelength Relation

It is possible to adjust a five-beam laser so that single mode operation is achieved in each beam when the wavelength of the central beam lies approximately at the center of Doppler distribution. Figure 16 shows the Haidinger fringes obtained with a 50-cm Fabry-Perot etalon arranged similarly to the optical system in figure 12. The wavelengths are all different and the central beam is located between the outer beams. The wavelength separation between adjacent fringes is found to be approximately 2.5×10^{-3} cm^{-1}, equal to the mode separation of the outer beams. Figure 17 shows the mode relation between beams and the gain distribution of the laser tube with respect to wavelength, λ.

L_1 and L_2 are, respectively, the total energy losses in the central and outer beams. In the central region, A, the net gain, $G-L_1$, of the central beam is much higher than those of the outer beams, so that oscillation cannot take place in these beams. In the region, B, no mode exists in the central beam and interaction is observed only between the outer

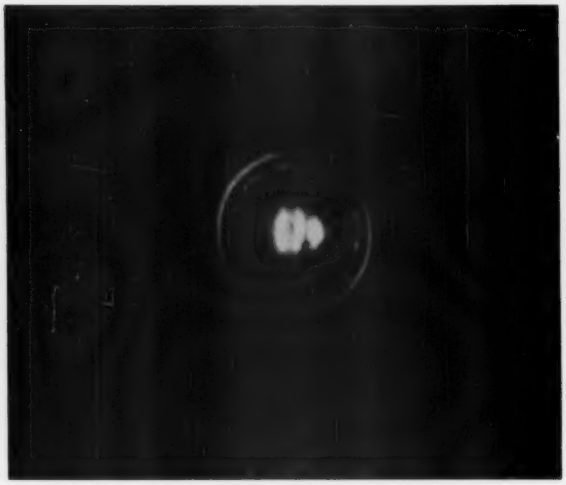

FIGURE 16. *Haidinger fringes showing single-mode operation in each beam.*

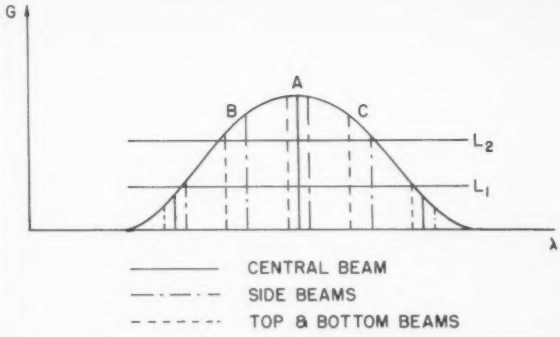

FIGURE 17. *Mode relation and gain distribution with respect to the wavelength corresponding to the fringes in figure 16.*
The region A corresponds to the mode of the central beam and the even modes of the outer beams. The regions B and C correspond to the odd modes of the outer beams.

beams. If $J_3/J_2 \geq (\alpha_{23}+1)/2\alpha_{23}$, the oscillation in the top and bottom beams is suppressed by the side beams. Here J_2 and J_3 are defined in the same way as in the previous section and α_{23} is the coupling constant between the two outer beams. The situation is reversed in the region C and oscillation takes place only in the top and bottom beams. When the effective cavity spacing changes due to, for example, the heat developed inside the tube, the wavelength relation changes as shown in figure 18. Here two modes are seen in the central beam and the modes of the outer beams lie in between, with approximately the same wavelength. The wavelength relation between these modes and the gain distribution are shown in figure 19. In region A, the ratio of J_3/J_2 is nearly equal to unity, so that both modes exist. In regions B and C only the central beam exists.

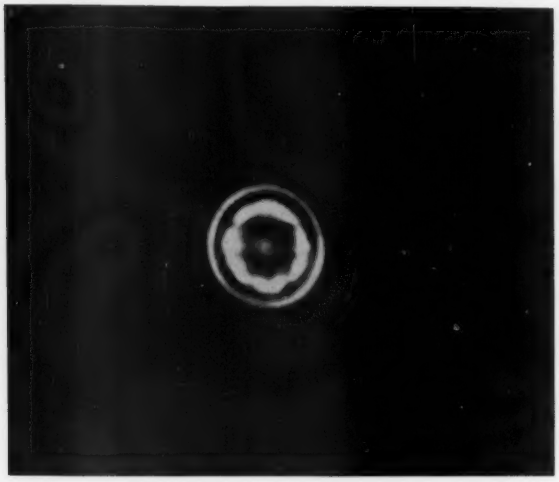

FIGURE 18. *Haidinger fringes showing two-mode operation in the central beam.*

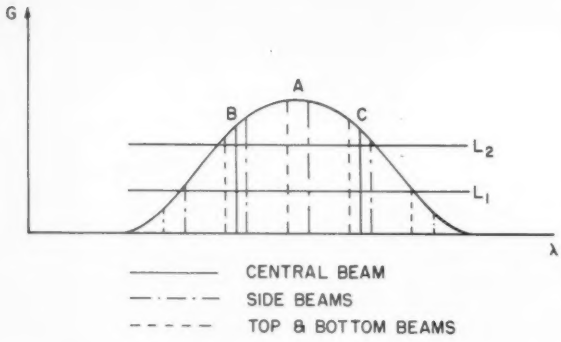

FIGURE 19. *Mode relation and gain distribution corresponding to fringes in figure 18.*

The region A corresponds to the odd modes of the outer beams. The region B and C correspond to the modes of the central beam and the even modes of the outer beams.

5. Wavelength Stabilization

It is possible for the laser to satisfy the following conditions by the use of a suitable diaphragm, and by the adjustment of both the position of the diaphragm and of the excitation energy for the laser medium.

1. The threshold value for the central beam must be low enough to supress the oscillation in the outer beams at the wavelengths almost equal to those of the outer beams.

2. This threshold value must be high enough so that single mode operation is attained when one of the modes is located approximately at the center of the laser line.

3. The outer beams must be kept in single modes, regardless of the change in the cavity spacing at least up to half a wavelength.

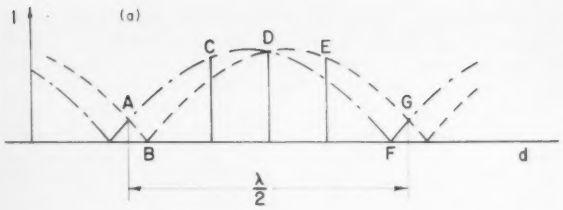

FIGURE 20a. *Intensity variation versus cavity spacing.*

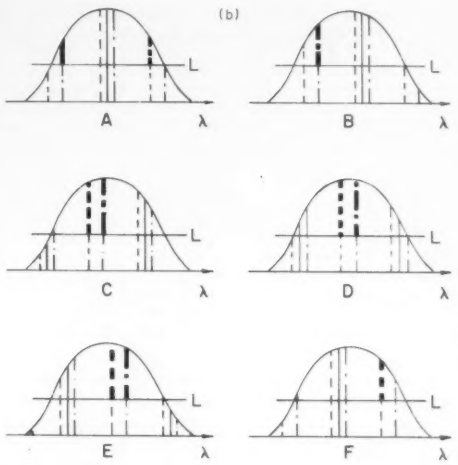

FIGURE 20b. *Mode relations at the spacings marked in (a).*

4. The intensities of the outer beams must not vanish at the same time.

These conditions are necessary to enable the outer beams to stabilize the wavelength of the central beam.

When the wavelength from a five-beam laser, with each beam in single mode, are located as shown in figure 17, the intensity of the side beams (3) in figure 2 increases and that of the top and bottom beams (2) decreases with a slight increase of the cavity spacing. They will change in a reverse manner with a slight decrease of the spacing. Figure 20a schematically shows the intensity variations with respect to the spacing, d.

This variation may be understood from figure 20b which shows the relations among the wavelengths, the gain distribution, and the threshold value, L, for the outer beams, at various spacings marked in figure 20a. Both intensities become equal at A and D. Between A and D, one of them is more intense than the other and this relation is reversed in the region between D and G. This effect can therefore be used to keep the spacing at A or G by means of a negative feedback. Thus the wavelength of the central beam can be kept approximately at the center of the gain distribution, if the spacing of the cavity is controlled

712-378—64——3

to be held at A. A phase plate can be inserted within the cavity, instead of making use of aberration in the Brewster's angle windows, in order to produce the mode relation shown in figure 20b. In this case, it is possible to bring the wavelength to the center of the Doppler distribution with either optical or electronic means. The reproducibility of the wavelength depends mainly upon the intensities of the beams. In this respect, a further experiment is to be carried out.

The author expresses his sincere thanks to K. F. Nefflen for his technical assistance throughout these experiments and for reviewing this paper and to K. D. Mielenz for helpful discussions.

6. References

[1] A. Javan, E. A. Ballik, and W. L. Bond, J. Opt. Soc. Am. Letters **52,** 96 (1962).
[2] T. S. Jaseja, A. Javan, and C. H. Townes, Phys. Rev Letters **10,** 165 (1963).
[3] G. Gould, Frequency **1,** 14 (1963).
[4] G. D. Boyd and J. P. Gordon, Bell System Tech. J. **40,** 489 (1961).
[5] A. G. Fox and T. Li, Bell System Tech. J. **40,** 453 (1961).
[6] W. R. Bennett, Jr., W. L. Faust, and R. A. McFarlane, Their work has been referred to on page 29 in the article by W. R. Bennett, Jr. in Supplement on Optical Masers, Applied Optics (1962).

(Paper 68C1–149)

JOURNAL OF RESEARCH of the National Bureau of Standards—C. Engineering and Instrumentation
Vol. 68C, No. 1, January–March 1964

Principles of Cryometric Impurity Determination as Applied to Samples of Small Sizes

Charles P. Saylor and Gaylon S. Ross

(October 21, 1963)

A consideration of the factors that tend to prevent attainment of thermal and thermodynamic equilibrium during thermometric methods of purity analysis suggests that the problems largely originate from spontaneously introduced inequalities in composition. During either a freezing or melting cycle, the solid phase settles in the liquid. This results in a greater average purity in the bottom than in the upper part of the vessel. The effects would be particularly strong during a melting sequence where the liquid released by melting of the solid would provide the compositional environment for the establishment of final temperature. This hypothesis has been tested by the design of a new cell for small samples. The design incorporates use of small gold pans to hold solid and liquid in close contact. The results are comparable in precision to those from conventional time-temperature curves with much larger samples, a condition not ordinarily possible with small samples.

1. Introduction

Cryometric techniques capable of accurate determinations of purity have been developed. When samples as large as 40 to 100 ml are used, the procedures available at the present time reduce successfully the errors resulting from imperfect attainment of equilibrium, both thermal and thermodynamic. These errors become progressively larger, however, with decreasing size of the sample. It was our purpose in this investigation to analyze the errors that persist in the ordinary large scale determinations of purity and also to alter the procedures in such a way that sufficient accuracy could be attained even with drastically reduced samples.

2. Principles

When a system is surrounded by, but relatively well-insulated from, a constant-temperature environment, the rate of loss or gain of heat by the system will be essentially constant, providing the difference in temperature between the system and the environment is very large with respect to the temperature change taking place within the test system. If there are no chemical reactions or phase transitions, the temperature of the system will change at a rate inversely proportional to the product of the specific heat of the system and the mass. In cryometry the system consists of a sample contained in a closed cell. As long as the sample is completely liquified, or fully solidified, the above relationship holds. However, when freezing or melting begins, the rate of change in temperature will be reduced because of the latent heat of the sample.

As long as compositional, thermal, and thermodynamic equilibrium are maintained and nothing occurs to disturb the uniform loss of heat from the sample container to its environment, the curve of temperature as a function of time during a freezing or melting sequence will be close to the hyperbolic form. One asymptote of this hyperbola will correspond to the melting point of the pure substance, and the other asymptote will represent the cooling rate of the solidified sample and the cell. A slight imperfection in the hyperbola is caused by the fact that the specific heat contribution during freezing is influenced proportionally by the specific heat of both the portion of the sample that is liquid and the portion that is solid. When the form of this hyperbola has been established, the intersection of the curve with the liquid line gives the melting point of the actual sample. The difference between freezing temperature of the sample and the calculated freezing point of the pure material is proportional to the mole fraction of impurity in the sample.

Influences that decrease the accuracy of this method during a freezing sequence are as follows: (1) Crystallization does not begin as soon as the freezing point is reached since some supercooling is unavoidable. Because of this supercooling, the rise in temperature after the onset of crystallization is not instantaneous and equilibrium temperature values are slowly approached. Since the heat from crystallization is proportional to the amount of solid produced and this amount of solid is in turn approximately proportional to the second power of the supercooling, recovery can never be complete, and the rate of approach to equilibrium becomes progressively slower. A large part of the curve is affected, and the error is particularly serious with very pure samples. (2) As crystallization advances, the total volume of the sample decreases. This decreases the total surface of the sample capable of radiating heat to the surrounding space and causes temperatures during the latter part of the freezing

experiment to be high. (3) During crystallization some of the solid forms on the wall of the container. Since this is less heated by the release of latent heat, it becomes colder than the rest of the sample. From this effect, at later times in the run, the recorded temperatures will tend to be high. (4) In unstirred systems the distribution of the solid throughout the cell may markedly change the thermal conduction pattern throughout the freezing. Further, in stirred systems, an increasing proportion of solid in the solid-liquid mixture increases the resistance to stirring, causing the stirring energy to increase and the observed temperatures to be high.

When the direction of this procedure is reversed, i.e., when a frozen sample is melted, there are a different group of factors which interfere with the accuracy of results. As we interpret the situation, these principal effects are as follows: (1) The solid, being more dense than its own liquid phase (except for ice and a few other materials) melts loose from the container and settles to the bottom. This is true even for stirred samples when stirring is achieved in the usual fashion. As a consequence, the heat sink created by the latent heat of fusion will be at the bottom of the container where the temperature will not rise above the equilibrium value. However, in the upper parts of the sample there will be little or no solid phase and the temperature here will tend to be higher than the thermodynamic equilibrium temperature for the complete sample. This effect, present from the beginning of the melt, would tend to distort the hyperbolic curve as so to decrease the final estimate of the difference between the actual melting point of the sample and that of the pure material. (2) As a consequence of the segregation of solid and liquid, the composition of the liquid phase is not homogeneous, unless the process is run very slowly. Since the liquid immediately surrounding the pure solid must necessarily be more pure than the bulk liquid, the local equilibrium temperature between solid and liquid in the vicinity of the solid will be high. This effect also would decrease the apparent steepness of the observed melting curve and so decrease the estimate of impurity in the sample. While this difficulty can be minimized by employing extremely slow melting, errors which result from the slower rate now tend to be more significant. (3) Ordinary techniques of stirring are not a feasible means of achieving compositional equilibrium since the solid is originally united in one piece and does not melt so as to fall apart. Inadequate stirring fails to abolish the inhomogeneity mentioned in (2) above.

Most precision calorimeters used for the determination of purity employ a metal vane system to provide temperature equality. Some calorimeters have vertical vanes all directed radially toward the thermometer well whereas others have parallel horizontal vanes normal to the axis of the well. The horizontal vane system would seem to be more suitable in that the vanes tend to keep the solid suspended throughout the cell and in intimate contact with the liquid. With the vertical vanes it is at least conceivable that all the solid would be at the bottom and all the liquid in the top portion of the well, making both thermal and compositional equality difficult to maintain. Even with the horizontal vanes there will be a tendency, during the contractions that accompany freezing, for the liquid to run off the upper vanes leaving the solid out of contact with the liquid during a significant amount of the freezing or melting process.

The principal difference between these vane systems and that described in this paper lies in the construction of the horizontal vanes. Instead of being flat disks, they are pans, arranged on a central support. In operation, each pan holds its own volume of material while maintaining thermal contact with the rest of the system throughout the central support. Now, despite volume changes, each pan represents in miniature what must be taking place in the other pans; each by holding both the solid and liquid phases in thin, horizontal sheets maintains good compositional and thermal contact. We anticipated that the experiments would confirm the attainment of a uniform solid-liquid equilibrium throughout the system during both freeze and subsequent melt.

3. Apparatus

In figure 1 is shown a portion of the cell, enough to illustrate the form and use of two of the pans. As represented, the sample is being melted. During the freezing process the sample contracts so that the space between the pans is no longer entirely filled. During the remelting, the liquid flows over the remaining solid, submerging it without anywhere permitting a large separation between the liquid and the solid from which it has formed.

The amount of sample used is such that, when all liquid is at its freezing point, the quantity of sample is just sufficient to cover the top pan. This corresponds to 1½ ml of sample in our case. Figure 3 depicts the

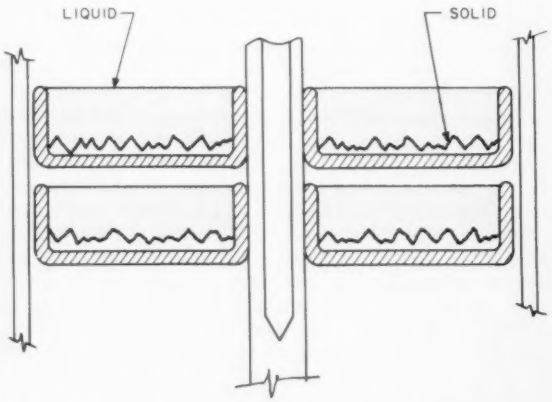

FIGURE 1. *Section of cell showing two pans.*
The pans are made from a soft gold sheet and are gold-soldered to the platinum support.

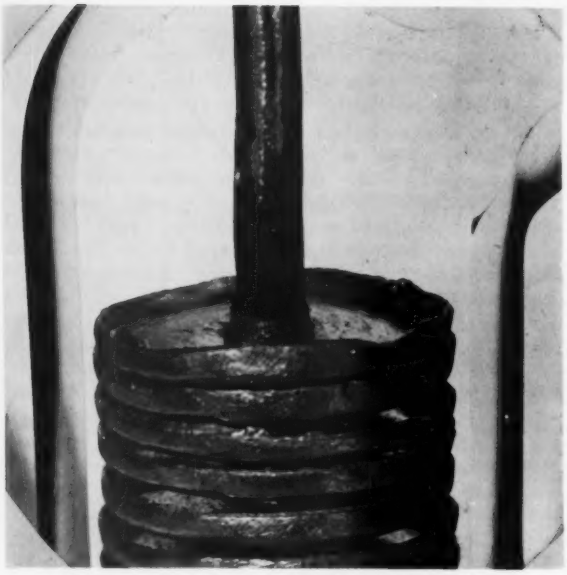

FIGURE 2. *Photomacrograph of cell details, ×5.5.*

The cell has been filled with 1,2-dibromoethane (refractive index about 1.54) and immersed in the same liquid. This has limited distortions that would have been caused by the glass envelope (refractive index about 1.51) and significantly increased depth of focus. The inner surface of the glass tube is only dimly shown.

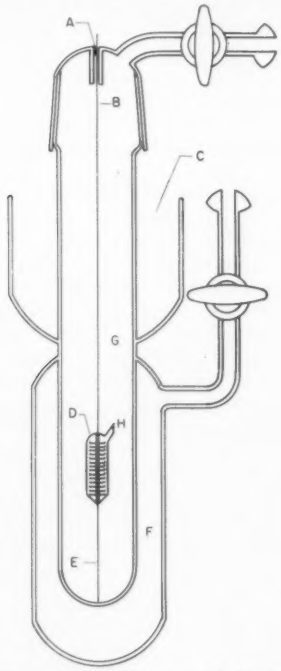

FIGURE 3. *Cryometric cell and its container.*

A. Vacuum-tight seal of cell container and thermocouple leads. Seal made with soft wax.
B. Thermocouple leads.
C. Well for thermostating liquid. Used to prevent heat leak down sides of wall.
D. The glass envelope of the cell.
E. Glass fiber to hold the cell in place.
F. Outer vacuum jacket.
G. Inner vacuum jacket.
H. Fused seal. Originally point at which cell was connected to transfer manifold.

normal assembly of the cell in its container. A 1.5 mm platinum rod, drilled so as to hold the thermocouple, serves as the support for the pans. These pans are made from 0.0006 in. sheet gold and are gold-soldered to the platinum rod. The rod is sealed into the thin-walled, soft-glass cell as shown. An insulated, copper-constantan thermocouple (No. 36 B & S wire) is inserted into the platinum support rod, and is secured to the rod with epoxy resin. The only cell supports are the copper and constantan wires, which are sealed at point (A) as they leave the container. The cell is centered and restrained from large oscillations by a thin glass fibre cemented to the bottom of the cell and the bottom of the inner container. All the interior surfaces of the container are silvered, as is the outside of the cell.

A water-ice triple-point cell is used to provide the reference junction temperature, and a thermally and electrically insulated potentiometer is used to balance the junction emf. The signal from the potentiometer is amplified and recorded on a potentiometric, strip-chart recorder. The amplifier and recording system have been previously described [1].[1]

4. Experimental Procedure [2]

The thermocouple was calibrated by comparing the junction emf with the temperature as determined with a calibrated platinum resistance thermometer while both sensing devices were being used to record simultaneously the freezing curve of a 50 ml sample of benzene. The thermometric cell and experimental details of this calibration are described in reference [2].

The cell was then sealed into a glass transfer manifold similar to that described previously [2]. After thorough evacuation of the manifold, a degassed benzene sample was distilled into the cell. The sample was frozen by immersion of the cell in a cold bath, and the cell was removed from the manifold by flame-fusion at (H).

The cell was assembled in its container as shown in figure 2, and the sample was frozen and cooled to −45 °C. Both of the vacuum jackets were evacuated, and the container was transferred to a water bath whose temperature was held constant. The well (C) was filled with a water-ice mixture to prevent any heat leak down the container wall.

The solid-warming rate was adjusted by varying the pressure in the two vacuum jackets. During the warming of the solid, time versus temperature recordings were made. The melting curves were recorded automatically using the programming sequences described in reference [2, 3]. One of the melting curves is shown in figure 4.

The end result of the time-temperature melting (freezing) experiment is, of course, the determination of the purity of the sample. The analyst must determine two numbers: T_f, the freezing point of the particular sample, and T_{f_0}, the freezing point of the

[1] Figures in brackets indicate the literature references at the end of this paper.
[2] The experimental procedure described herein is specifically that used with the benzene samples but of course could be generalized to apply to any sample.

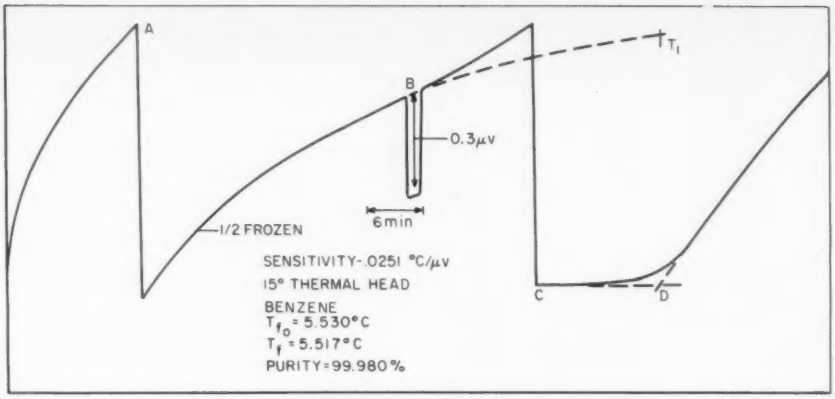

FIGURE 4. *Programmed freezing curve.*

A. Position at which zero of recorder was automatically shifted.
B. 0.3 μv signal used to determine experimental sensitivity.
C. Automatic reduction of amplification.
D. Intercept of melting curve and liquid warming line.

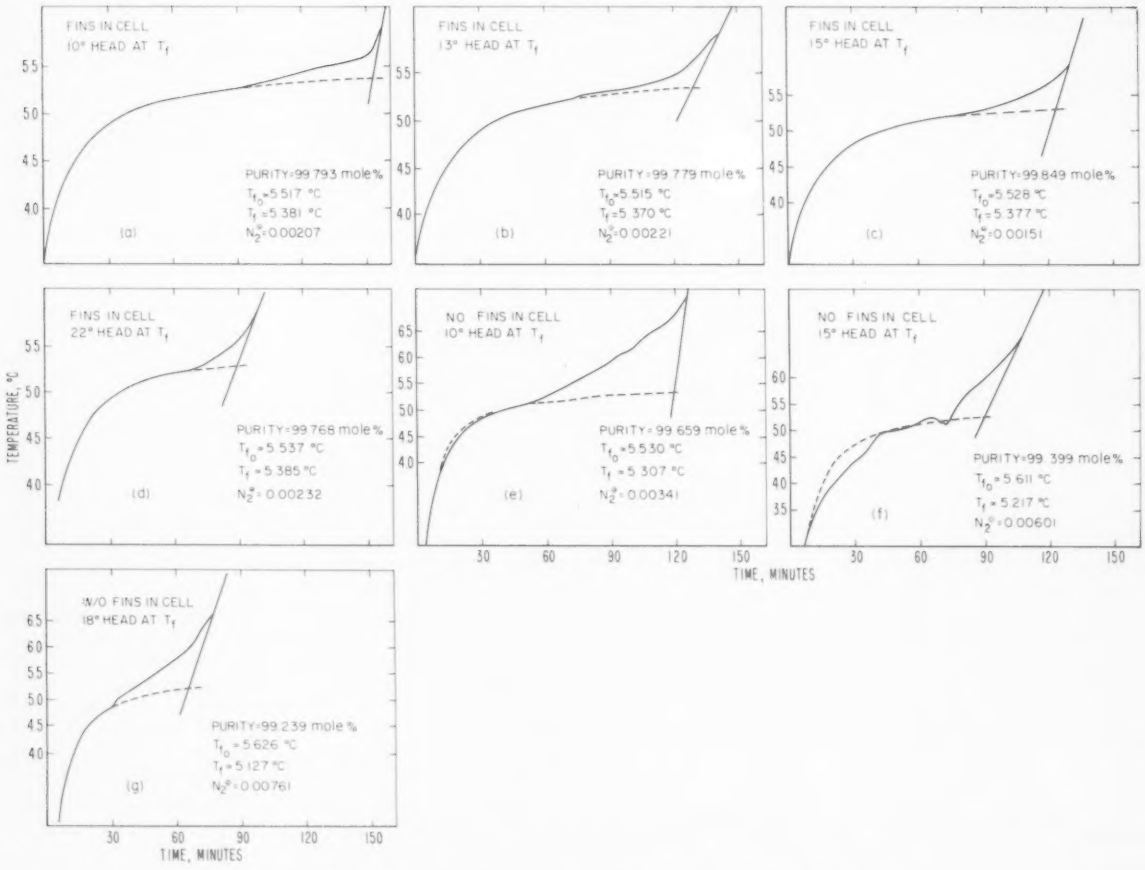

FIGURE 5. *Melting curves obtained using the two types of small cell.*

Benzene with a known purity of 99.79+ mole percent was used in both cells. Figures 5 (a,b,c,d) represent experiments conducted in cell with pan-shaped gold fins. Figure 5 (e,f,g) show experiments conducted in a cell without conducting vanes. In these experiments the difference between T_f and T_{f_0} is much more accurate than their absolute values.

pure material. Under the assumptions made in section 2, the time-temperature melting curve is hyperbolic, where T_f represents the intersection of the hyperbola with the liquid-warming curve and T_{f_0} represents the temperature corresponding to the horizontal asymptote of the hyperbola. One of the better ways of analyzing the experimental data lies in the direct comparison of the experimental curve with that of a mathematically exact hyperbola [4]. In this optical projection method, the mathematically exact hyperbola is projected, by means of a photographic enlarger, upon the experimental curve. By increasing or decreasing the magnification and shifting parallel to the coordinates, the best fit is obtained. Sufficient information is projected with the hyperbola so that the analyst can determine both T_f and T_{f_0}. The optical projection technique was used on all the curves included in this paper. The real, experimental curve is shown as a continuous line, whereas the projected hyperbolic function is dotted.

Two differrent samples of benzene were analyzed. In the first sample the purity as determined by the method described herein was compared with the purity as determined by time-temperature analysis using a 50-ml sample [2, 3]. When the second sample was analyzed a portion of the sample was placed in the small, gold-vaned cell and another identical portion was distilled into an all-glass cell, similar in shape and size. The all-glass cell differed only in that the thermocouple well was of glass and in that there were no conducting vanes of any kind. The construction of this type of cell has been described by Skau [5].

5. Discussion and Results

When the first sample was analyzed, two different thermal heads were used, namely 20 and 10 deg. The thermal head describes the difference in temperature between the constant-temperature warming bath and the melting point of the sample. The results of these analyzes were, respectively, 99.98_5 and 99.98_0 mole percent. When 50 ml of the sample was analyzed thermometrically [3], the purity was calculated to be 99.97_6 mole percent.

There was available for this work a sample of benzene contaminated with *n*-heptane. In an IUPAC project on purity analysis, the purity of this particular sample was known to be 99.79_7 mole percent. Four runs were made with a portion of this material in the gold-vaned cell, and three runs were made in the similar all-glass cell. A variety of thermal heads was employed. The curves are shown in figure 5. T_f and T_{f_0} were independently determined on each curve; the difference between their numbers in each case is more accurate than the absolute value of either. It is evident that with the cell containing the vanes a larger portion of the melt is at temperatures represented by the assumed hyperbola and that the calculated purities correspond much more nearly to the reference value. A tabulation of these results is given in table 1.

We believe that, within the limitations of the test, the gold-vaned cell and apparatus described are capable of approximately the same degree of accuracy as that obtainable from systems employing samples of much larger size. Further, the accuracy which appears to have been obtained with this apparatus is thought to be largely the result of the pan-shaped conducting vanes. We interpret this as a substantiation of the principle of avoiding the transfer of liquid away from the solid from which it has melted. If this is correct, it would seem that the incorporation of the principle into larger adiabatic calorimeters would permit shorter equilibration times and result in the attainment of better thermodynamic equilibrium.

TABLE 1. *Purity analysis of second benzene sample**

Cell [a]	Thermal head	T_{f_0}	Calculated values	
			T_f	Purity
	°C			*Mole %*
1	10	5.517	5.381	99.793
1	13	5.515	5.370	99.779
1	15	5.528	5.377	99.849
1	22	5.537	5.385	99.768
2	10	5.530	5.307	99.659
2	15	5.611	5.217	99.399
2	18	5.626	5.127	99.239

*Actual purity of sample was known to be 99.797 mole %.
[a] Cell (1) is the gold-vaned one and (2) is the all-glass one.

6. References

[1] G. S. Ross and H. D. Dixon, J. Research NBS **64C** (Engr. and Instr.) No. 4, 271–275 (1960).
[2] A. R. Glasgow, Jr., G. S. Ross, A. T. Horton, D. Enagonio, H. D. Dixon, C. P. Saylor, G. T. Furukawa, M. L. Reilly, and J. M. Henning, Anal. Chim. Acta **17,** 54 (1957).
[3] G. S. Ross and H. D. Dixon, J. Research NBS **67A** (Phys. and Chem.) No. 3, 247–251 (1963).
[4] C. P. Saylor, Anal. Chim. Acta **17,** 36 (1957).
[5] E. L. Skau, J. Phys. Chem. **37,** 609 (1933).

(Paper 68C1–150)

JOURNAL OF RESEARCH of the National Bureau of Standards—C. Engineering and Instrumentation
Vol. 68C, No. 1, January–March 1964

Reference Tables for Thermocouples of Iridium-Rhodium Alloys Versus Iridium

G. F. Blackburn and F. R. Caldwell

(September 11, 1963)

The program at the National Bureau of Standards to establish reference tables of temperature versus emf for thermocouples of iridium-rhodium alloys versus iridium has been extended to cover all three of the currently used thermocouples of this type. In addition to the values published in 1962 for the 40 Ir-60 Rh versus Ir thermocouples, tables now are available for thermocouples of 60 Ir-40 Rh and 50 Ir-50 Rh versus Ir. These tables give emfs for temperatures in degrees Celsius from 0 to 2150 °C and in degrees Fahrenheit from 32 to 3900 °F, and temperatures in these units with emf in millivolts as the argument.

In addition to the reference tables for these thermocouples, temperature-emf relationships are presented for other alloys containing 10, 25, 75, and 90 percent iridium versus iridium. It appears from the information obtained on all of the alloy versus iridium combinations tested that the 50 Ir-50 Rh alloy versus iridium gives about the maximum thermal emf (12.2 millivolts at 2150 °C), and as a result may provide the optimum thermocouple combination of this type.

1. Introduction

A program to establish reference tables of thermal emf of a number of alloys of iridium and rhodium versus iridium has been in progress at the National Bureau of Standards for several years. Tables for 40 percent iridium-60 percent rhodium versus iridium were published in 1962 [1].[1] The present paper includes tables for all the other alloys of the series studied at NBS viz, 10, 25, 40, 50, 75, and 90 percent rhodium.[2]

2. Apparatus and Procedure

The apparatus and procedure have been described previously [1]. Briefly, measurements of thermal emf were made at temperatures up to 2500 °F [3] (2000 °F in a few cases) using a conventional platinum-wound furnace. Temperatures in the furance were measured with a platinum-10 percent rhodium versus platinum thermocouple. Temperatures above the limit of this furnace were obtained in an iridium blackbody heated by electrical induction. A conventional optical pyrometer, modified to permit finer adjustment of current through the lamp filament, was used to measure temperature. The calibration of the pyrometer gave temperature as a function of lamp current.

Each thermocouple wire was annealed before testing by heating it electrically in air for about 1 min at approximately 400 °F below its melting point. The junction was welded in an oxyacetylene flame.

[1] Figures in brackets indicate the literature references at the end of this paper.
[2] For brevity, the expression "25 percent Rh," for example, will be used to indicate a thermocouple in which the positive leg is 75 percent Ir-25 percent Rh, and the negative is iridium.
[3] Degrees F (Fahrenheit) are based on the International Temperature Scale of 1948.

3. Thermocouples

Table 1 is a list of the thermocouples used, in order of increasing percentage of rhodium in the alloy leg. The letter in a thermocouple number designates the lot from which the wire was taken, and refers to a particular shipment received from the manufacturer. The first digit refers to the composition of the alloy as follows: 1 signifies 10 percent; 2, 25 percent; 4, 40 percent; 5, 50 percent; 7, 75 percent; and 9, 90 percent rhodium. The last two digits are the wire diameter in thousandths of an inch. Three lots of wire (A, D, and F) were supplied by the Sigmund Cohn Corporation, and two (C and G) by Engelhard Industries, Inc. Since lot D consisted of alloy wire only, iridium to pair with alloy wires from this lot was taken from other lots.

TABLE 1. *Description of thermocouples*

Percent Rh	Thermocouple No.	Diameter of wire in.	Manufacturer
10	A135	0.035	Sigmund Cohn
	G120	.020	Engelhard
25	A235	.035	Sigmund Cohn
	G220	.020	Engelhard
40	A435	.035	Sigmund Cohn
	C420	.020	Engelhard
	[1] D420C	.020	Sigmund Cohn
	[2] D435B	.035	Sigmund Cohn
50	A535	.035	Sigmund Cohn
	F530	.030	Sigmund Cohn
	F520	.020	Sigmund Cohn
75	A735	.035	Sigmund Cohn
	G720	.020	Engelhard
90	A935	.035	Sigmund Cohn
	G920	.020	Engelhard

[1] Iridium wire from lot C.
[2] Iridium wire from lot B (comprising 60 Rh and Ir wire).

712-378—64——4

4. Computations

For each alloy tested, the emf at a given temperature was taken as the average of the emfs of the different lots of that alloy. However, if a lot contained wires of more than 1 diam, the emf of each size wire was used as if it represented a different lot. For example, the emf for the 40 percent Rh thermocouple was taken as the average of the emfs of four: lot A, lot C, and the two wire sizes of lot D. With one exception each lot was represented by one thermocouple of a given alloy. Two thermocouples were used from lot C, and the mean of the emfs was taken as the emf for the lot.

The data for the alloys 25, 40, 50, and 75 percent rhodium were processed by the Computation Section of the NBS Applied Mathematics Division. An IBM 7090 Computer, employing programing procedures called OMNITAB [2], was used. With the object of finding a functional relation between emf and temperature such that tables could be generated entirely by a digital computer, trials were made in fitting polynominals of various degrees to the observed emfs for the 40 percent Rh thermocouple. It was determined that the data could be adequately represented by two equations, one of fourth degree for the range 32 °F to 1000 °F, the second of fifth degree for the range 1000 to 3900 °F. In computing the equation for the high range, the data from 1000 to 2500 °F were weighted 10 times those above 2500 °F, to take account of the higher precision that could be achieved at the lower temperatures.

The emf given for 32 °F by the equation for the lower range was less than 1 μv, and the difference between the emfs given by the two equations at the range juncture was also less than 1 μv. Deviations from observed emfs were randomly distributed, and were small—less than 5 μv at temperatures up to about 3000 °F, and only a few were over 10μv at the highest temperatures. Evidently, the equations as computed represented the observed data adequately, and could be used to generate the desired tables. However, it seemed desirable that the equation yield zero emf at 32 °F; and since this could be accomplished by changing the constant term by a fraction of a microvolt, this change was made. Similarly, the equation for the upper range was made to yield the same emf at the juncture of the two ranges as the modified equation for the lower range by changing the constant term slightly.

The procedure followed for the 40 percent Rh was found equally suitable for the 25, 50, and 75 percent Rh thermocouples. No change was as great as 1 μv except that for the 75 percent Rh thermocouple, which was 1.4 μv at 1000 °F.

The equations for the upper and lower ranges did not give the same value of dE/dT at the juncture for any of the thermocouples. However, they were so nearly the same that the equations yielded the same emf to within 1 μv at temperatures up to 20 °F on either side of the juncture.[4]

[4] It is feasible to use a computer program which performs the curve fitting in such a way that the conditions to be satisfied include zero emf at 32 °F and equality of both the emfs and the first derivatives at the juncture of the ranges.

5. Results

The derived polynominal equations were used to generate tables of emf with °F as the argument (values in tables 4–A, 8–A, and for the alloys 25 and 75 percent Rh in table 9–A). The coefficients of these equations are listed in table 2. For the 40 percent Rh and 50 percent Rh, the tables are fully developed, giving temperature in °C and °F with emf in 0.01-mv increments as the argument, and emf with °C and °F as the argument, in 10-deg increments. The computer techniques involved conversion from °C to °F and interpolation.

Table 9–A gives emfs for the 10, 25, 75, and 90 percent Rh thermocouples in 100 °F increments.

Electromotive force versus temperature curves for the alloys considered in this study are shown in figure 1. Figure 2 is a plot of dE/dT, derived by machine computation except for the 10 and 90 percent Rh thermocouples. Figure 3 shows the variation of emf with composition of the alloy leg for temperatures 2000, 2500, 3000, and 3500 °F. The emf at 2000 °F for 100 percent Rh is found from data by Caldwell [3] for Rh versus Pt27, together with a table of emfs for Ir versus Pt27 given in reference [1]. The point at 2500 °F is an extrapolation of Caldwell's data.

If the cold junction is at a temperature higher than 32 °F, the appropriate correction can be found by interpolating in the tables, or by the use of the corresponding equation. For the case where copper lead wires are used with the 40 or 50 percent Rh thermocouple the correction can be obtained from table 10–A, which gives the emfs of these alloys and iridium

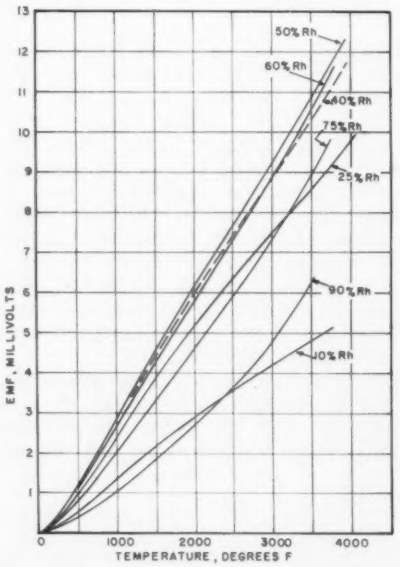

FIGURE 1. *Thermal emf of iridium-rhodium alloys against iridium.*

TABLE 2. *Values of coefficients in the equation*

$$E = A + BT + CT^2 + DT^3 + ET^4 + FT^5$$

*for four IrRh versus Ir thermocouples**

Coefficient	60 Ir-40 Rh		50 Ir-50 Rh	
	32 °F to 1000 °F	1000 °F to 3900 °F	32 °F to 1100 °F	1100 °F to 3900 °F
A	−0.052816	−0.353350	−0.054717	−0.143581
B	1.581377·10⁻³	2.406678·10⁻³	1.640880·10⁻³	1.877703·10⁻³
C	2.196393·10⁻⁶	1.366226·10⁻⁶	2.193392·10⁻⁶	1.981642·10⁻⁶
D	−1.136843·10⁻⁹	−0.791802·10⁻⁹	−1.127263·10⁻⁹	−1.091919·10⁻⁹
E	−0.204061·10⁻¹²	.178246·10⁻¹²	−0.202907·10⁻¹²	0.251008·10⁻¹²
F		−.013826·10⁻¹⁵		−.020415·10⁻¹⁵
	75 Ir-25 Rh		25 Ir-75 Rh	
	32 °F to 1000 °F	1000 °F to 4000 °F	32 °F to 1000 °F	1000 °F to 3700 °F
A	−0.043211	−0.110871	−0.036808	−0.031682
B	1.284913·10⁻³	1.449150·10⁻³	1.101287·10⁻³	.979634·10⁻³
C	2.079622·10⁻⁶	1.954721·10⁻⁶	1.552051·10⁻⁶	1.879813·10⁻⁶
D	−1.090633·10⁻⁹	−1.097890·10⁻⁹	−0.683930·10⁻⁹	−1.042899·10⁻⁹
E	0.193374·10⁻¹²	0.249149·10⁻¹²	.092373·10⁻¹⁹	0.263564·10⁻¹²
F		−.020193·10⁻¹⁵		−.023458·10⁻¹⁵

*E is emf in millivolts; T is temperature in degrees Fahrenheit.

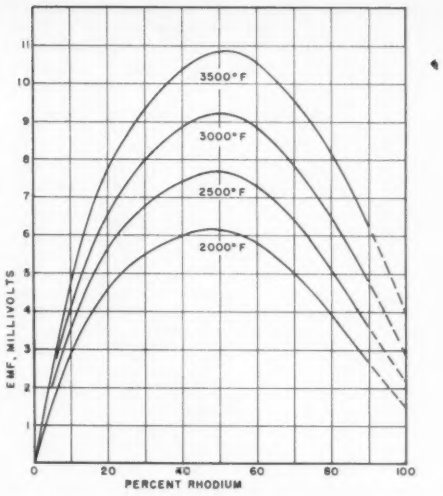

FIGURE 3. *Variation at constant temperature of thermal emf with percent rhodium in the alloy legs of iridium-rhodium versus iridium thermocouples.*

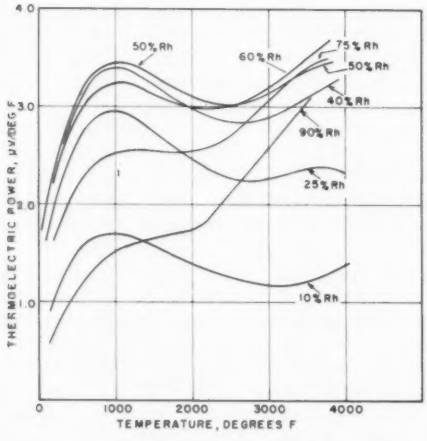

FIGURE 2. *Thermoelectric power of iridium-rhodium alloys against iridium.*

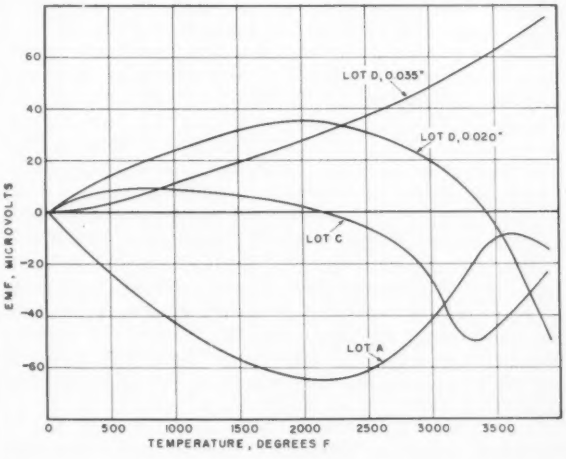

FIGURE 4. *Emf differences between the lots of 40 percent rhodium and the corresponding table values.*

(Thermocouple minus table values.)

versus copper for temperatures to 500 °F. This table is particularly useful when the two reference junctions of the thermocouple are at different temperatures.

6. Discussion

The maximum difference in emf between thermocouples of a given alloy occurred at the highest temperature associated with each alloy. This maximum for any alloy was that for the 40 percent Rh thermocouple, about 120 μv. This is comparable to the difference observed earlier for the 60 percent Rh, and is not considered unduly large. The emf differences for the four 40 percent Rh lots are plotted in figure 4. For comparison of thermal emfs from other sources, table 3 gives emfs from the present work and those of Zysk [4], and of Sine [5] as reported by Caldwell [6]. The largest difference is about 250 μv at approximately 1800 °F between Sine's and the NBS values. This corresponds to a temperature difference of about 80 °F, which is about twice the difference found between lots at NBS.

TABLE 3. *Emf of 60 percent* Ir-40 *percent* Rh *versus* Ir *thermocouples*

Temperature	NBS	Zysk	Sine
°F	*Millivolts*	*Millivolts*	*Millivolts*
200	0.342		0.32
400	.864		.82
600	1.468		1.39
800	2.119	2.101	2.00
1000	2.792	2.764	2.62
1200	3.469	3.433	3.26
1400	4.131	4.102	3.90
1600	4.775	4.741	4.53
1800	5.397	5.357	5.15
2000	6.000	5.956	5.76
2200	6.586	6.540	6.36
2400	7.159	7.106	6.95
2600	7.726		7.54
2800	8.291		8.14
3000	8.862		8.77
3200	9.444		9.42
3400	10.040		10.09
3600	10.653		10.78
3800	11.284		

For the 50 percent Rh thermocouple the maximum difference between lots was about 80 μv. The deviations from the table values were more regular than those for the 40 percent Rh thermocouples and increased to as much as 40 μv at 3900 °F. The deviations of lot A and those of the 0.030-in. wire of lot F were numerically about equal, and of opposite sign, while the emf of 0.020-in. wire of lot G was within 6 μv of the table values throughout the range.

As has been mentioned in a previous section and indicated in table 1, the alloys 10, 25, 75, and 90 percent Rh were each represented by two lots of wire. The maximum differences between their thermal emfs and the equivalent temperature differences are listed in table 4. For the 10 and 25 percent Rh the maximum differences occurred at a temperature under 2000 °F, lot A producing a higher output than lot G. With increasing temperature the differences diminished, until equal outputs were obtained from the two lots, at about 3350 °F for both compositions. For the 75 and 90 percent Rh the emf of lot G was lower than that of lot A at all temperatures, as indicated by the negative signs in table 4.

TABLE 4. *Maximum difference in thermal emf between thermocouples of lots A and G*

	Percent Rh			
	10	25	75	90
Maximum difference, μv	236	108	−180	−195
Equivalent temp. difference, °F	166	42	−52	−65
Temperature at maximum difference, °F	1900	1700	3700	3500

The output of 40 percent Rh is the same as that of the 60 percent Rh at about 3000 °F. Below that temperature the 40 percent Rh has a higher emf than the 60 percent Rh; above 3000 °F its emf is less. As the slopes of the emf-temperature curves for these two alloys do not differ greatly, the temperature at which equal emfs are observed may vary considerably from one thermocouple to another of the same nominal composition.

As was noted in the discussion of the work on the 60 percent Rh [1], several sources of error make increasingly large contributions to the uncertainty of the emfs obtained at temperatures above about 3500 °F. They combine to produce an uncertainty estimated not to exceed ±12 °F at the highest temperature.

The alloys of most interest from the standpoint of usefulness are the 40, 50, and 60 percent Rh. While the present work has not yielded results on which a definite preference can be based, the 50 percent Rh would seem to be a logical choice, inasmuch as its emf is higher than that of either the 40 or 60 percent Rh. If conditions of use were such as to bring about a change in composition at and near the measuring junction, as for example by preferential volatilization of one of the constituents of the alloy leg, the thermal emf would be changed relatively little over a range of several percent change of composition in the 50 percent Rh thermocouple. It is quite likely that extensive use of these thermocouples in different environments will indicate the superiority of one alloy over another, or different alloys may be best suited for different purposes. Even the alloys having less than 40 and more than 60 percent rhodium may have desirable properties.

The question of tolerances on composition has not been considered in this work, since the behavior of the thermocouples has indicated that other factors, some of them not identifiable, have predominated in causing differences or changes in thermocouple output.

It can be concluded from this study that a thermocouple of nominal composition 40, 50, or 60 percent Rh versus Ir can be used for measuring temperatures up to 3900 °F [5] to an accuracy of ±40 °F if the temperature of the thermocouple is determined from the appropriate table. Higher accuracy can be achieved by calibrating the particular thermocouple in question. A convenient method of performing such a calibration is to measure the emf of each thermoelement of the test thermocouple against the corresponding element of a thermocouple of known thermal emf. A higher degree of accuracy can be obtained above 1900 °F by using an optical pyrometer and a blackbody with the method described earlier. If the emf of a thermocouple is to be determined at temperatures between calibration points, a curve of deviations from the appropriate reference table can be constructed and used as described in reference 7.

[5] The temperature versus emf tables for the 60 percent Rh thermocouple extends to 3800 °F.

7. Appendix

TABLE 1–A. *Sixty percent iridium-forty percent rhodium versus iridium thermocouples*

Electromotive force in absolute millivolts. Temperatures in degrees C (Int. 1948). Reference junctions at 0 °C.

Millivolts	.000	.010	.020	.030	.040	.050	.060	.070	.080	.090	.100	Millivolts
	Degrees C											
0.000	0.0	3.2	6.4	9.5	12.6	15.6	18.7	21.6	24.6	27.5	30.4	0.000
0.100	30.4	33.2	36.1	38.9	41.6	44.4	47.1	49.8	52.5	55.1	57.8	0.100
0.200	57.8	60.4	63.0	65.5	68.1	70.6	73.2	75.7	78.1	80.6	83.1	0.200
0.300	83.1	85.5	87.9	90.3	92.7	95.1	97.5	99.8	102.2	104.5	106.8	0.300
0.400	106.8	109.1	111.4	113.7	116.0	118.2	120.5	122.7	124.9	127.1	129.4	0.400
0.500	129.4	131.6	133.8	135.9	138.1	140.3	142.4	144.6	146.7	148.8	151.0	0.500
0.600	151.0	153.1	155.2	157.3	159.4	161.5	163.5	165.6	167.7	169.7	171.8	0.600
0.700	171.8	173.8	175.8	177.9	179.9	181.9	183.9	185.9	187.9	189.9	191.9	0.700
0.800	191.9	193.9	195.9	197.9	199.8	201.8	203.7	205.7	207.6	209.6	211.5	0.800
0.900	211.5	213.4	215.4	217.3	219.2	221.1	223.0	224.9	226.8	228.7	230.6	0.900
1.000	230.6	232.5	234.4	236.3	238.2	240.1	241.9	243.8	245.7	247.5	249.4	1.000
1.100	249.4	251.2	253.1	254.9	256.8	258.6	260.4	262.3	264.1	265.9	267.7	1.100
1.200	267.7	269.6	271.4	273.2	275.0	276.8	278.6	280.4	282.2	284.0	285.8	1.200
1.300	285.8	287.6	289.4	291.2	293.0	294.8	296.6	298.3	300.1	301.9	303.6	1.300
1.400	303.6	305.4	307.2	308.9	310.7	312.5	314.2	316.0	317.7	319.5	321.2	1.400
1.500	321.2	323.0	324.7	326.5	328.2	329.9	331.7	333.4	335.2	336.9	338.6	1.500
1.600	338.6	340.3	342.1	343.8	345.5	347.2	349.0	350.7	352.4	354.1	355.8	1.600
1.700	355.8	357.6	359.3	361.0	362.7	364.4	366.1	367.8	369.5	371.2	372.9	1.700
1.800	372.9	374.6	376.3	378.0	379.7	381.4	383.1	384.8	386.5	388.2	389.8	1.800
1.900	389.8	391.5	393.2	394.9	396.6	398.3	399.9	401.6	403.3	405.0	406.7	1.900
2.000	406.7	408.4	410.0	411.7	413.4	415.1	416.7	418.4	420.1	421.7	423.4	2.000
2.100	423.4	425.1	426.7	428.4	430.1	431.7	433.4	435.1	436.7	438.4	440.1	2.100
2.200	440.1	441.7	443.4	445.1	446.7	448.4	450.0	451.7	453.4	455.0	456.7	2.200
2.300	456.7	458.3	460.0	461.6	463.3	464.9	466.6	468.2	469.9	471.6	473.2	2.300
2.400	473.2	474.9	476.5	478.2	479.8	481.5	483.1	484.8	486.4	488.1	489.7	2.400
2.500	489.7	491.4	493.0	494.6	496.3	497.9	499.6	501.2	502.9	504.5	506.2	2.500
2.600	506.2	507.8	509.5	511.1	512.8	514.4	516.1	517.7	519.3	521.0	522.6	2.600
2.700	522.6	524.3	525.9	527.6	529.2	530.8	532.5	534.1	535.8	537.4	539.1	2.700
2.800	539.1	540.7	542.3	544.0	545.6	547.2	548.8	550.5	552.1	553.7	555.4	2.800
2.900	555.4	557.0	558.6	560.3	561.9	563.5	565.2	566.8	568.4	570.1	571.7	2.900
3.000	571.7	573.4	575.0	576.6	578.3	579.9	581.5	583.2	584.8	586.5	588.1	3.000
3.100	588.1	589.7	591.4	593.0	594.7	596.3	597.9	599.6	601.2	602.9	604.5	3.100
3.200	604.5	606.1	607.8	609.4	611.1	612.7	614.4	616.0	617.7	619.3	621.0	3.200
3.300	621.0	622.6	624.3	625.9	627.6	629.2	630.9	632.5	634.2	635.8	637.5	3.300
3.400	637.5	639.1	640.8	642.4	644.1	645.7	647.4	649.1	650.7	652.4	654.0	3.400
3.500	654.0	655.7	657.3	659.0	660.7	662.3	664.0	665.6	667.3	669.0	670.6	3.500
3.600	670.6	672.3	674.0	675.6	677.3	679.0	680.6	682.3	684.0	685.6	687.3	3.600
3.700	687.3	689.0	690.7	692.3	694.0	695.7	697.3	699.0	700.7	702.4	704.0	3.700
3.800	704.0	705.7	707.4	709.1	710.8	712.4	714.1	715.8	717.5	719.2	720.8	3.800
3.900	720.8	722.5	724.2	725.9	727.6	729.3	730.9	732.6	734.3	736.0	737.7	3.900
4.000	737.7	739.4	741.1	742.8	744.5	746.2	747.9	749.6	751.3	753.0	754.6	4.000
4.100	754.6	756.3	758.0	759.7	761.4	763.1	764.9	766.6	768.3	770.0	771.7	4.100
4.200	771.7	773.4	775.1	776.8	788.5	780.2	781.9	783.6	785.3	787.1	788.8	4.200
4.300	788.8	790.5	792.2	793.9	795.6	797.4	799.1	800.8	802.5	804.2	806.0	4.300
4.400	806.0	807.7	809.4	811.1	812.8	814.6	816.3	818.0	819.8	821.5	823.2	4.400
4.500	823.2	824.9	826.7	828.4	830.1	831.9	833.6	835.3	837.1	838.8	840.6	4.500
4.600	840.6	842.3	844.0	845.8	847.5	849.3	851.0	852.8	854.5	856.3	858.0	4.600
4.700	858.0	859.8	861.5	863.3	865.0	866.8	868.5	870.3	872.0	873.8	875.5	4.700
4.800	875.5	877.3	879.0	880.8	882.6	884.3	886.1	887.9	889.6	891.4	893.2	4.800
4.900	893.2	894.9	896.7	898.5	900.2	902.0	903.8	905.5	907.3	909.1	910.9	4.900

TABLE 1–A. *Sixty percent iridium-forty percent rhodium versus iridium thermocouples*—Continued

Electromotive force in absolute millivolts. Temperatures in degrees C (Int. 1948). Reference junctions at 0 °C.

Millivolts	.000	.010	.020	.030	.040	.050	.060	.070	.080	.090	.100	Millivolts
	Degrees C											
5.000	910.9	912.6	914.4	916.2	918.0	919.8	921.5	923.3	925.1	926.9	928.7	5.000
5.100	928.7	930.5	932.3	934.0	935.8	937.6	939.4	941.2	943.0	944.8	946.6	5.100
5.200	946.6	948.4	950.2	952.0	953.8	955.6	957.4	959.2	961.0	962.8	964.6	5.200
5.300	964.6	966.4	968.2	970.0	971.8	973.6	975.4	977.3	979.1	980.9	982.7	5.300
5.400	982.7	984.5	986.3	988.1	990.0	991.8	993.6	995.4	997.2	999.1	1000.9	5.400
5.500	1000.9	1002.7	1004.5	1006.4	1008.2	1010.0	1011.9	1013.7	1015.5	1017.4	1019.2	5.500
5.600	1019.2	1021.0	1022.9	1024.7	1026.5	1028.4	1030.2	1032.1	1033.9	1035.7	1037.6	5.600
5.700	1037.6	1039.4	1041.3	1043.1	1045.0	1046.8	1048.7	1050.5	1052.4	1054.2	1056.1	5.700
5.800	1056.1	1057.9	1059.8	1061.6	1063.5	1065.3	1067.2	1069.1	1070.9	1072.8	1074.7	5.800
5.900	1074.7	1076.5	1078.4	1080.2	1082.1	1084.0	1085.8	1087.7	1089.6	1091.5	1093.3	5.900
6.000	1093.3	1095.2	1097.1	1098.9	1100.8	1102.7	1104.6	1106.5	1108.3	1110.2	1112.1	6.000
6.100	1112.1	1114.0	1115.9	1117.7	1119.6	1121.5	1123.4	1125.3	1127.2	1129.1	1130.9	6.100
6.200	1130.9	1132.8	1134.7	1136.6	1138.5	1140.4	1142.3	1144.2	1146.1	1148.0	1149.9	6.200
6.300	1149.9	1151.8	1153.7	1155.6	1157.5	1159.4	1161.3	1163.2	1165.1	1167.0	1168.9	6.300
6.400	1168.9	1170.8	1172.7	1174.6	1176.5	1178.5	1180.4	1182.3	1184.2	1186.1	1188.0	6.400
6.500	1188.0	1189.9	1191.8	1193.8	1195.7	1197.6	1199.5	1201.4	1203.3	1205.3	1207.2	6.500
6.600	1207.2	1209.1	1211.0	1212.9	1214.9	1216.8	1218.7	1220.6	1222.6	1224.5	1226.4	6.600
6.700	1226.4	1228.4	1230.3	1232.2	1234.1	1236.1	1238.0	1239.9	1241.9	1243.8	1245.7	6.700
6.800	1245.7	1247.7	1249.6	1251.5	1253.5	1255.4	1257.3	1259.3	1261.2	1263.2	1265.1	6.800
6.900	1265.1	1267.0	1269.0	1270.9	1272.9	1274.8	1276.8	1278.7	1280.6	1282.6	1284.5	6.900
7.000	1284.5	1286.5	1288.4	1290.4	1292.3	1294.3	1296.2	1298.2	1300.1	1302.1	1304.0	7.000
7.100	1304.0	1306.0	1307.9	1309.9	1311.8	1313.8	1315.7	1317.7	1319.6	1321.6	1323.5	7.100
7.200	1323.5	1325.5	1327.4	1329.4	1331.3	1333.3	1335.3	1337.2	1339.2	1341.1	1343.1	7.200
7.300	1343.1	1345.1	1347.0	1349.0	1350.9	1352.9	1354.9	1356.8	1358.8	1360.7	1362.7	7.300
7.400	1362.7	1364.7	1366.6	1368.6	1370.5	1372.5	1374.5	1376.4	1378.4	1380.4	1382.3	7.400
7.500	1382.3	1384.3	1386.2	1388.2	1390.2	1392.1	1394.1	1396.1	1398.0	1400.0	1402.0	7.500
7.600	1402.0	1403.9	1405.9	1407.9	1409.8	1411.8	1413.8	1415.7	1417.7	1419.6	1421.6	7.600
7.700	1421.6	1423.6	1425.5	1427.5	1429.5	1431.4	1433.4	1435.4	1437.3	1439.3	1441.3	7.700
7.800	1441.3	1443.2	1445.2	1447.2	1449.1	1451.1	1453.1	1455.0	1457.0	1459.0	1460.9	7.800
7.900	1460.9	1462.9	1464.9	1466.8	1468.8	1470.8	1472.7	1474.7	1476.7	1478.6	1480.6	7.900
8.000	1480.6	1482.6	1484.5	1486.5	1488.4	1490.4	1492.4	1494.3	1496.3	1498.3	1500.2	8.000
8.100	1500.2	1502.2	1504.2	1506.1	1508.1	1510.0	1512.0	1514.0	1515.9	1517.9	1519.9	8.100
8.200	1519.9	1521.8	1523.8	1525.7	1527.7	1529.7	1531.6	1533.6	1535.5	1537.5	1539.5	8.200
8.300	1539.5	1541.4	1543.4	1545.3	1547.3	1549.2	1551.2	1553.2	1555.1	1557.1	1559.0	8.300
8.400	1559.0	1561.0	1562.9	1564.9	1566.8	1568.8	1570.7	1572.7	1574.6	1576.6	1578.5	8.400
8.500	1578.5	1580.5	1582.4	1584.4	1586.3	1588.3	1590.2	1592.2	1594.1	1596.1	1598.0	8.500
8.600	1598.0	1600.0	1601.9	1603.9	1605.8	1607.7	1609.7	1611.6	1613.6	1615.5	1617.5	8.600
8.700	1617.5	1619.4	1621.3	1623.3	1625.2	1627.2	1629.1	1631.0	1633.0	1634.9	1636.8	8.700
8.800	1636.8	1638.8	1640.7	1642.6	1644.6	1646.5	1648.4	1650.4	1652.3	1654.2	1656.2	8.800
8.900	1656.2	1658.1	1660.0	1661.9	1663.9	1665.8	1667.7	1669.7	1671.6	1673.5	1675.4	8.900
9.000	1675.4	1677.3	1679.3	1681.2	1683.1	1685.0	1687.0	1688.9	1690.8	1692.7	1694.6	9.000
9.100	1694.6	1696.5	1698.4	1700.3	1702.3	1704.2	1706.1	1708.0	1709.9	1711.8	1713.7	9.100
9.200	1713.7	1715.6	1717.5	1719.4	1721.4	1723.3	1725.2	1727.1	1729.0	1730.9	1732.8	9.200
9.300	1732.8	1734.7	1736.6	1738.5	1740.4	1742.3	1744.2	1746.1	1748.0	1749.8	1751.7	9.300
9.400	1751.7	1753.6	1755.5	1757.4	1759.3	1761.2	1763.1	1765.0	1766.9	1768.7	1770.6	9.400
9.500	1770.6	1772.5	1774.4	1776.3	1778.2	1780.0	1781.9	1783.8	1785.7	1787.6	1789.4	9.500
9.600	1789.4	1791.3	1793.2	1795.1	1796.9	1798.8	1800.7	1802.5	1804.4	1806.3	1808.2	9.600
9.700	1808.2	1810.0	1811.9	1813.8	1815.6	1817.5	1819.3	1821.2	1823.1	1824.9	1826.8	9.700
9.800	1826.8	1828.6	1830.5	1832.4	1834.2	1836.1	1837.9	1839.8	1841.6	1843.5	1845.3	9.800
9.900	1845.3	1847.2	1849.0	1850.9	1852.7	1854.6	1856.4	1858.3	1860.1	1862.0	1863.8	9.900

TABLE 1–A. *Sixty percent iridium-forty percent rhodium versus iridium thermocouples* – Continued

Electromotive force in absolute millivolts. Temperatures in degrees C (Int. 1948). Reference junctions at 0°C.

Millivolts	.000	.010	.020	.030	.040	.050	.060	.070	.080	.090	.100	Millivolts
	Degrees C											
10.000	1863.8	1865.6	1867.5	1869.3	1871.2	1873.0	1874.8	1876.7	1878.5	1880.3	1882.2	10.000
10.100	1882.2	1884.0	1885.8	1887.7	1889.5	1891.3	1893.1	1895.0	1896.8	1898.6	1900.4	10.100
10.200	1900.4	1902.3	1904.1	1905.9	1907.7	1909.6	1911.4	1913.2	1915.0	1916.8	1918.6	10.200
10.300	1918.6	1920.5	1922.3	1924.1	1925.9	1927.7	1929.5	1931.3	1933.1	1934.9	1936.7	10.300
10.400	1936.7	1938.6	1940.4	1942.2	1944.0	1945.8	1947.6	1949.4	1951.2	1953.0	1954.8	10.400
10.500	1954.8	1956.6	1958.4	1960.2	1962.0	1963.7	1965.5	1967.3	1969.1	1970.9	1972.7	10.500
10.600	1972.7	1974.5	1976.3	1978.1	1979.9	1981.6	1983.4	1985.2	1987.0	1988.8	1990.6	10.600
10.700	1990.6	1992.4	1994.1	1995.9	1997.7	1999.5	2001.2	2003.0	2004.8	2006.6	2008.3	10.700
10.800	2008.3	2010.1	2011.9	2013.6	2015.4	2017.2	2019.0	2020.7	2022.5	2024.3	2026.0	10.800
10.900	2026.0	2027.8	2029.6	2031.3	2033.1	2034.8	2036.6	2038.4	2040.1	2041.9	2043.6	10.900
11.000	2043.6	2045.4	2047.2	2048.9	2050.7	2052.4	2054.2	2055.9	2057.7	2059.4	2061.2	11.000
11.100	2061.2	2062.9	2064.7	2066.4	2068.2	2069.9	2071.7	2073.4	2075.2	2076.9	2078.6	11.100
11.200	2078.6	2080.4	2082.1	2083.9	2085.6	2087.4	2089.1	2090.8	2092.6	2094.3	2096.0	11.200
11.300	2096.0	2097.8	2099.5	2101.2	2103.0	2104.7	2106.4	2108.2	2109.9	2111.6	2113.4	11.300
11.400	2113.4	2115.1	2116.8	2118.6	2120.3	2122.0	2123.7	2125.5	2127.2	2128.9	2130.6	11.400
11.500	2130.6	2132.4	2134.1	2135.8	2137.5	2139.3	2141.0	2142.7	2144.4	2146.1	2147.9	11.500
11.600	2147.9	2149.6										11.600

TABLE 2–A. *Sixty percent iridium-forty percent rhodium versus iridium thermocouples*

Electromotive force in absolute millivolts. Temperatures in degrees C (Int. 1948). Reference junctions at 0 °C.

°C	0	10	20	30	40	50	60	70	80	90	100	°C
	Millivolts											
0	0.000	0.032	0.064	0.099	0.134	0.171	0.209	0.247	0.287	0.329	0.371	0
100	0.371	0.414	0.458	0.503	0.549	0.595	0.643	0.691	0.740	0.790	0.841	100
200	0.841	0.892	0.944	0.997	1.050	1.103	1.158	1.212	1.268	1.323	1.379	200
300	1.379	1.436	1.493	1.550	1.608	1.666	1.724	1.783	1.842	1.901	1.960	300
400	1.960	2.020	2.080	2.139	2.200	2.260	2.320	2.381	2.441	2.502	2.562	400
500	2.562	2.623	2.684	2.745	2.806	2.867	2.928	2.989	3.051	3.112	3.173	500
600	3.173	3.233	3.294	3.355	3.415	3.476	3.536	3.596	3.656	3.716	3.776	600
700	3.776	3.835	3.895	3.954	4.014	4.073	4.131	4.190	4.249	4.307	4.365	700
800	4.365	4.423	4.481	4.539	4.597	4.654	4.711	4.768	4.825	4.882	4.939	800
900	4.939	4.995	5.051	5.107	5.163	5.219	5.274	5.330	5.385	5.440	5.495	900
1000	5.495	5.550	5.604	5.659	5.713	5.767	5.821	5.875	5.929	5.982	6.036	1000
1100	6.036	6.089	6.142	6.195	6.248	6.301	6.353	6.406	6.458	6.510	6.563	1100
1200	6.563	6.615	6.667	6.718	6.770	6.822	6.874	6.925	6.977	7.028	7.079	1200
1300	7.079	7.131	7.182	7.233	7.284	7.335	7.386	7.437	7.488	7.539	7.590	1300
1400	7.590	7.641	7.692	7.743	7.793	7.844	7.895	7.946	7.997	8.048	8.099	1400
1500	8.099	8.150	8.201	8.252	8.303	8.354	8.405	8.456	8.507	8.559	8.610	1500
1600	8.610	8.662	8.713	8.765	8.816	8.868	8.920	8.972	9.024	9.076	9.128	1600
1700	9.128	9.180	9.233	9.285	9.338	9.391	9.444	9.497	9.550	9.603	9.656	1700
1800	9.656	9.710	9.763	9.817	9.871	9.925	9.979	10.034	10.088	10.143	10.198	1800
1900	10.198	10.252	10.307	10.363	10.418	10.473	10.529	10.585	10.641	10.697	10.753	1900
2000	10.753	10.809	10.866	10.922	10.979	11.036	11.093	11.150	11.208	11.265	11.323	2000
2100	11.323	11.380	11.438	11.496	11.554	11.612						2100

TABLE 3–A. *Sixty percent iridium-forty percent rhodium versus iridium thermocouples*

Electromotive force in absolute millivolts. Temperatures in degrees F*. Reference junctions at 32 °F.

Millivolts	.000	.010	.020	.030	.040	.050	.060	.070	.080	.090	.100	Millivolts
	Degrees F											
0.000	32.0	37.8	43.5	49.1	54.7	60.2	65.6	70.9	76.2	81.5	86.7	0.000
0.100	86.7	91.8	96.9	101.9	106.9	111.9	116.7	121.6	126.5	131.2	136.0	0.100
0.200	136.0	140.7	145.3	150.0	154.6	159.1	163.7	168.2	172.6	177.1	181.5	0.200
0.300	181.5	185.9	190.3	194.6	198.9	203.2	207.5	211.7	215.9	220.1	224.3	0.300
0.400	224.3	228.4	232.5	236.6	240.7	244.8	248.9	252.9	256.9	260.9	264.9	0.400
0.500	264.9	268.8	272.8	276.7	280.6	284.5	288.4	292.2	296.1	299.9	303.7	0.500
0.600	303.7	307.5	311.3	315.1	318.9	322.6	326.4	330.1	333.8	337.5	341.2	0.600
0.700	341.2	344.9	348.5	352.2	355.8	359.5	363.1	366.7	370.3	373.9	377.5	0.700
0.800	377.5	381.0	384.6	388.1	391.7	395.2	398.7	402.2	405.7	409.2	412.7	0.800
0.900	412.7	416.2	419.7	423.1	426.6	430.0	433.5	436.9	440.3	443.8	447.2	0.900
1.000	447.2	450.6	453.9	457.3	460.7	464.1	467.5	470.8	474.2	477.5	480.9	1.000
1.100	480.9	484.2	487.5	490.9	494.2	497.5	500.8	504.1	507.4	510.7	513.9	1.100
1.200	513.9	517.2	520.5	523.8	527.0	530.3	533.5	536.8	540.0	543.3	546.5	1.200
1.300	546.5	549.7	552.9	556.1	559.4	562.6	565.8	569.0	572.2	575.4	578.6	1.300
1.400	578.6	581.7	584.9	588.1	591.3	594.4	597.6	600.8	603.9	607.1	610.2	1.400
1.500	610.2	613.4	616.5	619.7	622.8	625.9	629.0	632.2	635.3	638.4	641.5	1.500
1.600	641.5	644.6	647.7	650.8	654.0	657.1	660.2	663.2	666.3	669.4	672.5	1.600
1.700	672.5	675.6	678.7	681.8	684.8	687.9	691.0	694.1	697.1	700.2	703.2	1.700
1.800	703.2	706.3	709.4	712.4	715.5	718.5	721.6	724.6	727.6	730.7	733.7	1.800
1.900	733.7	736.8	739.8	742.8	745.9	748.9	751.9	754.9	758.0	761.0	764.0	1.900
2.000	764.0	767.0	770.1	773.1	776.1	779.1	782.1	785.1	788.1	791.1	794.1	2.000
2.100	794.1	797.1	800.2	803.2	806.2	809.2	812.2	815.1	818.1	821.1	824.1	2.100
2.200	824.1	827.1	830.1	833.1	836.1	839.1	842.1	845.1	848.0	851.0	854.0	2.200
2.300	854.0	857.0	860.0	862.9	865.9	868.9	871.9	874.9	877.8	880.8	883.8	2.300
2.400	883.8	886.7	889.7	892.7	895.7	898.6	901.6	904.6	907.5	910.5	913.5	2.400
2.500	913.5	916.4	919.4	922.4	925.3	928.3	931.3	934.2	937.2	940.1	943.1	2.500
2.600	943.1	946.1	949.0	952.0	955.0	957.9	960.9	963.8	966.8	969.8	972.7	2.600
2.700	972.7	975.7	978.6	981.6	984.6	987.5	990.5	993.5	996.4	999.4	1002.3	2.700
2.800	1002.3	1005.2	1008.2	1011.1	1014.0	1017.0	1019.9	1022.9	1025.8	1028.7	1031.7	2.800
2.900	1031.7	1034.6	1037.6	1040.5	1043.4	1046.4	1049.3	1052.3	1055.2	1058.1	1061.1	2.900
3.000	1061.1	1064.0	1067.0	1069.9	1072.9	1075.8	1078.8	1081.7	1084.7	1087.6	1090.6	3.000
3.100	1090.6	1093.5	1096.5	1099.4	1102.4	1105.3	1108.3	1111.3	1114.2	1117.2	1120.1	3.100
3.200	1120.1	1123.1	1126.0	1129.0	1131.9	1134.9	1137.9	1140.8	1143.8	1146.8	1149.7	3.200
3.300	1149.7	1152.7	1155.7	1158.6	1161.6	1164.6	1167.5	1170.5	1173.5	1176.5	1179.4	3.300
3.400	1179.4	1182.4	1185.4	1188.4	1191.4	1194.3	1197.3	1200.3	1203.3	1206.3	1209.3	3.400
3.500	1209.3	1212.2	1215.2	1218.2	1221.2	1224.2	1227.2	1230.1	1233.1	1236.1	1239.1	3.500
3.600	1239.1	1242.1	1245.1	1248.1	1251.1	1254.1	1257.1	1260.1	1263.1	1266.2	1269.2	3.600
3.700	1269.2	1272.2	1275.2	1278.2	1281.2	1284.2	1287.2	1290.2	1293.2	1296.3	1299.3	3.700
3.800	1299.3	1302.3	1305.3	1308.3	1311.4	1314.4	1317.4	1320.4	1323.5	1326.5	1329.5	3.800
3.900	1329.5	1332.5	1335.6	1338.6	1341.6	1344.7	1347.7	1350.8	1353.8	1356.8	1359.9	3.900
4.000	1359.9	1362.9	1366.0	1369.0	1372.1	1375.1	1378.2	1381.2	1384.3	1387.3	1390.4	4.000
4.100	1390.4	1393.4	1396.5	1399.5	1402.6	1405.7	1408.7	1411.8	1414.9	1417.9	1421.0	4.100
4.200	1421.0	1424.1	1427.2	1430.2	1433.3	1436.4	1439.5	1442.5	1445.6	1448.7	1451.8	4.200
4.300	1451.8	1454.9	1458.0	1461.0	1464.1	1467.2	1470.3	1473.4	1476.5	1479.6	1482.7	4.300
4.400	1482.7	1485.8	1488.9	1492.0	1495.1	1498.2	1501.3	1504.4	1507.5	1510.7	1513.8	4.400
4.500	1513.8	1516.9	1520.0	1523.1	1526.2	1529.4	1532.5	1535.6	1538.7	1541.9	1545.0	4.500
4.600	1545.0	1548.1	1551.3	1554.4	1557.6	1560.7	1563.8	1567.0	1570.1	1573.3	1576.4	4.600
4.700	1576.4	1579.6	1582.7	1585.9	1589.0	1592.2	1595.3	1598.5	1601.6	1604.8	1608.0	4.700
4.800	1608.0	1611.1	1614.3	1617.5	1620.6	1623.8	1627.0	1630.2	1633.3	1636.5	1639.7	4.800
4.900	1639.7	1642.9	1646.1	1649.2	1652.4	1655.6	1658.8	1662.0	1665.2	1668.4	1671.6	4.900

*Based on the International Temperature Scale of 1948.

TABLE 3–A. *Sixty percent iridium-forty percent rhodium versus iridium thermocouples*—Continued

Electromotive force in absolute millivolts. Temperatures in degrees F*. Reference junctions at 32 °F.

Millivolts	.000	.010	.020	.030	.040	.050	.060	.070	.080	.090	.100	Millivolts
	Degrees F											
5.000	1671.6	1674.8	1678.0	1681.2	1684.4	1687.6	1690.8	1694.0	1697.2	1700.4	1703.6	5.000
5.100	1703.6	1706.8	1710.1	1713.3	1716.5	1719.7	1723.0	1726.2	1729.4	1732.6	1735.9	5.100
5.200	1735.9	1739.1	1742.3	1745.6	1748.8	1752.0	1755.3	1758.5	1761.8	1765.0	1768.3	5.200
5.300	1768.3	1771.5	1774.8	1778.0	1781.3	1784.6	1787.8	1791.1	1794.3	1797.6	1800.9	5.300
5.400	1800.9	1804.1	1807.4	1810.7	1814.0	1817.2	1820.5	1823.8	1827.0	1830.3	1833.6	5.400
5.500	1833.6	1836.9	1840.2	1843.5	1846.8	1850.1	1853.4	1856.7	1860.0	1863.3	1866.6	5.500
5.600	1866.6	1869.9	1873.2	1876.5	1879.8	1883.1	1886.4	1889.7	1893.0	1896.4	1899.7	5.600
5.700	1899.7	1903.0	1906.3	1909.6	1912.9	1916.3	1919.6	1922.9	1926.3	1929.6	1932.9	5.700
5.800	1932.9	1936.3	1939.6	1943.0	1946.3	1949.7	1953.0	1956.3	1959.7	1963.0	1966.4	5.800
5.900	1966.4	1969.8	1973.1	1976.5	1979.8	1983.2	1986.5	1989.9	1993.3	1996.6	2000.0	5.900
6.000	2000.0	2003.4	2006.7	2010.1	2013.5	2016.9	2020.2	2023.6	2027.0	2030.4	2033.8	6.000
6.100	2033.8	2037.1	2040.5	2043.9	2047.3	2050.7	2054.1	2057.5	2060.9	2064.3	2067.7	6.100
6.200	2067.7	2071.1	2074.5	2077.9	2081.3	2084.7	2088.1	2091.6	2095.0	2098.4	2101.8	6.200
6.300	2101.8	2105.2	2108.6	2112.0	2115.5	2118.9	2122.3	2125.7	2129.2	2132.6	2136.0	6.300
6.400	2136.0	2139.5	2142.9	2146.3	2149.8	2153.2	2156.6	2160.1	2163.5	2167.0	2170.4	6.400
6.500	2170.4	2173.9	2177.3	2180.7	2184.2	2187.6	2191.1	2194.5	2198.0	2201.5	2204.9	6.500
6.600	2204.9	2208.4	2211.8	2215.3	2218.8	2222.2	2225.7	2229.1	2232.6	2236.1	2239.5	6.600
6.700	2239.5	2243.0	2246.5	2250.0	2253.4	2256.9	2260.4	2263.9	2267.4	2270.8	2274.3	6.700
6.800	2274.3	2277.8	2281.3	2284.8	2288.2	2291.7	2295.2	2298.7	2302.2	2305.7	2309.2	6.800
6.900	2309.2	2312.7	2316.2	2319.7	2323.2	2326.7	2330.2	2333.7	2337.1	2340.6	2344.1	6.900
7.000	2344.1	2347.7	2351.2	2354.7	2358.2	2361.7	2365.2	2368.7	2372.2	2375.7	2379.2	7.000
7.100	2379.2	2382.8	2386.3	2389.8	2393.3	2396.8	2400.3	2403.8	2407.3	2410.9	2414.4	7.100
7.200	2414.4	2417.9	2421.4	2424.9	2428.4	2432.0	2435.5	2439.0	2442.5	2446.1	2449.6	7.200
7.300	2449.6	2453.1	2456.6	2460.2	2463.7	2467.2	2470.7	2474.3	2477.8	2481.3	2484.9	7.300
7.400	2484.9	2488.4	2491.9	2495.4	2499.0	2502.5	2506.0	2509.6	2513.1	2516.6	2520.2	7.400
7.500	2520.2	2523.7	2527.2	2530.8	2534.3	2537.8	2541.4	2544.9	2548.4	2552.0	2555.5	7.500
7.600	2555.5	2559.1	2562.6	2566.1	2569.7	2573.2	2576.8	2580.3	2583.8	2587.4	2590.9	7.600
7.700	2590.9	2594.4	2598.0	2601.5	2605.1	2608.6	2612.1	2615.7	2619.2	2622.8	2626.3	7.700
7.800	2626.3	2629.8	2633.4	2636.9	2640.4	2644.0	2647.5	2651.1	2654.6	2658.1	2661.7	7.800
7.900	2661.7	2665.2	2668.8	2672.3	2675.8	2679.4	2682.9	2686.5	2690.0	2693.5	2697.1	7.900
8.000	2697.1	2700.6	2704.1	2707.7	2711.2	2714.7	2718.3	2721.8	2725.3	2728.9	2732.4	8.000
8.100	2732.4	2735.9	2739.5	2743.0	2746.5	2750.1	2753.6	2757.1	2760.7	2764.2	2767.7	8.100
8.200	2767.7	2771.3	2774.8	2778.3	2781.9	2785.4	2788.9	2792.5	2796.0	2799.5	2803.0	8.200
8.300	2803.0	2806.6	2810.1	2813.6	2817.1	2820.6	2824.1	2827.7	2831.2	2834.7	2838.2	8.300
8.400	2838.2	2841.7	2845.3	2848.8	2852.3	2855.8	2859.3	2862.8	2866.3	2869.9	2873.4	8.400
8.500	2873.4	2876.9	2880.4	2883.9	2887.4	2890.9	2894.4	2897.9	2901.4	2904.9	2908.4	8.500
8.600	2908.4	2911.9	2915.4	2918.9	2922.4	2925.9	2929.4	2932.9	2936.4	2939.9	2943.4	8.600
8.700	2943.4	2946.9	2950.4	2953.9	2957.4	2960.9	2964.4	2967.9	2971.4	2974.8	2978.3	8.700
8.800	2978.3	2981.8	2985.3	2988.8	2992.2	2995.7	2999.2	3002.7	3006.2	3009.6	3013.1	8.800
8.900	3013.1	3016.6	3020.0	3023.5	3027.0	3030.5	3033.9	3037.4	3040.8	3044.3	3047.8	8.900
9.000	3047.8	3051.2	3054.7	3058.1	3061.6	3065.0	3068.5	3071.9	3075.4	3078.8	3082.3	9.000
9.100	3082.3	3085.7	3089.2	3092.6	3096.1	3099.5	3102.9	3106.4	3109.8	3113.3	3116.7	9.100
9.200	3116.7	3120.1	3123.6	3127.0	3130.4	3133.9	3137.3	3140.7	3144.1	3147.6	3151.0	9.200
9.300	3151.0	3154.4	3157.8	3161.3	3164.7	3168.1	3171.5	3174.9	3178.3	3181.7	3185.1	9.300
9.400	3185.1	3188.5	3191.9	3195.4	3198.8	3202.2	3205.5	3208.9	3212.3	3215.7	3219.1	9.400
9.500	3219.1	3222.5	3225.9	3229.3	3232.7	3236.1	3239.5	3242.8	3246.2	3249.6	3253.0	9.500
9.600	3253.0	3256.3	3259.7	3263.1	3266.5	3269.8	3273.2	3276.6	3279.9	3283.3	3286.7	9.600
9.700	3286.7	3290.0	3293.4	3296.7	3300.1	3303.5	3306.8	3310.2	3313.5	3316.8	3320.2	9.700
9.800	3320.2	3323.5	3326.9	3330.2	3333.6	3336.9	3340.3	3343.6	3346.9	3350.3	3353.6	9.800
9.900	3353.6	3356.9	3360.3	3363.6	3366.9	3370.2	3373.5	3376.9	3380.2	3383.5	3386.8	9.900

*Based on the International Temperature Scale of 1948.

TABLE 3–A. *Sixty percent iridium-forty percent rhodium versus iridium thermocouples*—Continued

Electromotive force in absolute millivolts. Temperatures in degrees F*. Reference junctions at 32 °F.

Millivolts	.000	.010	.020	.030	.040	.050	.060	.070	.080	.090	.100	Millivolts
	Degrees F											
10.000	3386.8	3390.1	3393.5	3396.8	3400.1	3403.4	3406.7	3410.0	3413.3	3416.6	3419.9	10.000
10.100	3419.9	3423.2	3426.5	3429.8	3433.1	3436.4	3439.6	3442.9	3446.2	3449.5	3452.8	10.100
10.200	3452.8	3456.1	3459.4	3462.6	3465.9	3469.2	3472.5	3475.7	3479.0	3482.3	3485.6	10.200
10.300	3485.6	3488.8	3492.1	3495.4	3498.6	3501.9	3505.1	3508.4	3511.7	3514.9	3518.2	10.300
10.400	3518.2	3521.4	3524.7	3527.9	3531.2	3534.4	3537.6	3540.9	3544.1	3547.3	3550.6	10.400
10.500	3550.6	3553.8	3557.0	3560.3	3563.5	3566.7	3570.0	3573.2	3576.4	3579.7	3582.9	10.500
10.600	3582.9	3586.1	3589.3	3592.5	3595.8	3599.0	3602.2	3605.4	3608.6	3611.8	3615.0	10.600
10.700	3615.0	3618.2	3621.4	3624.6	3627.8	3631.0	3634.2	3637.4	3640.6	3643.8	3647.0	10.700
10.800	3647.0	3650.2	3653.4	3656.6	3659.7	3662.9	3666.1	3669.3	3672.5	3675.7	3678.9	10.800
10.900	3678.9	3682.0	3685.2	3688.4	3691.6	3694.7	3697.9	3701.1	3704.2	3707.4	3710.5	10.900
11.000	3710.5	3713.7	3716.9	3720.0	3723.2	3726.3	3729.5	3732.7	3735.8	3739.0	3742.1	11.000
11.100	3742.1	3745.3	3748.4	3751.6	3754.7	3757.9	3761.0	3764.2	3767.3	3770.4	3773.6	11.100
11.200	3773.6	3776.7	3779.8	3783.0	3786.1	3789.2	3792.4	3795.5	3798.6	3801.8	3804.9	11.200
11.300	3804.9	3808.0	3811.1	3814.3	3817.4	3820.5	3823.6	3826.7	3829.8	3833.0	3836.1	11.300
11.400	3836.1	3839.2	3842.3	3845.4	3848.5	3851.6	3854.8	3857.9	3861.0	3864.1	3867.2	11.400
11.500	3867.2	3870.3	3873.4	3876.5	3879.6	3882.7	3885.8	3888.9	3892.0	3895.0	3898.1	11.500
11.600	3898.1	3901.2										11.600

*Based on the International Temperature Scale of 1948.

TABLE 4–A. *Sixty percent iridium-forty percent rhodium versus iridium thermocouples*

Electromotive force in absolute millivolts. Temperatures in degrees F*. Reference junctions at 32 °F.

°F	0	10	20	30	40	50	60	70	80	90	100	°F
	Millivolts											
0					0.014	0.032	0.050	0.068	0.087	0.106	0.126	0
100	0.126	0.146	0.167	0.187	0.209	0.230	0.252	0.274	0.297	0.319	0.342	100
200	0.342	0.366	0.390	0.414	0.438	0.463	0.488	0.513	0.538	0.564	0.590	200
300	0.590	0.616	0.643	0.670	0.697	0.724	0.751	0.779	0.807	0.835	0.864	300
400	0.864	0.892	0.921	0.950	0.979	1.008	1.038	1.067	1.097	1.127	1.158	400
500	1.158	1.188	1.218	1.249	1.280	1.311	1.342	1.373	1.404	1.436	1.468	500
600	1.468	1.499	1.531	1.563	1.595	1.627	1.659	1.692	1.724	1.757	1.789	600
700	1.789	1.822	1.855	1.888	1.921	1.954	1.987	2.020	2.053	2.086	2.119	700
800	2.119	2.153	2.186	2.220	2.253	2.287	2.320	2.354	2.387	2.421	2.455	800
900	2.455	2.488	2.522	2.556	2.589	2.623	2.657	2.691	2.725	2.758	2.792	900
1000	2.792	2.826	2.860	2.894	2.928	2.962	2.996	3.030	3.064	3.098	3.132	1000
1100	3.132	3.166	3.200	3.233	3.267	3.301	3.335	3.368	3.402	3.435	3.469	1100
1200	3.469	3.502	3.536	3.569	3.603	3.636	3.669	3.703	3.736	3.769	3.802	1200
1300	3.802	3.835	3.869	3.902	3.935	3.967	4.000	4.033	4.066	4.099	4.131	1300
1400	4.131	4.164	4.197	4.229	4.262	4.294	4.327	4.359	4.391	4.423	4.456	1400
1500	4.456	4.488	4.520	4.552	4.584	4.616	4.648	4.680	4.711	4.743	4.775	1500
1600	4.775	4.806	4.838	4.869	4.901	4.932	4.964	4.995	5.026	5.057	5.089	1600
1700	5.089	5.120	5.151	5.182	5.213	5.244	5.274	5.305	5.336	5.367	5.397	1700
1800	5.397	5.428	5.458	5.489	5.519	5.550	5.580	5.610	5.641	5.671	5.701	1800
1900	5.701	5.731	5.761	5.791	5.821	5.851	5.881	5.911	5.941	5.970	6.000	1900
2000	6.000	6.030	6.059	6.089	6.118	6.148	6.177	6.207	6.236	6.265	6.295	2000
2100	6.295	6.324	6.353	6.382	6.412	6.441	6.470	6.499	6.528	6.557	6.586	2100
2200	6.586	6.615	6.644	6.672	6.701	6.730	6.759	6.788	6.816	6.845	6.874	2200
2300	6.874	6.902	6.931	6.959	6.988	7.017	7.045	7.074	7.102	7.131	7.159	2300
2400	7.159	7.188	7.216	7.244	7.273	7.301	7.330	7.358	7.386	7.415	7.443	2400
2500	7.443	7.471	7.499	7.528	7.556	7.584	7.613	7.641	7.669	7.697	7.726	2500
2600	7.726	7.754	7.782	7.810	7.839	7.867	7.895	7.923	7.952	7.980	8.008	2600
2700	8.008	8.037	8.065	8.093	8.121	8.150	8.178	8.206	8.235	8.263	8.291	2700
2800	8.291	8.320	8.348	8.377	8.405	8.433	8.462	8.490	8.519	8.547	8.576	2800
2900	8.576	8.604	8.633	8.662	8.690	8.719	8.747	8.776	8.805	8.834	8.862	2900
3000	8.862	8.891	8.920	8.949	8.978	9.006	9.035	9.064	9.093	9.122	9.151	3000
3100	9.151	9.180	9.210	9.239	9.268	9.297	9.326	9.356	9.385	9.414	9.444	3100
3200	9.444	9.473	9.503	9.532	9.562	9.591	9.621	9.650	9.680	9.710	9.740	3200
3300	9.740	9.769	9.799	9.829	9.859	9.889	9.919	9.949	9.979	10.010	10.040	3300
3400	10.040	10.070	10.100	10.131	10.161	10.191	10.222	10.252	10.283	10.314	10.344	3400
3500	10.344	10.375	10.406	10.436	10.467	10.498	10.529	10.560	10.591	10.622	10.653	3500
3600	10.653	10.684	10.715	10.747	10.778	10.809	10.841	10.872	10.904	10.935	10.967	3600
3700	10.967	10.998	11.030	11.061	11.093	11.125	11.157	11.189	11.220	11.252	11.284	3700
3800	11.284	11.316	11.348	11.380	11.413	11.445	11.477	11.509	11.541	11.574	11.606	3800
3900	11.606											3900

*Based on the International Temperature Scale of 1948.

TABLE 5–A. *Fifty percent iridium-fifty percent rhodium versus iridium thermocouples*

Electromotive force in absolute millivolts. Temperatures in degrees C (Int. 1948). Reference junctions at 0 °C.

Millivolts	.000	.010	.020	.030	.040	.050	.060	.070	.080	.090	.100	Millivolts
	Degrees C											
0.000	0.0	3.1	6.2	9.2	12.2	15.1	18.1	21.0	23.8	26.7	29.5	0.000
0.100	29.5	32.2	35.0	37.7	40.4	43.1	45.8	48.4	51.0	53.6	56.2	0.100
0.200	56.2	58.7	61.3	63.8	66.3	68.8	71.2	73.7	76.1	78.5	80.9	0.200
0.300	80.9	83.3	85.7	88.1	90.4	92.8	95.1	97.4	99.7	102.0	104.2	0.300
0.400	104.2	106.5	108.8	111.0	113.2	115.4	117.6	119.8	122.0	124.2	126.4	0.400
0.500	126.4	128.5	130.7	132.8	135.0	137.1	139.2	141.3	143.4	145.5	147.6	0.500
0.600	147.6	149.7	151.8	153.8	155.9	157.9	160.0	162.0	164.0	166.1	168.1	0.600
0.700	168.1	170.1	172.1	174.1	176.1	178.1	180.0	182.0	184.0	185.9	187.9	0.700
0.800	187.9	189.8	191.8	193.7	195.7	197.6	199.5	201.5	203.4	205.3	207.2	0.800
0.900	207.2	209.1	211.0	212.9	214.8	216.7	218.5	220.4	222.3	224.2	226.0	0.900
1.000	226.0	227.9	229.7	231.6	233.4	235.3	237.1	239.0	240.8	242.6	244.4	1.000
1.100	244.4	246.3	248.1	249.9	251.7	253.5	255.3	257.1	258.9	260.7	262.5	1.100
1.200	262.5	264.3	266.1	267.9	269.7	271.5	273.3	275.0	276.8	278.6	280.3	1.200
1.300	280.3	282.1	283.9	285.6	287.4	289.1	290.9	292.6	294.4	296.1	297.9	1.300
1.400	297.9	299.6	301.3	303.1	304.8	306.5	308.3	310.0	311.7	313.4	315.2	1.400
1.500	315.2	316.9	318.6	320.3	322.0	323.7	325.5	327.2	328.9	330.6	332.3	1.500
1.600	332.3	334.0	335.7	337.4	339.1	340.8	342.5	344.1	345.8	347.5	349.2	1.600
1.700	349.2	350.9	352.6	354.3	355.9	357.6	359.3	361.0	362.6	364.3	366.0	1.700
1.800	366.0	367.7	369.3	371.0	372.7	374.3	376.0	377.6	379.3	381.0	382.6	1.800
1.900	382.6	384.3	385.9	387.6	389.2	390.9	392.6	394.2	395.9	397.5	399.2	1.900
2.000	399.2	400.8	402.4	404.1	405.7	407.4	409.0	410.7	412.3	413.9	415.6	2.000
2.100	415.6	417.2	418.9	420.5	422.1	423.8	425.4	427.0	428.7	430.3	431.9	2.100
2.200	431.9	433.6	435.2	436.8	438.4	440.1	441.7	443.3	445.0	446.6	448.2	2.200
2.300	448.2	449.8	451.5	453.1	454.7	456.3	457.9	459.6	461.2	462.8	464.4	2.300
2.400	464.4	466.0	467.7	469.3	470.9	472.5	474.1	475.7	477.4	479.0	480.6	2.400
2.500	480.6	482.2	483.8	485.4	487.0	488.7	490.3	491.9	493.5	495.1	496.7	2.500
2.600	496.7	498.3	499.9	501.5	503.2	504.8	506.4	508.0	509.6	511.2	512.8	2.600
2.700	512.8	514.4	516.0	517.6	519.2	520.9	522.5	524.1	525.7	527.3	528.9	2.700
2.800	528.9	530.5	532.1	533.7	535.3	536.9	538.5	540.1	541.7	543.4	545.0	2.800
2.900	545.0	546.6	548.2	549.8	551.4	553.0	554.6	556.2	557.8	559.4	561.0	2.900
3.000	561.0	562.6	564.2	565.8	567.4	569.1	570.7	572.3	573.9	575.5	577.1	3.000
3.100	577.1	578.7	580.3	581.9	583.5	585.1	586.7	588.3	589.9	591.6	593.2	3.100
3.200	593.2	594.8	596.4	598.0	599.6	601.2	602.8	604.4	606.0	607.6	609.2	3.200
3.300	609.2	610.9	612.5	614.1	615.7	617.3	618.9	620.5	622.1	623.8	625.4	3.300
3.400	625.4	627.0	628.6	630.2	631.8	633.4	635.0	636.7	638.3	639.9	641.5	3.400
3.500	641.5	643.1	644.7	646.3	647.9	649.5	651.1	652.7	654.3	656.0	657.6	3.500
3.600	657.6	659.2	660.8	662.4	664.0	665.7	667.3	668.9	670.5	672.1	673.8	3.600
3.700	673.8	675.4	677.0	678.6	680.2	681.9	683.5	685.1	686.7	688.4	690.0	3.700
3.800	690.0	691.6	693.2	694.9	696.5	698.1	699.8	701.4	703.0	704.6	706.3	3.800
3.900	706.3	707.9	709.5	711.2	712.8	714.4	716.1	717.7	719.3	721.0	722.6	3.900
4.000	722.6	724.2	725.9	727.5	729.1	730.8	732.4	734.1	735.7	737.3	739.0	4.000
4.100	739.0	740.6	742.3	743.9	745.6	747.2	748.8	750.5	752.1	753.8	755.4	4.100
4.200	755.4	757.1	758.7	760.4	762.0	763.7	765.3	767.0	768.6	770.3	771.9	4.200
4.300	771.9	773.6	775.2	776.9	778.5	780.2	781.9	783.5	785.2	786.8	788.5	4.300
4.400	788.5	790.1	791.8	793.5	795.1	796.8	798.5	800.1	801.8	803.5	805.1	4.400
4.500	805.1	806.8	808.5	810.1	811.8	813.5	815.1	816.8	818.5	820.1	821.8	4.500
4.600	821.8	823.5	825.2	826.8	828.5	830.2	831.9	833.5	835.2	836.9	838.6	4.600
4.700	838.6	840.3	841.9	843.6	845.3	847.0	848.7	850.4	852.1	853.7	855.4	4.700
4.800	855.4	857.1	858.8	860.5	862.2	863.9	865.6	867.3	869.0	870.7	872.3	4.800
4.900	872.3	874.0	875.7	877.4	879.1	880.8	882.5	884.2	885.9	887.6	889.3	4.900

TABLE 5–A. *Fifty percent iridium-fifty percent rhodium versus iridium thermocouples*—Continued

Electromotive force in absolute millivolts. Temperatures in degrees C (Int. 1948). Reference junctions at 0 °C.

Millivolts	.000	.010	.020	.030	.040	.050	.060	.070	.080	.090	.100	Millivolts
	Degrees C											
5.000	889.3	891.0	892.7	894.5	896.2	897.9	899.6	901.3	903.0	904.7	906.4	5.000
5.100	906.4	908.1	909.8	911.5	913.3	915.0	916.7	918.4	920.1	921.8	923.6	5.100
5.200	923.6	925.3	927.0	928.7	930.4	932.2	933.9	935.6	937.3	939.0	940.8	5.200
5.300	940.8	942.5	944.2	946.0	947.7	949.4	951.1	952.9	954.6	956.3	958.1	5.300
5.400	958.1	959.8	961.5	963.3	965.0	966.8	968.5	970.2	972.0	973.7	975.5	5.400
5.500	975.5	977.2	978.9	980.7	982.4	984.2	985.9	987.7	989.4	991.2	992.9	5.500
5.600	992.9	994.7	996.4	998.2	999.9	1001.7	1003.4	1005.2	1006.9	1008.7	1010.4	5.600
5.700	1010.4	1012.2	1014.0	1015.7	1017.5	1019.2	1021.0	1022.8	1024.5	1026.3	1028.1	5.700
5.800	1028.1	1029.8	1031.6	1033.4	1035.1	1036.9	1038.7	1040.4	1042.2	1044.0	1045.7	5.800
5.900	1045.7	1047.5	1049.3	1051.1	1052.8	1054.6	1056.4	1058.2	1059.9	1061.7	1063.5	5.900
6.000	1063.5	1065.3	1067.1	1068.8	1070.6	1072.4	1074.2	1076.0	1077.7	1079.5	1081.3	6.000
6.100	1081.3	1083.1	1084.9	1086.7	1088.5	1090.3	1092.0	1093.8	1095.6	1097.4	1099.2	6.100
6.200	1099.2	1101.0	1102.8	1104.6	1106.4	1108.2	1110.0	1111.8	1113.6	1115.4	1117.2	6.200
6.300	1117.2	1119.0	1120.8	1122.6	1124.4	1126.2	1128.0	1129.8	1131.6	1133.4	1135.2	6.300
6.400	1135.2	1137.0	1138.8	1140.6	1142.4	1144.2	1146.0	1147.8	1149.6	1151.5	1153.3	6.400
6.500	1153.3	1155.1	1156.9	1158.7	1160.5	1162.3	1164.1	1166.0	1167.8	1169.6	1171.4	6.500
6.600	1171.4	1173.2	1175.0	1176.8	1178.7	1180.5	1182.3	1184.1	1185.9	1187.8	1189.6	6.600
6.700	1189.6	1191.4	1193.2	1195.0	1196.9	1198.7	1200.5	1202.3	1204.2	1206.0	1207.8	6.700
6.800	1207.8	1209.6	1211.5	1213.3	1215.1	1216.9	1218.8	1220.6	1222.4	1224.2	1226.1	6.800
6.900	1226.1	1227.9	1229.7	1231.6	1233.4	1235.2	1237.1	1238.9	1240.7	1242.6	1244.4	6.900
7.000	1244.4	1246.2	1248.0	1249.9	1251.7	1253.5	1255.4	1257.2	1259.1	1260.9	1262.7	7.000
7.100	1262.7	1264.6	1266.4	1268.2	1270.1	1271.9	1273.7	1275.6	1277.4	1279.2	1281.1	7.100
7.200	1281.1	1282.9	1284.8	1286.6	1288.4	1290.3	1292.1	1294.0	1295.8	1297.6	1299.5	7.200
7.300	1299.5	1301.3	1303.1	1305.0	1306.8	1308.7	1310.5	1312.3	1314.2	1316.0	1317.9	7.300
7.400	1317.9	1319.7	1321.5	1323.4	1325.2	1327.1	1328.9	1330.8	1332.6	1334.4	1336.3	7.400
7.500	1336.3	1338.1	1340.0	1341.8	1343.6	1345.5	1347.3	1349.2	1351.0	1352.8	1354.7	7.500
7.600	1354.7	1356.5	1358.4	1360.2	1362.0	1363.9	1365.7	1367.6	1369.4	1371.3	1373.1	7.600
7.700	1373.1	1374.9	1376.8	1378.6	1380.5	1382.3	1384.1	1386.0	1387.8	1389.7	1391.5	7.700
7.800	1391.5	1393.3	1395.2	1397.0	1398.9	1400.7	1402.5	1404.4	1406.2	1408.0	1409.9	7.800
7.900	1409.9	1411.7	1413.6	1415.4	1417.2	1419.1	1420.9	1422.7	1424.6	1426.4	1428.2	7.900
8.000	1428.2	1430.1	1431.9	1433.8	1435.6	1437.4	1439.3	1441.1	1442.9	1444.8	1446.6	8.000
8.100	1446.6	1448.4	1450.3	1452.1	1453.9	1455.8	1457.6	1459.4	1461.2	1463.1	1464.9	8.100
8.200	1464.9	1466.7	1468.6	1470.4	1472.2	1474.1	1475.9	1477.7	1479.5	1481.4	1483.2	8.200
8.300	1483.2	1485.0	1486.8	1488.7	1490.5	1492.3	1494.1	1496.0	1497.8	1499.6	1501.4	8.300
8.400	1501.4	1503.2	1505.1	1506.9	1508.7	1510.5	1512.3	1514.2	1516.0	1517.8	1519.6	8.400
8.500	1519.6	1521.4	1523.2	1525.1	1526.9	1528.7	1530.5	1532.3	1534.1	1535.9	1537.8	8.500
8.600	1537.8	1539.6	1541.4	1543.2	1545.0	1546.8	1548.6	1550.4	1552.2	1554.0	1555.8	8.600
8.700	1555.8	1557.7	1559.5	1561.3	1563.1	1564.9	1566.7	1568.5	1570.3	1572.1	1573.9	8.700
8.800	1573.9	1575.7	1577.5	1579.3	1581.1	1582.9	1584.7	1586.5	1588.3	1590.1	1591.9	8.800
8.900	1591.9	1593.6	1595.4	1597.2	1599.0	1600.8	1602.6	1604.4	1606.2	1608.0	1609.8	8.900
9.000	1609.8	1611.5	1613.3	1615.1	1616.9	1618.7	1620.5	1622.3	1624.0	1625.8	1627.6	9.000
9.100	1627.6	1629.4	1631.2	1632.9	1634.7	1636.5	1638.3	1640.0	1641.8	1643.6	1645.4	9.100
9.200	1645.4	1647.1	1648.9	1650.7	1652.5	1654.2	1656.0	1657.8	1659.5	1661.3	1663.1	9.200
9.300	1663.1	1664.8	1666.6	1668.4	1670.1	1671.9	1673.6	1675.4	1677.2	1678.9	1680.7	9.300
9.400	1680.7	1682.4	1684.2	1686.0	1687.7	1689.5	1691.2	1693.0	1694.7	1696.5	1698.2	9.400
9.500	1698.2	1700.0	1701.7	1703.5	1705.2	1707.0	1708.7	1710.5	1712.2	1714.0	1715.7	9.500
9.600	1715.7	1717.4	1719.2	1720.9	1722.7	1724.4	1726.1	1727.9	1729.6	1731.4	1733.1	9.600
9.700	1733.1	1734.8	1736.6	1738.3	1740.0	1741.8	1743.5	1745.2	1747.0	1748.7	1750.4	9.700
9.800	1750.4	1752.1	1753.9	1755.6	1757.3	1759.0	1760.8	1762.5	1764.2	1765.9	1767.6	9.800
9.900	1767.6	1769.4	1771.1	1772.8	1774.5	1776.2	1778.0	1779.7	1781.4	1783.1	1784.8	9.900

TABLE 5–A. *Fifty percent iridium-fifty percent rhodium versus iridium thermocouples*—Continued

Electromotive force in absolute millivolts. Temperatures in degrees C (Int. 1948). Reference junctions at 0 °C.

Millivolts	.000	.010	.020	.030	.040	.050	.060	.070	.080	.090	.100	Millivolts
	Degrees C											
10.000	1784.8	1786.5	1788.2	1789.9	1791.6	1793.4	1795.1	1796.8	1798.5	1800.2	1801.9	10.000
10.100	1801.9	1803.6	1805.3	1807.0	1808.7	1810.4	1812.1	1813.8	1815.5	1817.2	1818.9	10.100
10.200	1818.9	1820.6	1822.3	1824.0	1825.7	1827.4	1829.1	1830.7	1832.4	1834.1	1835.8	10.200
10.300	1835.8	1837.5	1839.2	1840.9	1842.6	1844.3	1845.9	1847.6	1849.3	1851.0	1852.7	10.300
10.400	1852.7	1854.4	1856.0	1857.7	1859.4	1861.1	1862.7	1864.4	1866.1	1867.8	1869.4	10.400
10.500	1869.4	1871.1	1872.8	1874.5	1876.1	1877.8	1879.5	1881.1	1882.8	1884.5	1886.2	10.500
10.600	1886.2	1887.8	1889.5	1891.2	1892.8	1894.5	1896.1	1897.8	1899.5	1901.1	1902.8	10.600
10.700	1902.8	1904.5	1906.1	1907.8	1909.4	1911.1	1912.7	1914.4	1916.1	1917.7	1919.4	10.700
10.800	1919.4	1921.0	1922.7	1924.3	1926.0	1927.6	1929.3	1930.9	1932.6	1934.2	1935.9	10.800
10.900	1935.9	1937.5	1939.2	1940.8	1942.4	1944.1	1945.7	1947.4	1949.0	1950.7	1952.3	10.900
11.000	1952.3	1953.9	1955.6	1957.2	1958.9	1960.5	1962.1	1963.8	1965.4	1967.1	1968.7	11.000
11.100	1968.7	1970.3	1972.0	1973.6	1975.2	1976.9	1978.5	1980.1	1981.8	1983.4	1985.0	11.100
11.200	1985.0	1986.6	1988.3	1989.9	1991.5	1993.2	1994.8	1996.4	1998.0	1999.7	2001.3	11.200
11.300	2001.3	2002.9	2004.5	2006.2	2007.8	2009.4	2011.0	2012.7	2014.3	2015.9	2017.5	11.300
11.400	2017.5	2019.1	2020.8	2022.4	2024.0	2025.6	2027.2	2028.8	2030.5	2032.1	2033.7	11.400
11.500	2033.7	2035.3	2036.9	2038.5	2040.2	2041.8	2043.4	2045.0	2046.6	2048.2	2049.8	11.500
11.600	2049.8	2051.4	2053.1	2054.7	2056.3	2057.9	2059.5	2061.1	2062.7	2064.3	2065.9	11.600
11.700	2065.9	2067.6	2069.2	2070.8	2072.4	2074.0	2075.6	2077.2	2078.8	2080.4	2082.0	11.700
11.800	2082.0	2083.6	2085.2	2086.8	2088.4	2090.0	2091.6	2093.2	2094.9	2096.5	2098.1	11.800
11.900	2098.1	2099.7	2101.3	2102.9	2104.5	2106.1	2107.7	2109.3	2110.9	2112.5	2114.1	11.900
12.000	2114.1	2115.7	2117.3	2118.9	2120.5	2122.1	2123.7	2125.3	2126.9	2128.5	2130.1	12.000
12.100	2130.1	2131.7	2133.3	2134.9	2136.5	2138.1	2139.7	2141.3	2142.9	2144.5	2146.1	12.100
12.200	2146.1	2147.7	2149.3									12.200

TABLE 6–A. *Fifty percent iridium-fifty percent rhodium versus iridium thermocouples*

Electromotive force in absolute millivolts. Temperatures in degrees C (Int. 1948). Reference junctions at 0 °C.

°C	0	10	20	30	40	50	60	70	80	90	100	°C
	Millivolts											
0	0.000	0.033	0.067	0.102	0.138	0.176	0.215	0.255	0.296	0.338	0.381	0
100	0.381	0.426	0.471	0.517	0.564	0.612	0.660	0.710	0.760	0.811	0.862	100
200	0.862	0.915	0.968	1.021	1.076	1.130	1.186	1.242	1.298	1.355	1.412	200
300	1.412	1.470	1.528	1.587	1.646	1.705	1.764	1.824	1.884	1.945	2.005	300
400	2.005	2.066	2.127	2.188	2.250	2.311	2.373	2.434	2.496	2.558	2.620	400
500	2.620	2.683	2.745	2.807	2.869	2.931	2.994	3.056	3.118	3.180	3.243	500
600	3.243	3.305	3.367	3.429	3.491	3.553	3.615	3.677	3.738	3.800	3.862	600
700	3.862	3.923	3.984	4.045	4.106	4.167	4.228	4.288	4.349	4.409	4.469	700
800	4.469	4.529	4.589	4.649	4.708	4.768	4.827	4.886	4.945	5.004	5.063	800
900	5.063	5.121	5.179	5.237	5.296	5.353	5.411	5.469	5.526	5.583	5.640	900
1000	5.640	5.697	5.754	5.811	5.868	5.924	5.980	6.037	6.093	6.149	6.204	1000
1100	6.204	6.260	6.316	6.371	6.427	6.482	6.537	6.592	6.647	6.702	6.757	1100
1200	6.757	6.812	6.867	6.921	6.976	7.031	7.085	7.140	7.194	7.249	7.303	1200
1300	7.303	7.357	7.412	7.466	7.520	7.575	7.629	7.683	7.738	7.792	7.846	1300
1400	7.846	7.901	7.955	8.010	8.064	8.119	8.173	8.228	8.283	8.337	8.392	1400
1500	8.392	8.447	8.502	8.557	8.612	8.668	8.723	8.778	8.834	8.890	8.945	1500
1600	8.945	9.001	9.057	9.114	9.170	9.226	9.283	9.339	9.396	9.453	9.510	1600
1700	9.510	9.567	9.625	9.682	9.740	9.798	9.856	9.914	9.972	10.030	10.089	1700
1800	10.089	10.148	10.207	10.266	10.325	10.384	10.444	10.503	10.563	10.623	10.683	1800
1900	10.683	10.743	10.804	10.864	10.925	10.986	11.047	11.108	11.169	11.231	11.292	1900
2000	11.292	11.354	11.415	11.477	11.539	11.601	11.663	11.725	11.787	11.850	11.912	2000
2100	11.912	11.974	12.037	12.099	12.162	12.224						2100

TABLE 7–A. *Fifty percent iridium-fifty percent rhodium versus iridium thermocouples*

Electromotive force in absolute millivolts. Temperatures in degrees F*. Reference junctions at 32 °F.

Millivolts	.000	.010	.020	.030	.040	.050	.060	.070	.080	.090	.100	Millivolts
	Degrees F											
0.000	32.0	37.6	43.1	48.6	53.9	59.3	64.5	69.7	74.9	80.0	85.0	0.000
0.100	85.0	90.0	95.0	99.9	104.8	109.6	114.4	119.1	123.8	128.5	133.1	0.100
0.200	133.1	137.7	142.3	146.8	151.3	155.8	160.2	164.6	169.0	173.4	177.7	0.200
0.300	177.7	182.0	186.3	190.5	194.8	199.0	203.1	207.3	211.4	215.5	219.6	0.300
0.400	219.6	223.7	227.8	231.8	235.8	239.8	243.8	247.7	251.7	255.6	259.5	0.400
0.500	259.5	263.4	267.3	271.1	275.0	278.8	282.6	286.4	290.2	293.9	297.7	0.500
0.600	297.7	301.4	305.2	308.9	312.6	316.3	319.9	323.6	327.3	330.9	334.5	0.600
0.700	334.5	338.1	341.7	345.3	348.9	352.5	356.1	359.6	363.2	366.7	370.2	0.700
0.800	370.2	373.7	377.2	380.7	384.2	387.7	391.2	394.6	398.1	401.5	404.9	0.800
0.900	404.9	408.4	411.8	415.2	418.6	422.0	425.4	428.7	432.1	435.5	438.8	0.900
1.000	438.8	442.2	445.5	448.9	452.2	455.5	458.8	462.1	465.4	468.7	472.0	1.000
1.100	472.0	475.3	478.6	481.8	485.1	488.4	491.6	494.9	498.1	501.3	504.6	1.100
1.200	504.6	507.8	511.0	514.2	517.4	520.6	523.8	527.0	530.2	533.4	536.6	1.200
1.300	536.6	539.8	542.9	546.1	549.3	552.4	555.6	558.7	561.9	565.0	568.2	1.300
1.400	568.2	571.3	574.4	577.5	580.7	583.8	586.9	590.0	593.1	596.2	599.3	1.400
1.500	599.3	602.4	605.5	608.6	611.7	614.7	617.8	620.9	624.0	627.0	630.1	1.500
1.600	630.1	633.2	636.2	639.3	642.3	645.4	648.4	651.5	654.5	657.5	660.6	1.600
1.700	660.6	663.6	666.6	669.7	672.7	675.7	678.7	681.7	684.7	687.8	690.8	1.700
1.800	690.8	693.8	696.8	699.8	702.8	705.8	708.8	711.8	714.7	717.7	720.7	1.800
1.900	720.7	723.7	726.7	729.7	732.6	735.6	738.6	741.6	744.5	747.5	750.5	1.900
2.000	750.5	753.4	756.4	759.4	762.3	765.3	768.2	771.2	774.1	777.1	780.1	2.000
2.100	780.1	783.0	785.9	788.9	791.8	794.8	797.7	800.7	803.6	806.5	809.5	2.100
2.200	809.5	812.4	815.3	818.3	821.2	824.1	827.1	830.0	832.9	835.8	838.8	2.200
2.300	838.8	841.7	844.6	847.5	850.5	853.4	856.3	859.2	862.1	865.0	868.0	2.300
2.400	868.0	870.9	873.8	876.7	879.6	882.5	885.4	888.3	891.2	894.1	897.1	2.400
2.500	897.1	900.0	902.9	905.8	908.7	911.6	914.5	917.4	920.3	923.2	926.1	2.500
2.600	926.1	929.0	931.9	934.8	937.7	940.6	943.5	946.4	949.3	952.2	955.1	2.600
2.700	955.1	958.0	960.9	963.8	966.6	969.5	972.4	975.3	978.2	981.1	984.0	2.700
2.800	984.0	986.9	989.8	992.7	995.6	998.5	1001.4	1004.3	1007.1	1010.0	1012.9	2.800
2.900	1012.9	1015.8	1018.7	1021.6	1024.5	1027.4	1030.3	1033.2	1036.1	1038.9	1041.8	2.900
3.000	1041.8	1044.7	1047.6	1050.5	1053.4	1056.3	1059.2	1062.1	1065.0	1067.9	1070.8	3.000
3.100	1070.8	1073.7	1076.6	1079.4	1082.3	1085.2	1088.1	1091.0	1093.9	1096.8	1099.7	3.100
3.200	1099.7	1102.6	1105.5	1108.4	1111.2	1114.1	1117.0	1119.9	1122.8	1125.7	1128.6	3.200
3.300	1128.6	1131.5	1134.4	1137.3	1140.2	1143.1	1146.0	1148.9	1151.8	1154.7	1157.6	3.300
3.400	1157.6	1160.5	1163.4	1166.3	1169.2	1172.1	1175.0	1177.9	1180.8	1183.7	1186.6	3.400
3.500	1186.6	1189.5	1192.4	1195.3	1198.2	1201.1	1204.0	1206.9	1209.8	1212.7	1215.6	3.500
3.600	1215.6	1218.5	1221.5	1224.4	1227.3	1230.2	1233.1	1236.0	1238.9	1241.9	1244.8	3.600
3.700	1244:8	1247.7	1250.6	1253.5	1256.4	1259.4	1262.3	1265.2	1268.1	1271.1	1274.0	3.700
3.800	1274.0	1276.9	1279.8	1282.8	1285.7	1288.6	1291.6	1294.5	1297.4	1300.4	1303.3	3.800
3.900	1303.3	1306.2	1309.2	1312.1	1315.0	1318.0	1320.9	1323.8	1326.8	1329.7	1332.7	3.900
4.000	1332.7	1335.6	1338.6	1341.5	1344.5	1347.4	1350.4	1353.3	1356.3	1359.2	1362.2	4.000
4.100	1362.2	1365.1	1368.1	1371.0	1374.0	1377.0	1379.9	1382.9	1385.8	1388.8	1391.8	4.100
4.200	1391.8	1394.7	1397.7	1400.7	1403.6	1406.6	1409.6	1412.5	1415.5	1418.5	1421.5	4.200
4.300	1421.5	1424.4	1427.4	1430.4	1433.4	1436.4	1439.3	1442.3	1445.3	1448.3	1451.3	4.300
4.400	1451.3	1454.3	1457.3	1460.2	1463.2	1466.2	1469.2	1472.2	1475.2	1478.2	1481.2	4.400
4.500	1481.2	1484.2	1487.2	1490.2	1493.2	1496.2	1499.2	1502.2	1505.2	1508.3	1511.3	4.500
4.600	1511.3	1514.3	1517.3	1520.3	1523.3	1526.3	1529.4	1532.4	1535.4	1538.4	1541.5	4.600
4.700	1541.5	1544.5	1547.5	1550.5	1553.6	1556.6	1559.6	1562.7	1565.7	1568.7	1571.8	4.700
4.800	1571.8	1574.8	1577.9	1580.9	1583.9	1587.0	1590.0	1593.1	1596.1	1599.2	1602.2	4.800
4.900	1602.2	1605.3	1608.3	1611.4	1614.4	1617.5	1620.6	1623.6	1626.7	1629.7	1632.8	4.900

*Based on the International Temperature Scale of 1948.

TABLE 7–A. *Fifty percent iridium-fifty percent rhodium versus iridium thermocouples*—Continued

Electromotive force in absolute millivolts. Temperature in degrees F*. Reference junctions at 32 °F.

Millivolts	.000	.010	.020	.030	.040	.050	.060	.070	.080	.090	.100	Millivolts
	Degrees F											
5.000	1632.8	1635.9	1638.9	1642.0	1645.1	1648.2	1651.2	1654.3	1657.4	1660.5	1663.5	5.000
5.100	1663.5	1666.6	1669.7	1672.8	1675.9	1678.9	1682.0	1685.1	1688.2	1691.3	1694.4	5.100
5.200	1694.4	1697.5	1700.6	1703.7	1706.8	1709.9	1713.0	1716.1	1719.2	1722.3	1725.4	5.200
5.300	1725.4	1728.5	1731.6	1734.7	1737.8	1740.9	1744.1	1747.2	1750.3	1753.4	1756.5	5.300
5.400	1756.5	1759.7	1762.8	1765.9	1769.0	1772.2	1775.3	1778.4	1781.6	1784.7	1787.8	5.400
5.500	1787.8	1791.0	1794.1	1797.2	1800.4	1803.5	1806.7	1809.8	1812.9	1816.1	1819.2	5.500
5.600	1819.2	1822.4	1825.5	1828.7	1831.9	1835.0	1838.2	1841.3	1844.5	1847.6	1850.8	5.600
5.700	1850.8	1854.0	1857.1	1860.3	1863.5	1866.6	1869.8	1873.0	1876.1	1879.3	1882.5	5.700
5.800	1882.5	1885.7	1888.9	1892.0	1895.2	1898.4	1901.6	1904.8	1908.0	1911.1	1914.3	5.800
5.900	1914.3	1917.5	1920.7	1923.9	1927.1	1930.3	1933.5	1936.7	1939.9	1943.1	1946.3	5.900
6.000	1946.3	1949.5	1952.7	1955.9	1959.1	1962.3	1965.5	1968.7	1971.9	1975.2	1978.4	6.000
6.100	1978.4	1981.6	1984.8	1988.0	1991.2	1994.5	1997.7	2000.9	2004.1	2007.4	2010.6	6.100
6.200	2010.6	2013.8	2017.0	2020.3	2023.5	2026.7	2030.0	2033.2	2036.4	2039.7	2042.9	6.200
6.300	2042.9	2046.1	2049.4	2052.6	2055.9	2059.1	2062.4	2065.6	2068.8	2072.1	2075.3	6.300
6.400	2075.3	2078.6	2081.8	2085.1	2088.3	2091.6	2094.9	2098.1	2101.4	2104.6	2107.9	6.400
6.500	2107.9	2111.1	2114.4	2117.7	2120.9	2124.2	2127.5	2130.7	2134.0	2137.2	2140.5	6.500
6.600	2140.5	2143.8	2147.1	2150.3	2153.6	2156.9	2160.1	2163.4	2166.7	2170.0	2173.2	6.600
6.700	2173.2	2176.5	2179.8	2183.1	2186.4	2189.6	2192.9	2196.2	2199.5	2202.8	2206.1	6.700
6.800	2206.1	2209.3	2212.6	2215.9	2219.2	2222.5	2225.8	2229.1	2232.4	2235.7	2238.9	6.800
6.900	2238.9	2242.2	2245.5	2248.8	2252.1	2255.4	2258.7	2262.0	2265.3	2268.6	2271.9	6.900
7.000	2271.9	2275.2	2278.5	2281.8	2285.1	2288.4	2291.7	2295.0	2298.3	2301.6	2304.9	7.000
7.100	2304.9	2308.2	2311.5	2314.8	2318.1	2321.4	2324.7	2328.0	2331.3	2334.6	2338.0	7.100
7.200	2338.0	2341.3	2344.6	2347.9	2351.2	2354.5	2357.8	2361.1	2364.4	2367.7	2371.0	7.200
7.300	2371.0	2374.4	2377.7	2381.0	2384.3	2387.6	2390.9	2394.2	2397.5	2400.8	2404.2	7.300
7.400	2404.2	2407.5	2410.8	2414.1	2417.4	2420.7	2424.0	2427.4	2430.7	2434.0	2437.3	7.400
7.500	2437.3	2440.6	2443.9	2447.2	2450.6	2453.9	2457.2	2460.5	2463.8	2467.1	2470.4	7.500
7.600	2470.4	2473.7	2477.1	2480.4	2483.7	2487.0	2490.3	2493.6	2496.9	2500.3	2503.6	7.600
7.700	2503.6	2506.9	2510.2	2513.5	2516.8	2520.1	2523.4	2526.8	2530.1	2533.4	2536.7	7.700
7.800	2536.7	2540.0	2543.3	2546.6	2549.9	2553.2	2556.6	2559.9	2563.2	2566.5	2569.8	7.800
7.900	2569.8	2573.1	2576.4	2579.7	2583.0	2586.3	2589.6	2592.9	2596.2	2599.5	2602.9	7.900
8.000	2602.9	2606.2	2609.5	2612.8	2616.1	2619.4	2622.7	2626.0	2629.3	2632.6	2635.9	8.000
8.100	2635.9	2639.2	2642.5	2645.8	2649.1	2652.4	2655.7	2658.9	2662.2	2665.5	2668.8	8.100
8.200	2668.8	2672.1	2675.4	2678.7	2682.0	2685.3	2688.6	2691.9	2695.2	2698.4	2701.7	8.200
8.300	2701.7	2705.0	2708.3	2711.6	2714.9	2718.2	2721.4	2724.7	2728.0	2731.3	2734.6	8.300
8.400	2734.6	2737.8	2741.1	2744.4	2747.7	2750.9	2754.2	2757.5	2760.8	2764.0	2767.3	8.400
8.500	2767.3	2770.6	2773.8	2777.1	2780.4	2783.6	2786.9	2790.2	2793.4	2796.7	2800.0	8.500
8.600	2800.0	2803.2	2806.5	2809.7	2813.0	2816.3	2819.5	2822.8	2826.0	2829.3	2832.5	8.600
8.700	2832.5	2835.8	2839.0	2842.3	2845.5	2848.8	2852.0	2855.3	2858.5	2861.7	2865.0	8.700
8.800	2865.0	2868.2	2871.5	2874.7	2877.9	2881.2	2884.4	2887.6	2890.9	2894.1	2897.3	8.800
8.900	2897.3	2900.6	2903.8	2907.0	2910.2	2913.5	2916.7	2919.9	2923.1	2926.3	2929.6	8.900
9.000	2929.6	2932.8	2936.0	2939.2	2942.4	2945.6	2948.8	2952.1	2955.3	2958.5	2961.7	9.000
9.100	2961.7	2964.9	2968.1	2971.3	2974.5	2977.7	2980.9	2984.1	2987.3	2990.5	2993.7	9.100
9.200	2993.7	2996.8	3000.0	3003.2	3006.4	3009.6	3012.8	3016.0	3019.2	3022.3	3025.5	9.200
9.300	3025.5	3028.7	3031.9	3035.0	3038.2	3041.4	3044.6	3047.7	3050.9	3054.1	3057.2	9.300
9.400	3057.2	3060.4	3063.6	3066.7	3069.9	3073.0	3076.2	3079.4	3082.5	3085.7	3088.8	9.400
9.500	3088.8	3092.0	3095.1	3098.3	3101.4	3104.6	3107.7	3110.8	3114.0	3117.1	3120.3	9.500
9.600	3120.3	3123.4	3126.5	3129.7	3132.8	3135.9	3139.1	3142.2	3145.3	3148.5	3151.6	9.600
9.700	3151.6	3154.7	3157.8	3160.9	3164.1	3167.2	3170.3	3173.4	3176.5	3179.6	3182.7	9.700
9.800	3182.7	3185.9	3189.0	3192.1	3195.2	3198.3	3201.4	3204.5	3207.6	3210.7	3213.8	9.800
9.900	3213.8	3216.9	3220.0	3223.0	3226.1	3229.2	3232.3	3235.4	3238.5	3241.6	3244.7	9.900

*Based on the International Temperature Scale of 1948.

TABLE 7–A. *Fifty percent iridium-fifty percent rhodium versus iridium thermocouples*—Continued

Electromotive force in absolute millivolts. Temperature in degrees F*. Reference junctions at 32 °F.

Millivolts	.000	.010	.020	.030	.040	.050	.060	.070	.080	.090	.100	Millivolts
	Degrees F											
10.000	3244.7	3247.7	3250.8	3253.9	3257.0	3260.0	3263.1	3266.2	3269.3	3272.3	3275.4	10.000
10.100	3275.4	3278.5	3281.5	3284.6	3287.7	3290.7	3293.8	3296.8	3299.9	3302.9	3306.0	10.100
10.200	3306.0	3309.1	3312.1	3315.2	3318.2	3321.3	3324.3	3327.3	3330.4	3333.4	3336.5	10.200
10.300	3336.5	3339.5	3342.5	3345.6	3348.6	3351.7	3354.7	3357.7	3360.7	3363.8	3366.8	10.300
10.400	3366.8	3369.8	3372.9	3375.9	3378.9	3381.9	3384.9	3388.0	3391.0	3394.0	3397.0	10.400
10.500	3397.0	3400.0	3403.0	3406.0	3409.0	3412.1	3415.1	3418.1	3421.1	3424.1	3427.1	10.500
10.600	3427.1	3430.1	3433.1	3436.1	3439.1	3442.1	3445.1	3448.0	3451.0	3454.0	3457.0	10.600
10.700	3457.0	3460.0	3463.0	3466.0	3469.0	3471.9	3474.9	3477.9	3480.9	3483.9	3486.8	10.700
10.800	3486.8	3489.8	3492.8	3495.8	3498.7	3501.7	3504.7	3507.7	3510.6	3513.6	3516.6	10.800
10.900	3516.6	3519.5	3522.5	3525.4	3528.4	3531.4	3534.3	3537.3	3540.2	3543.2	3546.1	10.900
11.000	3546.1	3549.1	3552.1	3555.0	3558.0	3560.9	3563.9	3566.8	3569.8	3572.7	3575.6	11.000
11.100	3575.6	3578.6	3581.5	3584.5	3587.4	3590.3	3593.3	3596.2	3599.2	3602.1	3605.0	11.100
11.200	3605.0	3608.0	3610.9	3613.8	3616.8	3619.7	3622.6	3625.5	3628.5	3631.4	3634.3	11.200
11.300	3634.3	3637.2	3640.2	3643.1	3646.0	3648.9	3651.9	3654.8	3657.7	3660.6	3663.5	11.300
11.400	3663.5	3666.4	3669.4	3672.3	3675.2	3678.1	3681.0	3683.9	3686.8	3689.7	3692.7	11.400
11.500	3692.7	3695.6	3698.5	3701.4	3704.3	3707.2	3710.1	3713.0	3715.9	3718.8	3721.7	11.500
11.600	3721.7	3724.6	3727.5	3730.4	3733.3	3736.2	3739.1	3742.0	3744.9	3747.8	3750.7	11.600
11.700	3750.7	3753.6	3756.5	3759.4	3762.3	3765.2	3768.1	3771.0	3773.8	3776.7	3779.6	11.700
11.800	3779.6	3782.5	3785.4	3788.3	3791.2	3794.1	3797.0	3799.8	3802.7	3805.6	3808.5	11.800
11.900	3808.5	3811.4	3814.3	3817.2	3820.0	3822.9	3825.8	3828.7	3831.6	3834.5	3837.4	11.900
12.000	3837.4	3840.2	3843.1	3846.0	3848.9	3851.8	3854.6	3857.5	3860.4	3863.3	3866.2	12.000
12.100	3866.2	3869.1	3871.9	3874.8	3877.7	3880.6	3883.5	3886.3	3889.2	3892.1	3895.0	12.100
12.200	3895.0	3897.8	3900.7									12.200

*Based on the International Temperature Scale of 1948.

TABLE 8–A. *Fifty percent iridium-fifty percent rhodium versus iridium thermocouples*

Electromotive force in absolute millivolts. Temperature in degrees F*. Reference junctions at 32 °F.

°F	0	10	20	30	40	50	60	70	80	90	100	°F
	Millivolts											
0					0.014	0.033	0.051	0.071	0.090	0.110	0.130	0
100	0.130	0.151	0.172	0.193	0.215	0.237	0.259	0.282	0.305	0.329	0.352	100
200	0.352	0.377	0.401	0.426	0.451	0.476	0.501	0.527	0.553	0.580	0.606	200
300	0.606	0.633	0.660	0.688	0.715	0.743	0.771	0.799	0.828	0.857	0.886	300
400	0.886	0.915	0.944	0.974	1.003	1.033	1.064	1.094	1.124	1.155	1.186	400
500	1.186	1.217	1.248	1.279	1.311	1.342	1.374	1.406	1.438	1.470	1.502	500
600	1.502	1.535	1.567	1.600	1.632	1.665	1.698	1.731	1.764	1.797	1.831	600
700	1.831	1.864	1.898	1.931	1.965	1.998	2.032	2.066	2.100	2.134	2.168	700
800	2.168	2.202	2.236	2.270	2.304	2.338	2.373	2.407	2.441	2.476	2.510	800
900	2.510	2.545	2.579	2.613	2.648	2.683	2.717	2.752	2.786	2.821	2.855	900
1000	2.855	2.890	2.924	2.959	2.994	3.028	3.063	3.097	3.132	3.167	3.201	1000
1100	3.201	3.236	3.270	3.305	3.339	3.374	3.408	3.443	3.477	3.512	3.546	1100
1200	3.546	3.581	3.615	3.649	3.684	3.718	3.752	3.786	3.821	3.855	3.889	1200
1300	3.889	3.923	3.957	3.991	4.025	4.059	4.093	4.127	4.160	4.194	4.228	1300
1400	4.228	4.261	4.295	4.329	4.362	4.396	4.429	4.463	4.496	4.529	4.563	1400
1500	4.563	4.596	4.629	4.662	4.695	4.728	4.761	4.794	4.827	4.860	4.893	1500
1600	4.893	4.925	4.958	4.991	5.023	5.056	5.089	5.121	5.153	5.186	5.218	1600
1700	5.218	5.250	5.283	5.315	5.347	5.379	5.411	5.443	5.475	5.507	5.539	1700
1800	5.539	5.571	5.602	5.634	5.666	5.697	5.729	5.761	5.792	5.824	5.855	1800
1900	5.855	5.886	5.918	5.949	5.980	6.012	6.043	6.074	6.105	6.136	6.167	1900
2000	6.167	6.198	6.229	6.260	6.291	6.322	6.353	6.384	6.414	6.445	6.476	2000
2100	6.476	6.507	6.537	6.568	6.598	6.629	6.660	6.690	6.721	6.751	6.782	2100
2200	6.782	6.812	6.842	6.873	6.903	6.934	6.964	6.994	7.025	7.055	7.085	2200
2300	7.085	7.115	7.146	7.176	7.206	7.236	7.267	7.297	7.327	7.357	7.387	2300
2400	7.387	7.418	7.448	7.478	7.508	7.538	7.569	7.599	7.629	7.659	7.689	2400
2500	7.689	7.719	7.750	7.780	7.810	7.840	7.870	7.901	7.931	7.961	7.991	2500
2600	7.991	8.022	8.052	8.082	8.113	8.143	8.173	8.204	8.234	8.264	8.295	2600
2700	8.295	8.325	8.356	8.386	8.417	8.447	8.478	8.508	8.539	8.569	8.600	2700
2800	8.600	8.631	8.661	8.692	8.723	8.754	8.785	8.815	8.846	8.877	8.908	2800
2900	8.908	8.939	8.970	9.001	9.032	9.064	9.095	9.126	9.157	9.189	9.220	2900
3000	9.220	9.251	9.283	9.314	9.346	9.377	9.409	9.440	9.472	9.504	9.535	3000
3100	9.535	9.567	9.599	9.631	9.663	9.695	9.727	9.759	9.791	9.823	9.856	3100
3200	9.856	9.888	9.920	9.952	9.985	10.017	10.050	10.082	10.115	10.148	10.180	3200
3300	10.180	10.213	10.246	10.279	10.312	10.345	10.378	10.411	10.444	10.477	10.510	3300
3400	10.510	10.543	10.576	10.610	10.643	10.677	10.710	10.743	10.777	10.811	10.844	3400
3500	10.844	10.878	10.912	10.945	10.979	11.013	11.047	11.081	11.115	11.149	11.183	3500
3600	11.183	11.217	11.251	11.285	11.319	11.354	11.388	11.422	11.457	11.491	11.525	3600
3700	11.525	11.560	11.594	11.629	11.663	11.698	11.732	11.767	11.801	11.836	11.871	3700
3800	11.871	11.905	11.940	11.974	12.009	12.044	12.079	12.113	12.148	12.183	12.217	3800
3900	12.217											3900

*Based on the International Temperature Scale of 1948.

TABLE 9–A. *Iridium-rhodium versus iridium thermocouples Electromotive force in absolute millivolts*

Temperatures in degrees F. Reference junctions at 32° F.

Temperature	10% Rh	25% Rh	75% Rh	90% Rh
°F	*Millivolts*	*Millivolts*	*Millivolts*	*Millivolts*
32	0	0	0	0
100	.052	.105	.088	.031
200	.146	.289	.240	.092
300	.260	.502	.416	.168
400	.392	.739	.611	.260
500	.536	.995	.822	.366
600	.690	1.266	1.047	.483
700	.852	1.548	1.282	.610
800	1.019	1.836	1.525	.747
900	1.188	2.130	1.774	.889
1000	1.360	2.424	2.025	1.038
1100	1.530	2.719	2.280	1.192
1200	1.700	3.012	2.537	1.349
1300	1.868	3.301	2.793	1.510
1400	2.032	3.585	3.049	1.672
1500	2.192	3.864	3.304	1.836
1600	2.349	4.136	3.558	2.002
1700	2.501	4.402	3.811	2.170
1800	2.649	4.662	4.064	2.342
1900	2.793	4.916	4.316	2.517
2000	2.935	5.163	4.570	2.691
2100	3.076	5.406	4.825	2.865
2200	3.212	5.644	5.082	3.046
2300	3.343	5.877	5.342	3.234
2400	3.472	6.107	5.607	3.437
2500	3.600	6.335	5.876	3.646
2600	3.724	6.561	6.150	3.868
2700	3.846	6.785	6.431	4.098
2800	3.962	7.010	6.718	4.332
2900	4.086	7.234	7.013	4.576
3000	4.203	7.460	7.316	4.830
3100	4.320	7.687	7.626	5.097
3200	4.438	7.917	7.944	5.373
3300	4.556	8.148	8.270	5.653
3400	4.676	8.381	8.602	5.947
3500	4.799	8.617	8.941	6.265
3600	4.926	8.854	9.284	
3700	5.055	9.092	9.631	
3800	5.185	9.330		
3900	5.316	9.567		
4000	5.450	9.805		

TABLE 10–A. *Emf of 50 percent iridium–50 percent rhodium and 60 percent iridium–40 percent rhodium alloys and iridium relative to copper**

Temperature	50% Ir–50% Rh vs Cu	60% Ir–40% Rh vs Cu	Cu vs Ir
°F	*Millivolts*	*Millivolts*	*Millivolts*
32	0.000	0.000	0.000
50	.027	.026	.006
75	.067	.064	.014
100	.107	.103	.023
125	.147	.142	.035
150	.188	.181	.049
175	.228	.220	.065
200	.268	.258	.084
225	.308	.296	.105
250	.347	.334	.129
275	.385	.371	.155
300	.422	.406	.184
350	.496	.477	.247
400	.571	.549	.315
450	.638	.613	.395
500	.701	.673	.485

*These alloys are thermoelectrically positive to copper. Copper is positive to iridium.

8. References

[1] G. F. Blackburn and F. R. Caldwell, Reference tables for 40 percent iridium-60 percent rhodium versus iridium thermocouples, J. Res. NBS **66C** (Engr. and Instr.) No. 1, 1–12 (Jan.–Mar. 1962); Temperature—Its Measurement and Control in Science and Industry **3,** Part 2 (Reinhold Pub. Corp., New York, N.Y., 1962).

[2] J. Hilsenrath, G. G. Ziegler, C. G. Messina, and P. J. Walsh, OMNITAB, a general purpose machine program for the calculation of tables of functions and statistical and numerical analysis of tabular data, to be issued as an NBS publication.

[3] F. R. Caldwell, Thermoelectric properties of platinum-rhodium alloys, BS J. Research **10,** 373 (1933) RP537.

[4] E. D. Zysk, Private communication, January 20, 1960.

[5] J. D. Sine, Pyrometer Supplies Division, Minneapolis-Honeywell Regulator Company, Philadelphia, Pa., private communication to F. R. Caldwell (July 1960).

[6] F. R. Caldwell, Thermocouple materials, NBS Mono. 40, March 1, 1962; Temperature—Its Measurement and Control in Science and Industry **3,** part 2 (Reinhold Pub. Corp., New York, N.Y., 1962).

[7] W. F. Roeser and S. T. Lonberger, Methods of testing thermocouples and thermocouple materials, NBS Cir. 590 (1958) supersedes RP768).

(Paper 68C1–151)

JOURNAL OF RESEARCH of the National Bureau of Standards—C. Engineering and Instrumentation
Vol. 68C, No. 1, January–March 1964

Publications of the National Bureau of Standards*

Selected Abstracts

Recalibration of the NBS glass standards of spectral transmittance, H. J. Keegan, J. C. Schleter, and M. A. Belknap, *J. Res. NBS* **67A** (*Phys. and Chem.*), *No. 6, 577* (*Nov.-Dec. 1963*), *70 cents.*

In 1934, Gibson, Walker, and Brown developed sets of four colored glass filters to serve as working standards of spectral transmittance for checking the reliability of spectrophotometers. Several sets of these glasses were measured carefully and reserved and designated as future reference standards. Duplicate standards evaluated by comparison with the reference standards are available by purchase to the public. The current set of reference standards was established in the years 1945 to 1947, and one of these reference standards (selenium-red) was recalibrated in 1952. This paper reports a recalibration, made in 1961 and 1962, of all four glasses (selenium-red, carbon-yellow, copper-green, cobalt-blue) on three spectrophotometers (Cary 14, Beckman DU, König-Martens). Except for the cobalt-blue standard, the values of spectral transmittance found differ from those previously assigned by amounts differing at some wavelengths by as much as or slightly more than the uncertainties estimated for the present values, though not by amounts exceeding the combined uncertainties of the present and previous determinations. The indicated changes for these three standards are fairly regular, however, and support the view that the selenium-red and carbon-yellow standards are changing chiefly by formation of a reflectance-reducing film on the surfaces. The indicated rate of upward drift is slow, and suggests that it takes about 10 years for the drift to exceed the assigned uncertainty.

Thermal behavior of muscovite sheet mica, S. Ruthberg, *J. Res. NBS* **67A** (*Phys. and Chem.*), *No. 6, 585* (*Nov.-Dec 1963*), *70 cents.*

The three spectral types of muscovite sheet mica, i.e., very pink ruby, light green, and dark green, were subjected to heat treatments at temperatures up to 600 °C. The changes in the apparent optic axial angle and in the absorption spectra (0.3 − 15 μ) were studied along with color.

The differentiation of muscovite sheet according to these spectral types extends to the behavior of apparent optic axial angle and to certain regions of the spectrum under heat treatment. The pink associated absorption region (0.47 to 0.6 μ) can be enhanced or bleached away by appropriate thermal treatment although the associated infrared multiplet at 3 to 3.5 μ is little affected. The absorption band at 12 μ increases in intensity with temperature of treatment. It is suspected that the 0.47 to 0.6 μ absorption is the result of color centers.

Chemical purity by dielectric cryometry, G. S. Ross and L. J. Frolen, *J. Res NBS* **67A** (*Phys. and Chem.*), *No. 6, 607* (*Nov.-Dec. 1963*), *70 cents.*

A consideration of the deficiencies in standard methods used for the cryometric determination of purity has led to a new approach in which the measurement of an intensive rather than an extensive property is the controlling factor. This method, measurement of the dielectric constant as a function of the fraction melted and correlation with the accompanying change in temperature, allows calculation of purity with high precision. The apparatus used and experimental work performed to ascertain the scope of the method are described. Determination of purity for organic compounds with diverse polarizabilities and dipole moments indicate a rather wide applicability of the method. The large change in the dielectric constant of a high purity compound as it passes from solid to liquid state, with an accompanying small change in temperature, may allow automatic control of temperature within extremely narrow limits.

Optimal periodic inspection programs for randomly failing equipment, G. H. Weiss, *J. Res. NBS* **67B** (*Math. and Math. Phys.*), *No. 4, 223–228* (*Oct.–Dec.1963*), *75 cents.*

There have been many analyses made of models for equipment inspection, i.e., where a system may suffer a breakdown, but such an event is only discovered by an inspection. Most analyses assume that the failures follow a negative exponential law which implies that only periodic inspection programs need be considered. Another model which has been analyzed by Barlow, Hunter, and Proschan finds the optimal program of inspections when the equipment reliability function is of general form, but a particular loss function is given. In this paper we find the optimal periodic inspection program for systems which do not have negative exponential reliability functions. These programs have the virtue of simplicity even though they may not be optimal in an absolute sense. Besides the periodic inspection programs, we derive results for random inspection programs.

On the index of refraction of air, the absorption and dispersion of centimeter waves by gases, G. Boudouris. *Translated from French by G. Wm. Curtis, J. Res. NBS* **67D** (*Radio Prop.*), *No. 6, 631, 631–684* (*Nov.–Dec. 1963*), *70 cents.*

The index of refraction, the absorption and dispersion are studied for several gases and vapors (pressure from 0 to 1 atm. temperature from 0 to 50 °C, frequency from 7,000 to 12,000Mc/s). The first part is devoted to a description of the microwave spectrometer used, while the second part is a survey of the several theories implied in the interpretation of the results.

In the third part, we present first the results concerning the index of refraction of atmospheric gases, of dry air and of damp air. Then we study the absorption and dispersion by several vapors, and of ammonia and chloroform, principally. Finally, we indicate a new method making use of gaseous mixtures.

Our original results are discussed and presented within the frame of reference of works of other authors by means of comparison and intensive bibliographis.

Effects of wall perturbations in multimode waveguides, S. W. Maley and E. Bahar, *J. Res. NBS* **68D** (*Radio Sci.*), *No. 1, 35–42* (*Jan. 1964*), *$1.00*

An experimental investigation has been made of the effects of wall perturbations in multimode rectangular waveguides, whose dimensions were such that the modes TE_{n0} for n=1, 2 . . . 15 were propagating modes and all of the others were cut off. Measurements were made at X-band frequencies. The investigation has shown that when the lowest ordered mode is incident upon a perturbation in the waveguide wall, all of the higher ordered propagating modes will be excited in both directions in the waveguide, but the distribution of energy among the modes is critically dependent upon the shape and size of the perturbation.

Measurements on this waveguide with various wall perturbations may be used to gain insight into the effects of ionospheric perturbations on terrestrial VLF propagation.

Bibliography of temperature measurement, July 1960 to December 1962, C. Halpern, *NBS Mono. 27, Suppl. 1* (*Sept. 13, 1963*), *20 cents.*

There are presented in this supplement to NBS Monograph 27, "Bibliography of Temperature Measurement, January 1953 to June 1960" issued April 6, 1961, about 700 additional references to the field of temperature measurement. The period covered is from July 1960 to December 1962 with some earlier references which came to our attention. The arrangement of material is the same as in Monograph 27, and the journal abbreviations used are those employed in Chemical Abstracts.

Tensile and impact properties of selected materials from 20 to 300 ° K, K. A. Warren and R. P. Reed, *NBS Mono. 63 (June 28, 1963), 35 cents.*
The tensile and impact properties of structural materials were experimentally determined at temperatures from 20 to 300 °K. Tensile properties of a few materials were also determined at 4 °K. The materials included forty-two commercial alloys of iron, aluminum, titanium, copper, nickel, and cobalt, and two metal-bonded carbides. The properties experimentally determined were the yield strength, tensile strength, elongation, and reduction of area, the stress versus strain curve, and the impact energy. The test equipment and procedures are described. The individual data are presented in tables, and the average results are displayed in graphs.

Experimental statistics, M. G. Natrella, *NBS Handb. 91 (Aug. 1, 1963), $4.25.*
This Handbook is a collection of statistical procedures which are useful in research and development programs. It is intended for the user with a scientific or engineering background who has an occasional need for statistical techniques, but does not have the time or inclination to become an expert on statistical theory or methodology. It is organized in five sections. Section 1 provides an elementary introduction to basic statistical concepts and furnishes full details on standard statistical techniques for the analysis and interpretation of measurement data. Section 2 provides detailed procedures for the analysis and interpretation of enmerative and classificatory data. Section 3 has to do with the planning and analysis of comparative experiments. Section 4 is devoted to consideration and exemplification of a number of important but as yet non-standard statistical techniques, and to discussion of other special topics. Section 5 contains all the mathematical tables needed for application of the procedures given in Sections 1 through 4.

Proceedings of the 1962 Standards Laboratory Conference, *NBS Misc. Publ. 248 (Aug. 16, 1963), $1.75.*
This publication comprises technical papers together with discussions thereof, presented at the 1962 Standards Laboratory Conference, August 8–10, 1962.

A bibliography of foreign developments in machine translation and information processing, J. L. Walkowicz, *NBS Tech. Note 193 (July 10, 1963), $1.00.*
The bibliography presents 714 references to the literature translated in the Joint Publications Research Service series on foreign developments in machine translation and information processing. In addition to a conventional subject index to the literature cited, a permuted title index is provided as an experiment in the comparative efficiency of two methods of indexing. Also provided are an author index, an index to conferences and organizations cited, and a listing of the original source documents.

Report on technical investigation of odometers, D. R. Mackay, *NBS Tech. Note 195 (Aug. 6, 1963), 25 cents.*
A technical investigation of the accuracy of vehicle odometers was conducted by the Office of Weights and Measures. This report describes (1) the determination of the accuracy of odometers, (2) the identification of the factors that affect accuracy, and (3) the development of testing equipment and procedures to be used in the testing of odometers. Included in the investigation were fifth-wheel tests, road tests, wheel tests, and simulated-road tests. Each type of test is described, and the results discussed.

Report on the investigation of slow-flow meters for fuel oil distribution systems, D. R. Mackay, *NBS Tech. Note 196 (Sept. 5, 1963), 20 cents.*
A recent development in the retail distribution of fuel oil to individual residences and to mobile homes involves the use of small, slow-flow meters. A technical investigation was conducted by the Office of Weights and Measures to develop testing equipment and test procedures that could be used to evaluate the accuracy characteristics of these meters. This report describes the testing systems and test procedures that were developed, as well as the data that were obtained during the course of the investigation.

Research on crystal growth and characterization at the National Bureau of Standards during the period January to June 1963, *Ed. by H. S. Peiser, NBS Tech. Note 197 (Sept. 23, 1963), 30 cents.*
The National Bureau of Standards with partial support from the Advanced Research Projects Agency is continuing diverse research projects on the growth and characterization of crystals. This note summarizes the individual NBS activities in this and closely related fields during January to July 1963. Lists of NBS publications appertaining to that period and of participating NBS scientists are appended.

Pressure induced shifts of infrared lines due to polar molecules, E. K. Plyler, M. A. Hirshfield, and J. H. Jaffe, *J. Chem. Phys.* **38,** *No. 1, 257–258 (Jan. 1963).*
Most of the studies of pressure induced shifts of lines in the infrared spectra of molecules have been concerned with systems involving noble gases as perturbers. In this communication the problem of polar perturbers is discussed and a striking example is given.

Design of an interferometric oil manometer for vacuum measurement, A. M. Thomas, D. P. Johnson, and J. W. Little, *1962 Trans. Ninth Natl. Vacuum Symp., Am. Vacuum Soc., pp. 468–473 (1962).*
The oil manometer under discussion is one which uses an interferometer to measure the changes in height of the oil surfaces as a change in pressure is applied. Interference fringes are developed between the lower surface of an optical flat and the oil surfaces of the manometer. Di-octyl sebacate is distilled into the manometer after outgassing the system and oil. A fringe shift of fifty-five fringes is produced by a pressure of 10^{-3} torr. A sensitivity of 2×10^{-6} torr can be attained by detecting a shift of one-tenth of a fringe.

Vacuum-tight cylinder joints and ball-and-socket joints, L. A. Guildner and H. F. Stimson, *Rev. Sci. Instr.* **34,** *No. 6, 658–659 (June 1963).*
Two types of vacuum tight joint have been developed for articulation of the connecting lines of a mercury manometer. The design and construction of each joint are described. The cylinder type has a seal around the circumference of a tube. The exit tube of the cylinder joint can be moved in a plane normal to the joint axis. The ball and socket type has a seal around the equator of the ball. The exit tube of the ball and socket joint can be deflected 15°. The joints are packed with Teflon and they remain vacuum tight without causing excessive resistance to movement.

Statistical interpretations, W. J. Youden, *Book, Standard Methods of Chemical Analysis, IIA, ch. 16, 319–325 (D. Van Nostrand Co., Princeton, New Jersy, 1963).*
This paper has been prepared for the chapter on Statistics in the new (6th) edition of Scott's Standard Methods of Chemical Analysis published by Van Nostrand. The first part of the paper goes into detail regarding the steps required to obtain meaningful estimates of the errors in analytical determinations. The remainder takes up a few recurring problems in analytical chemistry along with the appropriate statistical techniques.

Study of Knudsen's method of pressure division as a means of calibrating vacuum gauges, S. Schuhmann, *Trans. Ninth Natl. Vacuum Symp. Am. Vacuum Soc., pp. 463–467 (1962).*
A glass apparatus which enables one to produce low gas pressures in a controlled manner is described. In this apparatus, the gas which is present in a small container of accurately determined volume, at relatively high pressure, escapes into a much larger volume. Boyle's law enables one to calculate the resultant lower pressure. Volume ratios are chosen so as to obtain low pressures covering at least three decades. These ratios are accurate to within 0.5%. Values of pressure obtained in this manner are compared to corresponding values read with an ionization gage.

Design of low voltage electron guns, J. A. Simpson and C. E. Kuyatt, *Rev. Sci. Instr.* **34**, *No. 3, 265–268 (Mar. 1963).*
It is shown that by use of a multi-stage technique in which electrons are drawn from a cathode by a high potential and decelerated to the required final energy, guns can be designed capable of forming beams in which the current is limited only by space charge in the beam itself. The design principles and procedures are given and illustrated by two examples of electron guns giving highly collimated beams and operating at energies of 30 and 500 electron volts. The measured currents obtained are somewhat greater than the space charge limited beam maximum because of ion neutralization.

Plastics, G. M. Kline, *Americana Annual, p. 535 (American Corp., Chicago, Ill., 1963).*
A brief summary of developments in the plastics industry in 1962, prepared by invitation for publication in The 1963 Americana Annual.

Precision of simultaneous measurement procedures, W. A. Thompson, Jr., *J. Am. Stat. Assoc.* **58**, *No. 302, 474–479 (June 1963).*
We consider the problem of measurement under the following conditions: The process of gathering the data is such that on any given item only one opportunity for measurement occurs, but simultaneous observation by several instruments is possible. The items to be measured are variable so that one cannot obtain replicate observations with the same instrument which would show directly the variance of the instrument readings. Procedures are discussed for estimating the precisions of the instruments and the variability of the items being measured.

Mathematical analysis of thermal environment in underground shelters, P. R. Achenbach, T. Kusuda, and F. J. J. Drapeau, *ASHRAE Symp. Survival Shelters, pp. 9–33 (June 1962).*
The National Bureau of Standards has employed numerical methods and some simplified analytical solutions to predict temperatures and humidities in underground shelters. These techniques have been applied to the family-size shelter on the grounds of the National Bureau of Standards, so that comparisons between calculated conditions and those observed during five simulated occupancy tests could be made. In a typical illustration, the predicted shelter air and surface temperatures differed from the observed values by 2 °F or less and the disparity between calculated and observed relative humidities ranged from 0 to 2 percent.

Effect of insulation on the weathering of smooth-surfaced, built-up roofs exposed to solar heating, W. C. Cullen and W. H. Appleton, *Am. Roofer and Building Improvement Building Contractor Mag. pt. I,* **53**, *No. 3, 19–22 (Mar. 1963); pt. II,* **53**, *No. 4, 14 (Apr. 1963).*
The effects of solar heating on the weathering characteristics of smooth-surfaced, built-up roofings applied over insulation are discussed. Data are presented giving the temperatures attained at the underside of smooth-surfaced, built-up roofings placed either over insulation or directly on a concrete deck. Photographs are given showing the differences in the weathering between the insulated and non-insulated roofings observed in the laboratory and in the field. The data show that roofings placed over insulation are subjected to much higher maximum temperatures, more rapid temperature changes, and greater sub-cooling on clear nights than similar roofings placed directly on concrete decks.

The precise evaluation of lens distortion, F. E. Washer, *Photogrammetric Eng., 327–332 (Mar. 1963)*
Four methods of radial distortion measurement are described. Comparison of results obtained on the same lens using each of the four methods is used to locate systematic errors and to evaluate the reliability of each method. Several sources of error are discussed. It is concluded that a precision of ± 2 microns can be achieved using any one of the four methods, provided adequate attention is given to the reduction of all potential errors to negligible proportions; that is, the PE_s of D_β does not exceed 2 microns where D_β is the value of distortion obtained at angle β and PE_s is the probable error of a single determination.

Factorial designs and the direct product, B. Kurkjian and M. Zelen, *Bull. Intern. Stat. Inst.* **XXXIX**, pt. *2, 509–519 (1962).*
This paper presents new notation and associated operations for treating a general factorial experiment, and to apply it to the analysis of confounded asymmetric factorial designs. The aim of the new notation and operations is to unify the analysis of the general problem and make complicated arithmetic operations easy. The chief tool is the use of the direct (or Kronecker) product and its associated operations.

The contact properties of thin films on semiconductors, T. Higier and G. G. Harman, *November 1961 Contact Symp. Proc. Univ. Maine (Mar. 20, 1963).*
The surface and bulk properties of semiconductors have been studied by a two-terminal method using dirty contacts. These contacts are defined as ones that are easily applied and removed and that are separated from the bulk by surface states, oxides, adhered gases, and chemical films. The method essentially involves measuring the resistance-voltage (R–V) characteristics from the millivolt range up to about 100 V, and from these data the sample resistivity can be obtained directly. By observation of the shape of the R–V curves it is possible to separate the bulk from the surface effects, calculate the surface barrier height and thickness from tunneling equations, and determine whether the barrier is a surface film or due to metal-semiconductor contact potential difference. In this paper, an application of the theory of electric field tunneling of Holm to the data of silicon carbide gives values of about 2.4 eV for the barrier height and 13 Å for the barrier width of the film on the surface. For gallium arsenide, these values are about 3.0 eV and 10 Å respectively.

The present status of radiometric calibrations in the ultraviolet spectrum, R. Stair, *Symp. on Military Applications of Ultraviolet Radiation, Rept. No. LAS–TR–199–37 (Nov. 1962).*
Until recently all radiometric calibrations in the ultraviolet spectrum at the National Bureau of Standards were based upon the thermal-radiation standards as established and maintained since 1913 (1, 2, 3). As originally set up these standards were based primarily upon the emission of a blackbody, using the Stefan-Boltzman constant of total radiation $\sigma = 5.70 \times 10^{-12}$ watt/(cm^2 °K^4). A recent review of changes (a) in the atomic constants involved and (b) in probable atmospheric humidities encountered in the calibration of the standards (4) has indicated no need for adjustment of the values assigned to the standards.

Acoustic properties of liquids, M. Greenspan, *Am. Inst. Phys. Handb. 2d Ed. Sec. 3e, pp. 71–82 (1963).*
Tables of acoustical properties of various liquids, abstracted from the literature, are presented.

Gas measurement and other services of the National Bureau of Standards, C. T. Collett, *Am. Gas Assoc. Preprint DMC–63, pp. 1–3 (1963).*
A brief description of the National Bureau of Standards, its staff, physical facilities, and general services, is followed by a discussion of services of particular interest to gas measurement personnel.

Discussion of errors of a recommended standard resistor-noise test system, M. Newman and G. T. Conrad, Jr., *IRE Trans. Component Parts* **CP-9,** *No. 4, 180–192 (Dec. 1962).*
This paper supplements an earlier report which describes a recommended standard resistor-noise test system. It treats of the nautre and the magnitude of the errors associated with the use of the test system. The sources and types of errors are discussed for different operating procedures. Means are provided in summary form for estimating accuracy of current-noise measurements under a broad range of operating conditions.

Conditions for second-order waves in hypo-elasticity, B. Bernstein, *Trans. Soc. Rheology* **VI,** *No. 1, 263–273 (1962).*
The study in hypo-elasticity of second order waves, regarded as propagating singular surfaces of order two in displacement, yields results similar to those in general elasticity theory. The amplitude of a wave must be an eigenvector of a certain matrix, the acoustical tensor, which depends on the stress and direction of propagation, and the product square of the wave speed with the mass density must be the corresponding eigenvalue. Conditions are stated that at least one wave is possible in each direction and that the existence of a longitudinal amplitude imply the possibility of a longitudinal wave. The condition that the acoustical tensor be always symmetric is the same as that of a Cauchy-elastic hypo-elastic material possess a strain energy.

Research in American Society for Testing Materials, B. L. Wilson, *Mater. Res. Std.* **2,** *No. 8, 694–695 (Aug. 1962).*
The early recognition of the importance of research in ASTM is discussed. Attention is called to the importance of the cooperative research done in technical committees and methods of giving appropriate recognition to this work are suggested.

Atomic flame reactions involving N-atoms, H-atoms and ozone, D. Garvin and H. P. Broida, *9th Intern. Combustion Symp., pp. 678–688 (1963).*
Although no radiation is observable from the fast exothermic reaction

$$N+O_3 \rightarrow NO+O_2$$

the addition of H atoms produces a flame with ultraviolet and visible emission. The emitters in the flames are OH, NH, NO, N_2 and, under certain conditions, NH_2.
The characteristics of this prototype combustion system are:
(a) N atoms, H atoms and O_3 must all be present in the reaction zone.
(b) H atoms catalyze the consumption of ozone beyond that expected from $H+O_3 \rightarrow OH+O_2$.
(c) NO and NO_2 are not important intermediates.
(d) The nitrogen emission (1st positive bands) is not the result of the mechanism operating in the Lewis-Rayleigh nitrogen afterglow.
(e) Vibrationally excited OH radicals are important in the mechanism for forming NH and in the excitation of the emitters.
The rate constant for the reaction $N+OH \rightarrow NO+H$ is estimated to be greater than 10^{-11} cc/molecule-second.

The effect of moisture on heat transfer through insulated flat-roof constructions, F. J. Powell, *Suppl. Bull. Intern. Inst. Refrigeration, Annexe 1962–1, 61–70 (Aug. 1962).*
Laboratory determinations were made of the effect of moisture on heat flow in insulated flat-roof constructions exposed to roofing surface temperatures simulating winter and summer conditions with daily solar heating. Two methods of heat transfer measurement were used. One employed heat-flow meters and the other a calorimetric technique. Over a period of six years, 63 specimens were tested. The results indicated that wetted insulation over a vapor barrier and/or a dense concrete deck dried very slowly under the exposure conditions used and that, if initially moist, or wetted by a roof leak, such insulation applications had greatly impaired resistance to heat flow. Some constructions made without vapor barriers, and with under-decks of moderate permeance to water vapor, showed good self-drying characteristics as a result of moisture loss through the under-deck during the summer exposure condition. The insulations in such constructions, if wetted, approached dryness in a period comparable to a year's service. Current research is aimed at determining how heat transmission and self-drying characteristics of wetted insulated constructions are affected by such factors as ambient conditions, the arrangement and thickness of the component materials, and their thermal and moisture permeance and capacity properties.

Convergence to normality of powers of a normal random variable, N. Severo and L. J. Montzingo, Jr., *Bull. Intern. Stat. Inst.* **XXXIX**: *pt. 2, 491–500 (1962).*
Let Y be a normally distributed random variable, and let p be a real number such that y^p is also real, $-\infty \leq y \leq +\infty$. Let μ_y and σ_y be the mean and standard deviation of Y, respectively. Let $X=Y^p$. It is shown that, if the mean μ_x and the standard deviation σ_x of X exist, then X is asymptotically normally distributed with mean μ_x and standard deviation σ_x as $\mu_y/\sigma_y \rightarrow \infty$. If μ_x and σ_x do not exist, then X is asymptotically normally distributed with mean $\mu_0=\mu_y^p[1+0(\eta^{-2})]$ and standard deviation $\sigma_0=(p\mu_y^{p/\eta})[1+0(\eta^{-2})]$ as $\mu_y/\sigma_y \rightarrow \infty$. When μ_x and σ_x exist, it is shown that $\mu_y/\sigma_y \rightarrow \infty$ is necessary and sufficient to insure that $\mu_x/\sigma_x \rightarrow \infty$.

A note on domain conversions of $BaTiO_3$, P. H. Fang and W. S. Brower, *J. Appl. Phys.* **34,** *No. 5, 1516 (May 1963).*
Some peculiar properties of $BaTiO_3$ single crystals, which have been converted into a-domain form, are discussed. The a-domain form shows a time instability, in that an intrusion of c-domains is observed, by use of X-ray techniques and polarizing microscope with a monochromatic light source, to occur after several weeks.

An alignment interferometer, J. B. Saunders, *Appl. Opt.* **2,** *No. 5, 541 (May 1963).*
An alignment interferometer is described that permits accurate alignment of points along a straight line several miles long. The interferometer is relatively easy to construct, is rugged, and can be used with currently available light sources.

An application of the peek-a-boo principle to information retrieval, J. Stern, *Proc. Symp. Materials Information Retrieval, pp. 93–115 (Nov. 28–29, 1962).*
The Peek-a-Boo technique is defined to distinguish it from Peek-a-Boo systems of which it constitutes a major element. Experience in applying the technique to a collection of instrumentation references is described. A philosophy of information retrieval that has resulted from that experience is outlined. The performance of improved equipment developed to implement that philosophy is discussed and further projected improvements are described.

Burning behavior of building finish materials: Two-test methods, A. R. Robertson, *Spec. Publ. Fed. Fire Council, pp. 21–35 (Apr. 1962).*
An argument is made for a more analytical approach during measurement of the fire behavior of materials. It is suggested that the flammability of solids may be considered as a function of the ratio of heat release rate to critical ignition energy of the material being studied. Based on this concept, the radiant panel flammability test method has shown its usefulness as a research and production control tool. A review is presented of previous studies made by use of this method.
A brief description is also furnished of the horizontal panel fire test method of SS–A–118b. It is emphasized that this method of test measures more than surface flammability. It provides some indication of the combustible character of the backing material. It is suggested that this method has been unjustly criticised as a result of improper understanding of the way in which it should be used. It is concluded that, although the test methods discussed have achieved some recognition, it would be a mistake to assume that any one known test method would be ideal for prediction of the surface flammability hazard of all materials in all situations.

Dependence of the electrical conductivity and thermoelectric power of pure and aluminum-doped rutile on equilibrium oxygen pressure and temperature, J. Yahia, *Phys. Rev.* **130,** *No. 5, 1711–1719 (June 1, 1963).*
The electrical conductivity σ and thermoelectric power Q have been measured as a function of equilibrium oxygen pressure in crystals of pure and Al-doped rutile. The pressure was varied over the range 10^{-4} mm Hg to $\sim 10^3$ mm Hg with the temperature held constant at several fixed values in the vicinity of 1000°K. The electrical conductivity of the pure material varied with pressure according to the relation $\sigma \propto p^{-1/x}$ with $x \approx 6$ for $p > 10$ mm Hg and $x \approx 5$ for $p < 10$ mm Hg. For the Al-doped crystal, σ reached a minimum for $p=p_0$ mmHg. At low pressures σ followed a relation of the form $\sigma \propto p^{-1/x}$ with $x \sim 5$, whereas at high pressures a relation

of the form $\sigma \propto p^{+1/x}$ with $x \sim 5$ was obeyed. The thermoelectric power exhibited a reversal near p_0, being negative at lower pressures and positive for $p > p_0$. For pure rutile a defect model involving anion vacancies and estimated values of equilibrium constants leads to a pressure dependence of the conductivity: $\sigma \propto p^{-1/6}$, whereas for a model involving titanium interstitials the pressure dependence is $\sigma \propto p^{-1/3}$. On the basis of the present measurements it seems that for pure rutile the anion vacancy mechanism obtains at "high" pressures with the titanium interstitials mechanism predominating at "low" pressures. For Al-doped rutile, both the anion vacancy model and the titanium interstitials model are shown to give rise to approximately the observed pressure dependence of conductivity. The anion vacancy model equations are solved in detail (assuming certain values of the equilibrium constants). The titanium interstitials model equations are not solved explicity for this case but it is shown that for a certain combination of reaction constants the observed pressure dependence may be approximated. Assuming a two-band formalism to be valid—and therefore, a formalism into which the results derived from any defect model must fit—we have analyzed the data and shown that reasonable agreement with observation results. Some indications that hole mobilities at 1000°K are considerably larger ($\sim$180 cm^2/V sec) than those of the electrons are discussed. Assuming high-temperature polar scattering to obtain, a hole effective mass 10^{-2} m_0 (where m_0 is the free-electron mass) is deduced as a consequence of the mobility calculations.

A portable impedance tube, R. D. Berendt and H. A. Schmidt, Jr., *J. Acoust. Soc. Am.* **35,** *No. 7, 1049–1052 (July 1963).*
A light-weight impedance tube has been developed primarily as an instrument for practical research. It can be used also for precision measurements of acoustical impedance and sound absorption coefficients in both laboratory and field installations, over the frequency range 400 to 900 c/s. It is useful for the development and manufacturing control of acoustical materials, acceptance testing of acoustical installations in the field and determination of aging, staining and redecoration effects on the absorptivity of acoustical materials. Experimental results are presented.

Inertial seismograph design—limitations in principle and practice, B. [illegible] Melton and D. P. Johnson, *Proc. IRE* **50,** *No. 11, 2328–2339 (Nov. 1962).*
Seismograph design is discussed in the general terms of bandpass, control of response characteristics through mechanical and electrical modifications of the system; and the limitations imposed on sensitivity when some seemingly innocuous numbers are ignored. Earth vibration ampiitudes of one Angstrom or less, and power sensing levels as low as 10^{-20} watts are considered, implying that instrumental noise levels should be even lower under some circumstances. A discussion of transducer elements leads to the conclusion that the incorporation of a galvanometer into the motion amplifying system offers at least as good a system as can be devised by other means. The concept of a platform stabilized against seismic disturbances is outlined as an interesting and probably important sidelight on seismograph design. Remarks on mechanical construction are included as guidance to designers because certain details, such as spring proportions, lever systems, crossed flexure plate hinges and suspension members with controlled regions of bending have been found extremely effective while other details of design have produced elusive troubles. Some design features are illustrated in the construction of certain seismographs in whose design the authors have an interest. The problem of level-sensitivity for horizontal component seismometers is outlined to show its basic nature, and some possible solutions.

Whistlers, R. M. Gallet, *Grenoble, Univ. Ecole Phys. Theorique, Les Houches, Geophysique Exterieur, pp. 551–590 (Gordon and Breach, New York, N.Y., 1963).*
The whistlers and the very low frequency emissions (VLF Emissions) are two different classes of natural radio phenomena observed at very low frequency (few kilocycles per second). Both classes are characterized by very distinctive variations of frequency with time, which give them quasi-musical qualities in listening. They can be heard after the voltage, which the electromagnetic signals induce in an antenna, is amplified by a wide band audio-amplifier without frequency conversion. Their principal physical interest is that their characteristics are directly due to the structure of the Earth's exosphere. They can be considered as natural and highly sensitive electromagnetic probes for studying the physics of the exosphere. In both classes a radio-propagation phenomenon is experienced, which has the unique property of *guiding* the energy of radio waves along curved paths defined by the magnetic lines of force of the Earth's magnetic field. These paths reach far out into space, as far as 3 or 4 earth's radii in the plane of the magnetic equator, and bring the energy back to earth at the point in the opposite hemisphere which is the magnetic conjugate of the position of the radio emission in the case of the whistlers. The length of such one way path can easily be as long as 30,000 to 50,000 km. Furthermore, the energy can be almost perfectly reflected at the end of the path, and propagating again along the same path can be received in the area near the original point of emission. Along such long paths the speed of propagation of the energy is very slow (as low as c/10 to c/100), and its local value depends strongly on frequency.

Ten year weathering data on aluminum alloys, W. H. Ailor, Jr., and F. M. Reinhart, *Materials Protect.* **2,** *No. 6, 30–36 (June 1963).*
A series of ten aluminum sheet alloys was exposed in urban and marine atmospheres and in sea water at mean tide level for periods of time varying from six months to ten years. The results of these exposures were evaluated by changes in mechanical properties and pit depth measurements. The mechanical properties of the alloys were not affected by exposure in either urban or marine atmospheres for periods of exposure up to ten years. In tidewater exposure, the mechanical properties of the aluminum-manganese alloy were significantly reduced after two years of exposure.
The cladding of the aluminum-copper alloys was not penetrated by pitting after ten years of exposure in any one of the three environments. The rates of penetration for the other alloys were greater than for the alclad alloys, with those of the purer alloys (1050 and 8099) being less than the aluminum-magnesium alloys. The exception to this was the aluminum-manganese alloy in the tidewater which was perforated after two years of exposure.

A He^3 cryostat for performing experiments with oriented nuclei, E. Ambler, R. Dove, and R. Kaeser, (*Proc. 1962 Cryogenic Engineering Conf.), Book, Advances in Cryogenic Engineering* **8,** *Sec. H–2, 443–554 (Plenum Press, Inc., New York, N.Y., 1963).*
An all-metal cryostat is described for carrying out experiments on nuclear reactions with certain oriented nuclei. The cryostat contains a continuously operating He^3 refrigerator, and is of such a construction as to make possible experiments with various types of particle accelerators. The apparatus has been employed successfully so far for measuring the (γ,n) cross-section for aligned Ho^{165} nuclei in conjunction with a betatron.

The redefinition of the second and the velocity of light, G. E. Hudson and W. Atkinson, *Physics Today* **16,** *No. 5, 30–36 (May 1963).*
Two subjects were discussed at an informal session during the International Conference on Precision Electromagnetic Measurements, August 14 to 17, 1962, viz, "An Atomic Definition for the Unit of Time" and "Determination of the Velocity of Light." The session was presided over by Professor Norman Ramsey of Harvard University.
This article summarizes, examines, and comments on the discussions.

Radiation, L. S. Taylor, *Americana Annual pp. 620–622 (Americana Corporation, Chicago, Ill., 1961).*
This is a brief statement of the current status with regard to general thinking on radiation protection criteria together with brief mention of some of the events during the past year or two relative to protection matters. This was re-

quested by the Editor of the Americana Annual. The general topics covered are in accordance with the specific request from the Editor.

The calibration of inductive voltage dividers, T. L. Zapf, *ISA Proc. 1962, 17, pt. I, pp. 10.2.62-1 to 10.2.62-8 (1962).*
A review of recent work in a-c voltage ratio measurements at NBS is followed by a discussion of equipment and methods of measurement now under investigation. Improvements in the accuracy of measurement of a-c voltage ratio by capacitance bridge methods have reduced the limit of error in the calibration of voltage ratio of inductive voltage dividers to less than 2×10^{-7}. Calibrated inductive voltage dividers have been used as standards for the calibration of other dividers by a comparison method with relatively little degradation of accuracy. Recent investigations on the design and construction of inductive voltage dividers have demonstrated the feasibility of compensation of ratio errors arising from internal loading, and several inductive voltage dividers have been designed and constructed having ratio errors less than 5×10^{-8} at a frequency of 1000 cycles per second.

The stress-corrosion cracking of type 304 stainless steel at 455 to 615 F, H. L. Logan, M. J. McBee, and M. Romanoff, *Mater. Res. Std. 3, No. 8, 625–639 (Aug. 1963).*
The resistance of type 304 austenitic stainless steel to stress-corrosion cracking in solutions containing the chloride ion was determined in the temperature range of 455 to 615°F using a specimen that was itself an autoclave. Cracking was produced in specimens exposed to a corrodent containing as little as 5 ppm of chloride ion and subjected to stresses of 20,000 lb/in^2 or more at a temperature of 570°F. The presence of oxygen was necessary for crack initiation.

Bolometric microwave power calibration techniques at NBS, R. F. Desch and R. E. Larson, *Proc. ISA 17th Annual Instrument-Automation Conf. & Exhibit (Oct. 1962).*
A bolometric method of calibrating low-level microwave power measuring devices is currently employed at the National Bureau of Standards in Boulder, Colorado. The technique is one of direct comparison between the standard and the unknown, and utilizes NBS working standard bolometer units and self-balancing d-c bridges. In general, the unknown is calibrated to an accuracy of one percent. The following quantities and associated errors are discussed: (A) Calibration factor of a bolometer unit in combination with a directional coupler, (B) Calibration factor of a bolometer unit, and, (C) Effective efficiency of a bolometer unit.

Photographic dosimetry, megaroentgen range, W. L. McLaughlin, *Encyclopaedia of X-rays and Gamma Rays, Ed. G. L. Clark, pp. 307–309 (Rheinhold Publ. Corp., New York, N.Y., 1963).*
One of the oldest of photographic processes—print-out image formation—can be used to measure very large X- and γ-radiation exposure doses. The direct photochemical print-out darkening of the photographic material is usually measured photometrically, in terms of net transmission or reflection density. This net density is then related to the exposure dose by means of a calibration curve.
Commercial silver-halide X-ray films are widely available and have relatively uniform emulsion coatings; their print-out response is rate independent and permits γ-ray measurements in the 10^4–10^7r range with a precision of 5 percent. Special silver halide print-out emulsions, such as those containing silver citrate and silver azide have a useful range of approximately 10^3–10^4r; however, they may be subject to high-intensity rate dependence. Treating the commercial emulsions with certain halide acceptors prior to exposure sensitizes their print-out response by more than a factor of 10. The response can be enhanced further if, after the treated films receive γ-ray exposures, they are exposed briefly to a bright light. Other photographic materials which respond in the megaroentgen range are non-halide silver-salt emulsions, with development, and non-silver print-out systems. The photographic methods of measuring large exposure doses have several important limitations, which need consideration. These limitations are due to energy dependence, temperature dependence, and non-linearity of the film response, and to sensitivity of the films to blue light.

Proposed experiment to measure effects of ground roughness on the dose rate from fallout radiation, C. Eisenhauer, *Health Phys.* **9,** *503–506 (1963).*
An experiment designed to measure the effects of microscopic ground roughness on dose rates from fallout radiation is described. Existing calculational procedures for predicting these effects are first discussed. The effect of rough ground is then discussed in terms of a correction factor to the angular distribution of radiation above a smooth plane. An experiment designed to measure this correction factor is discussed in detail.

A study of embrittlement of high strength steels by hydrogen isotopes. I. Testing of steel rings as specimens, a comparison of hydrogen and deuterium embrittlement, and permeation studies, G. B. Wood, *J. Electrochem. Soc. 110: No. 8, 867–877 (Aug. 1963).*
Embrittlement of steel produced from electrolytic charging in H_2O- and D_2O-solutions is discussed. A comparison of the retention of embrittlement with retained gas content in uncoated steel is given. The separation factor for the electrodeposition of hydrogen and deuterium on SAE 4130 steel was found to be 5.9. Permeation of the mixture of these isotopes through steel results in further enrichment with respect to hydrogen. The diffusion coefficients and permeation rates for hydrogen and deuterium in steel are compared.

A study of embrittlement of high strength steels by hydrogen isotopes. II. A comparison of gas contents and hydrogen or deuterium embrittlement resulting from electroplating processes, G. B. Wood, *J. Electrochem. Soc.* **110,** *No. 8, 877–885 (Aug. 1963).*
Plating processes introduce more deuterium into steel from heavy water solutions than hydrogen from ordinary water solutions, yet hydrogen embrittles steel more than deuterium. There is no simple relation between the total gas content and embrittlement. Embrittlement appears to be dependent on factors other than the total gas content. The present work does not preferentially support any one of the mechanisms which have been proposed for hydrogen embrittlement. The difference in the chemical affinity of steel for hydrogen and deuterium is demonstrated.

Klystron protection circuit, W. E. Case and N. T. Larsen, *Rev. Sci. Instr.* **34,** *No. 7, 809–810 (July 1963).*
The design of a circuit to protect a klystron from either overvoltage or undervoltage on the heater is complicated by the high potential difference which exists between the klystron heater and ground. The insulation and control problems created by this potential difference are solved in this circuit by means of a light-beam controlled relay circuit. Thermal protection also is provided.

Optical observation of pressure induced transitions in polymers, A. Van Valkenburg and J. Powers, *J. Appl. Phys.* **34,** *No. 8, 2433–2434 (Aug. 1963).*
Pressure induced transitions in polytetrafluoroethylene, nylon 6, natural rubber, and polyethylene were observed optically between diamond anvils. In all polymers examined, the decrease in thickness and in birefringence is irreversible, at least on the time scale of a few months.

The wear of magnetic recording tape and solubility of the binder, F. Nesh, *IEEE Trans. Audio* **AU-11,** *No. 3, 97 (May–June 1963).*
The ability of magnetic recording tape to perform satisfactorily after repeated use is a characteristic of critical importance in computer service. Wear tests of tapes are time consuming and have not always shown good agreement in the rank ordering of tape between different transport mechanisms and different criteria of end of life. The ability to withstand repeated use is governed to a certain extent by the composition of the binder and its adhesion to the plastic backing. Since the solubility of the binder in various solvents depends on its compositions, experiments were run to see how well solubility could be correlated with wear. This letter is to bring attention to this work which is reported in more detail in other reports.

Special techniques for use in sugar analysis, V. R. Deitz and F. G. Carpenter, *Cane Sugar Handb. Ed. G. P. Meade, 9th Edition, pp. 605–619 (John Wiley and Sons, Inc., New York, N.Y., Aug. 1963).*
In addition to the standard analytical methods that are given in other chapters, new methods based on recent developments show some promise of utility to sugar technology. Some of these will now be described in sufficient detail to acquaint the reader with the possibilities and limitations of the methods and to furnish pertinent references to those who wish to read further. EDTA titration for Ca+Mg is given in detail since this procedure has attained wide usage. Some of the new techniques lend themselves readily to instrumental and even automatic analysis and thus may be useful in control.

Humidity (measurement of moisture in gas), A. Wexler, *ISA Transducer Compendium, pp. 502–508 (Sept. 1963).*
This paper is a state-of-the-art review of the measurement of water vapor content in gases. It is intended to serve as introductory material for the chapter on Humidity of the Transducer Compendium to be published by the ISA.

Convection phenomena from plants in still air, D. M. Gates and C. M. Benedict, *Am. J. Botany* **50,** *563–673 (July 1963).*
The free convection from leaves in still air was observed by means of schlieren photographs of broad leaves and of coniferous plants. A quantitative measure of the rate at which energy was convected away from the leaf was obtained by photographing the size of the convection plume, measuring its rate of flow by means of movie photography, and measuring the temperature of the plume with a fine thermocouple. The heat load on a leaf and the surface temperature of the leaf were obtained with a total hemispherical radiometer and an infrared radiometer respectively. The observations of free convection from broad-leaved plants confirmed the values predicted, using heat transfer theory for heated plates. The schlieren system can also be used to observe forced convection from plants in wind.

Portable 2 flow counter for the detection of α and β particles in smear samples, L. Costrell, A. Schwebel, and G. W. Zimmer, *Health Phys.* **9,** *No. 6, 643 (June 1963).*
A portable 2π flow counter has been developed for α and β smears. The instrument has proved useful in on-the-spot analysis of accidental spills and in routine smear tests.

An unmodulated twin channel microwave attenuation measurement system, D. H. Russell, *ISA 18th Annual Conf., pp. 1–17 (Sept. 1963).*
A two channel microwave attenuation measurement system is described which has the possibility of using the maximum linear range of a heterodyne mixer. The error of the system approaches that of the mixer alone. Theory of operation is presented and a practical system is detailed. No error is contributed by i-f amplifier slope or ripple as no modulation is required. The i-f amplifier is a null detector only. The system is completely phase-locked and with minor modification will also give the phase angle of the measured device. Experimental results and sources of error for two operating frequencies are discussed. The simplicity of the system and its use of standard components suggest its practical application in many standards laboratories.

Application of distillation techniques to radiochemical separations, J. R. DeVoe, *Natl. Acad. Sci.-Natl. Res. Council Nuclear Science Series, Radiochemical Techniques NAS–NS3108 (Aug. 1962).*
The use of vacuum distillation of inorganic compounds and metals for radiochemical separations is reviewed. A brief description of the experimental apparatus which is most often used for the distillation is outlined. Advantages and disadvantages of the various techniques are discussed. Detailed separation procedures are described using wet chemical distillation separations as well as for separations of daughter radioactivity from target materials by direct heating of the target.

The National Bureau of Standards reactor facility, C. O. Muehlhause, *Capital Chemist* **12,** *No. 1, 7–10 (Jan. 1962).*
The Bureau of Standards will construct a 10 MW research reactor-laboratory on its new campus near Gaithersburg, Maryland. The facility will be utilized by the Bureau and other participating institutions of the Washington area. In addition to nuclear standards, radiation standards, and standards in the field of radiation effects, the Bureau will engage in research and measurement of material parameters basic to science and engineering. This paper briefly describes the reactor facility and outlines some of the research objectives.

Determination of rhodium in rhodium-uranium alloys by precipitation with hydrogen sulfide, E. J. Maienthal, *Anal. Chem.* **35,** *1094–1095 (July 1963).*
The separation of rhodium from uranium by precipitation of rhodium as the sulfide in dilute hydrochloric acid media provides a simple and quantitative method for its determination in binary alloys containing from 44 to 98% of uranium.

Determination of bitumen content in expansion joint fillers, E. Horowitz and J. Mandel, *Mater. Res. Std.* **3,** *No. 9, 723–725 (Sept. 1963).*
A Soxhlet extraction method for the determination of bitumen content in expansion joint fillers made of bitumen and cellulose fiber, cork, or glass wool is compared with the ASTM centrifuge method. The Soxhlet extraction procedure requires less operator time and smaller amounts of solvent, and makes it possible to analyze a large number of samples concurrently with a minimum amount of attention. The results obtained by the Soxhlet method are in good agreement with those obtained by the centrifuge method. Furthermore, an evaluation of the data indicates that ACS carbon tetrachloride, ACS benzene, and technical benzene yield essentially the same results. It was found that the 4×4-inch specimen tended to give slightly higher results for bitumen content than did the 2×2-inch specimen.

Distillation, A. T. Leslie and E. C. Kuehner, *Analytical Chemistry Handb.* **XIII,** *Methods of Separation, Ed. L. Meites, Sect. 10, pp. 10–23—10–42 (1963).*
Tables of data and other information pertinent to laboratory distillation have been compiled for the convenience of laboratory workers using distillation as a method of analysis. The tables are to be included in a Handbook of Analytical Chemistry, edited by Prof. Louis Meites, and to be published by McGraw-Hill Co. in 1961.

Other NBS Publications

Journal of Research 67A (Phys. and Chem.), No. 6 (Nov.–Dec. 1963), 70 cents.

Analysis of the spectrum of neutral atomic bromine (Br I). J. L. Tech.
Matrices of spin-orbit interaction in the electron configurations $np^2\ n'\ p$ and $np^4\ n'\ p$. J. L. Tech.
A study of the gas-stabilized arc as an emission source for the measurement of oscillator strengths. Determination of some relative *gf*-values for Fe I. M. Morgoshes and B. F. Scribner.
Tritium-labeled compounds. IX. Determination of isotope effects in reactions yielding water-*t* from nonvolatile reactants. Oxidation of aldoses-*l*-*t* with iodine. H. S. Isbell and L. T. Sniegoski.
Buffer solutions of potassium dihydrogen phosphate and sodium succinate at 25 °C. M. Paabo, R. G. Bates, and R. A. Robinson.
Recalibration of the NBS glass standards of spectral transmittance. H. J. Keegan, J. C. Schleter, and M. A. Belknap. (See above abstracts.)
Thermal behavior of muscovite sheet mica. S. Ruthberg. (See above abstracts.)
Absolute configuration and chemical topology. S. J. Tauber.
Reversibility of polyester adsorption on glass. R. R. Stromberg and W. H. Grant.
Chemical purity by dielectric cryometry. G. S. Ross and L. J. Frolen. (See above abstracts.)

Adsorption, desorption, resorption. W. V. Loebenstein.
Color phenomena in polymer fracture. S. B. Newman and I. Wolock.

Journal of Research 68A (Phys. and Chem.), No. 1 (Jan.–Feb. 1964), 70 cents.

Fast neutron dose measurements for a D-D source in water. W. B. Beverly and V. Spiegel, Jr.
X-ray spectrometric analysis of noble metal dental alloys. B. W. Mulligan, H. J. Caul, S. D. Rasberry, and B. F. Scribner.
The first spectrum of manganese, Mn I. Miguel A. Catalán, William F. Meggers, and Olga Garcia-Riquelme.
Transition probabilities of forbidden lines. R. H. Garstang.
Franck-Condon factors to high vibrational quantum numbers III: CN. R. W. Nicholls.
Infrared absorption spectrum of nitrous oxide (N_2O) from 1830 cm^{-1} to 2270 cm^{-1}. E. K. Plyler, E. D. Tidwell, and A. G. Maki.
An absolute light scattering photometer: II. Direct determination of scattered light from solutions. D. McIntyre.
High pressure microscopy of the silver and cuprous halides. A. Van Valkenburg.
Lattice parameters and lattice energies of high-pressure polymorphs of some alkali halides. C. E. Weir and G. J. Piermarini.
Calculation of the higher order dipole-dipole effect in paramagnetic crystals. P. H. E. Meijer.
Second and third virial coefficients for hydrogen. R. D. Goodwin, D. E. Diller, H. M. Roder, and L. A. Weber.
Heats of solution, transition, and formation of three crystalline forms of metaboric acid. M. V. Kilday and E. J. Prosen.
Publications of the National Bureau of Standards.

Journal of Research 67B (Math. and Math. Phys.), No. 4 (Oct.–Dec. 1963), 75 cents.

Zonal harmonic perturbations of an accurate reference orbit of an artificial satellite. J. P. Vinti.
Optimal periodic inspection programs for randomly failing equipment. G. H. Weiss. (See above abstracts.)
An analysis of pedestrian queueing. G. H. Weiss.
Solutions of the equation $\Psi_{xx}+\frac{1}{x}\Psi_x+Kx^ne^{\Psi}=0$ E. A. Kearsley.
On the graphs of finite idempotent Boolean relation matrices. D. Rosenblatt.

Journal of Research 67D (Radio Prop.), No. 6 (Nov.–Dec. 1963), 70 cents.

A radiometeorological study, part I. Existing radiometeorological parameters. J. A. Lane and B. R. Bean.
A radiometeorological study part II. An analysis of VHF field strength variations and refractive index profiles. B. R. Bean, V. R. Frank, and J. A. Lane.
A radiometeorological study, part III. A new turbulence parameter. B. R. Bean, E. J. Dutton, J. A. Lane, and W. B. Sweezy.
Reflection of radio waves from undulating tropospheric layers. A. T. Waterman, Jr., and J. W. Strohbehn.
Oblique propagation of groundwaves across a coastline—Part I. J. R. Wait.
Oblique propagation of groundwaves across a coastline—Part II. J. R. Wait and C. M. Jackson.
On the index of refraction of air, the absorption and dispersion of centimeter waves by gases. G. Boudouris. Translated from French by G. Wm. Curtis. (See above abstract.)
A numerical approach to the solution of radio diffraction problems. J. K. Hargreaves and S. Hargreaves.
Inversion of radio wave absorption data to establish ionospheric properties. I. Nondeviative absorption. D. A. Wheelon.
Radiation in a lossless magneto-ionic medium at frequencies high relative to the electron gyrofrequency. J. W. Marini.
Radiation through cylindrical plasma sheaths. J. H. Harris.
Chart for determining the effects of ionospheric tilts using an idealized model. T. A. Croft and R. B. Fenwick.
Reflection of VLF radio wave from an inhomogeneous ionosphere. Part III. Exponential model with hyperbolic transition. J. R. Wait and L. C. Walters.
Families of distributions for hourly median power and instantaneous power of received radio signals. M. M. Siddiqui and G. H. Weiss.
Statistical methods in radar astronomy. Determination of surface roughness. H. S. Hayre.
Electrical conductivity of the Great Lakes. L. H. Doherty.

Journal of Research 68D (Radio Sci.), No. 1 (Jan. 1964), $1.00.

Comparison of observed VLF attenuation rates and excitation factors with theory. A. D. Watt and R. D. Croghan.
Field Intensity measurements at 10.2 kc/s over reciprocal paths. J. C. Hanselman, C. J. Casselman, M. L. Tibbals, and J. E. Bickel.
The propagation of VLF waves over distances between 1000 and 3000 km. B. Burgess.
Some experimental results concerning non-reciprocal east-west VLF wave propagation. B. Burgess.
An experimental study of the phase stability of VLF signals. D. E. Hampton.
Some particular observations on diurnal phase variations of VLF transmission received in Paris. B. Decaux and A. Gabry.
Periodic fading of VLF signals received over long paths during sunrise and sunset. D. D. Crombie.
Effects of wall perturbations in multimode waveguides. S. W. Maley and E. Bahar. (See above abstracts.)
VLF Utilization at NASA satellite tracking stations. C. H. Looney, Jr.
Long waves associated with disturbances produced in plasmas. H. Bremmer.
Some remarks on the Watson transformation and mode theory. L. A. Berry.
Concerning limitations and further corrections to geometric-optical theory for LF/VLF propagation between the ionosphere and the ground. J. R. Johler.
Some remarks on mode and ray theories of VLF radio propagation. J. R. Wait.
Two-dimensional treatment of mode theory of the propagation of VLF radio waves. J. R. Wait.
Reflection of electromagnetic waves from a lossy magnetoplasma. J. R. Wait and L. C. Walters.
Propagation of ELF waves below an inhomogeneous anisotropic ionosphere. J. Galejs and R. V. Row.
VLF propagation under the ionosphere in the lowest mode of horizontal polarization. H. A. Wheeler.
Propagation of VLF waves under disturbed conditions. B. Burgess.
VLF disturbances caused by trapped beta-rays from the decay of neutrons produced in high-altitude nuclear explosions. A. J. Zmuda, B. W. Shaw, and C. R. Haave.
VLF anomalies observed at State College, Pa., during the U.S. 1962 high-altitude nuclear tests. C. F. Sechrist.

Journal of Research 68D (Radio Sci.), No. 2 (Feb. 1964) $1.00.

Generation of an electromagnetic pulse by an expanding plasma in a conducting half-space. A. P. Stogryn and R. N. Ghose.
Impedance of a monopole antenna with a radial-wire ground system on an imperfectly conducting half-space, part II. S. W. Maley and R. J. King.
Capacitor type biconical antennas. Janis Galejs.
Simulated angular response patterns for transhorizon propagation. J. W. Strohbehn and A. T. Waterman, Jr.
Radio-star scintillations from ionospheric waves. J. W. Warwick.
Ionosonde studies of some chemical releases in the ionosphere. J. W. Wright.
Diurnal changes and transmission time in the arctic propagation of VLF waves. W. T. Blackband.
Geometrical optics convergence coefficient for the whistler case. J. H. Crary.
Comments on a paper 'Collisional Detachment and the Formation of an Ionospheric' by E. T. Pierce. H. R. Arnold.

The quasi-longitudinal approximation in the generalized theory of radio wave absorption. R. F. Benson.

Diurnal phase variation of VLF waves at medium distances. H. Volland.

Application of diffractions by convex surfaces to irregular terrain situations. H. T. Dougherty and L. J. Maloney.

Effect of lossy earth on antenna gain. R. J. Coe and W. L. Curtis.

Propagation of radio waves with frequency 99.9 Mhz as a function of the vertical structure of the atmosphere derived from daily radiosonde observations. G. P. A. Braam.

Electron optical studies of low-pressure gases, L. Marton, D. C. Schubert, and S. R. Mielczarek, NBS Mono. 66 (Aug. 16, 1963), 35 cents.

1963 Supplement Screw-thread standards for federal services (Parts I, II and III) Handbook H28 (1957) (Oct. 15, 1963), 70 cents.

Clinical Dosimetry, Recommendations of the International Commission on Radiological Units and Measurements, NBS Handb. 87 (Aug. 9, 1963), 40 cents. (This publication supersedes parts of H78. Handbooks 84 through 89 will completely replace H78.)

Methods of evaluating radiological equipment and materials, Recommendations of the International Commission on Radiological Units and Measurements, NBS Handb. 89 (Aug. 23, 1963), 35 cents. (This publication supersedes parts of H78. Handbooks 84 through 89 will completely replace H78.)

Hydraulic research in the United States, 1963, NBS Misc. Publ. 249 (Aug. 9, 1963), $1.00.

Mean electron density variations of the quiet ionosphere, No. 11, January 1960, J. W. Wright, L. R. Wescott, and D. J. Brown, NBS Tech. Note 40–11 (Aug. 30, 1963), 40 cents.

Mutual interference between surface and satellite communication systems, W. J. Hartman and M. T. Decker, NBS Tech. Note 126 (Aug. 1, 1963), 35 cents.

Choking two-phase flow literature summary and idealized design solutions for hydrogen, nitrogen, oxygen, and refrigerants 12 and 11, R. V. Smith, NBS. Tech. Note 179 (Aug. 3, 1963), 75 cents.

Antenna beam elevation angle for control of tropospheric interference between space system earth terminals and terrestrial stations, S. G. Lutz and W. J. Hartman, NBS Tech. Note 180 (Aug. 25, 1963), 15 cents.

Computer program for ionospheric mapping by numerical methods, M. E. Hinds and W. B. Jones, NBS Tech. Note 181 (Aug. 20, 1963), 50 cents.

A note on antipodal focussing, J. R. Wait, NBS Tech. Note 182 (Aug. 20, 1963), 15 cents.

Impedance of commercial Leclanché dry cells and batteries, R. J. Brodd and H. J. Dewane, NBS Tech. Note 190 (July 5, 1963), 40 cents.

Calculations of the potential and effective diffusion constant in a polyelectrolyte solution, S. R. Coriell and J. L. Jackson, NBS Tech. Note 192 (June 28, 1963), 25 cents.

A comparison of two independent atomic time scales, J. Newman, L. Fay, and W. R. Atkinson, Proc. IEEE **51,** No. 3, 498–499 (Mar. 1963).

Symmetry conditions for internal friction caused by jumping of point defects in crystals, J. B. Wachtman, Jr., and H. S. Peiser, J. Appl. Phys. Letter **1,** No. 1, 20–22 (Sept. (1962).

Change in occulsion of complete dentures caused by a pipe habit; a case report, J. B. Woefel and G. C. Paffenbarger, J. Am. Dental Assoc. **66,** No. 4, 478–485 (Apr. 1963).

Measurement of a maximum in the isothermal crystallization rate-temperature curve for polypentene-1, F. A. Quinn, Jr., and J. Powers, Polymer Letters (J. Polymer Sci., Pt. B) **1,** No. 7, 341–344 (July 1963).

The maximum number of zeros in the powers of an undecomposable matrix, M. Marcus and F. May, Duke Math. J. **29,** No. 4, 581–588 (Dec. 1962).

Radio spectrum of SH, H. E. Radford and M. Linzer, Phys. Rev. Letters **10,** No. 10, 443–444 (May 15, 1963).

Electrophoretic deposits of barium titanate, V. A. Lamb and H. I. Salmon, J. Am. Ceram. Bull. **41,** No. 11, 781 (1962).

Measurement of the lattice constants of neon isotopes in the temperature range 4°-24°K, L. H. Bolz and F. A. Mauer, Proc. 11th Annual Conf. Applications of X-ray Analysis, Denver, Res. Inst. (Plenum Press, Inc., New York, N.Y., 1962).

Thermodynamic properties of gases, J. Hilsenrath, Am. Inst. Phys. Handb. 2d Ed., sec. 4h, 101–157 (1963).

The decoration of dislocations in aluminum oxide, H. E. Bond and K. B. Harvey, J. Appl. Phys. **34,** No. 2, 440–441 (Feb. 1963).

The effect of geomagnetic crochet on cosmic ray intensity, C. S. Warwick, J. Geophys. Res. **68,** No. 10, 3303–3304 (May 15, 1963).

Packing inequalities for circles, P. J. Davis, Michigan Math. J. **10,** pp. 25–31 (1963).

Lower bounds to eigenvalues using operator decompositions of the form B*B, N. W. Bazley and D. W. Fox, Arch. Rat. Mech. Anal. **10,** p. 352 (1962).

Transference numbers in pure molten sodium nitrate, R. J. Labrie and V. A. Lamb, J. Electrochem. Soc. **110,** No. 7, 810–814 (July 1963).

Unstable detonation near a hypervelocity missile, F. W. Ruegg and W. W. Dorsey, Ninth Symp. Intern. Combustion, pp. 476–477 (1963).

Exchange processes in the reaction of boron trichloride with triethylamineboron trifluoride, T. D. Coyle, Proc. Chem. Soc. (London), p. 172 (June 1963).

Analysis of the third spectrum of praseodymium, J. Sugar, J. Opt. Soc. Am. **53,** No. 7, 831–838 (July 1963).

Classification of two-electron excitation levels of helium, J. W. Cooper, U. Fano, and F. Prats, Phys. Rev. Letters **10,** No. 12, 518–521 (June 1963).

Photodisintegration of light nuclei, E. Hayward, Rev. Mod. Phys. **35,** No. 2, 324–331 (Apr. 1963).

Solid state physics, H. P. R. Frederikse (Editor and part author), Book, Am. Inst. Phys. Handbook Sec. 9, 2d Ed. (McGraw Hill Book Co., New York, N.Y., 1963).

Very low temperature data. Properties of paramagnetic salts, R. P. Hudson, AIP Handb. 2d Ed. Sec. 5g, pp. 222–223 (1963).

VLF propagation—theory and experiment, J. R. Wait, Monograph, Electromagnetic Waves in Stratified Media, Ch. IX, pp. 264–288 (Pergamon Press, Inc., Oxford, England, 1962).

Sum rules relating coherent X-ray scattering data to the diamagnetic nuclear shielding constant and to the self-energy of the charge distribution of the scatterer, J. N. Silverman and Y. Obata, J. Chem. Phys. **38,** No. 5, 1254–1255 (1963).

Determining fastest routes using fixed schedules, B. M. Levin and S. Hedetniemi, Proc. Conf. American Federation for Information Processing Soc. **23,** pp. 1–9 (1963).

Dielectric relaxation in a high temperature dipole lattice, R. Zwanzig, J. Chem. Phys. **38,** No. 11, 2766 (1963).

Present status of our knowledge of atomic transition probabilities, W. L. Wiese, Proc. Xth Colloq. Spectroscopicum Intern., pp. 37–56, Ed. E. R. Lippincott and M. Margoshes (Spartan Books, Washington, D.C., 1963).

Collective correlation of plasma, C. M. TchenCzechoslovak J. Phys., Proc. 2d Conf. Electronics **XXI,** No. 5–6, 516–521 (Apr. 1961).

Double-photon photodetachment of negative ions, S. Geltman, Phys. Rev. Letters **4,** No. 3, 168–169 (Apr. 1, 1963).

Effect of insulation on the weathering of smooth-surfaced, built-up roofs exposed to solar heating, W. C. Cullen and W. H. Appleton, Am. Roofer and Building Improvement Building Contractor Mag. pt. I, **53,** No. 3, 19–22 (Mar. 1963); pt. II, **53,** No. 4, 14 (Apr. 1963).

Pressure broadening as a prototype of relaxation, U. Fano, Phys. Rev. **131,** No. 1, 259–268 (July 1, 1963).

The atomic spectra of the rare earths: their presence in the sun, C. E. Moore, Appl. Opt. **2,** No. 7, 665–674 (July 1963).

The conductive-disk method of measuring the thermal conductivity of insulations, H. E. Robinson, Suppl. Bull. Intern. Inst. Refrigeration, Annexe 1962–1, 43–50 (Aug. 1962).

Electrodeposition of alloys. Principles and practice. Vol. I. General Survey, principles, and alloys of copper and of silver, and Vol. II, Practical and specific information, A. Brenner, Book (Academic Press, Inc., New York, N.Y., 1963).

Electron affinity of atomic iodine, B. Steiner, M. L. Seman, and L. M. Branscomb, J. Chem. Phys, **37,** No. 6, 1200–1202 (June 1962).

Temperature scales, thermocouples and resistance thermometers, H. F. Stimson, J. F. Swindells, and R. E. Wilson, Am. Inst. Phys. Handb. 2d Ed., sec. 4a, pp. 2–21 (1963).

Field-emission study of carbon monoxide on tantalum, R. Klein and L. B. Leder, J. Chem. Phys. **38,** No. 8, 1866–1872 (Apr. 15, 1963).

Field emission observations of carbon on tantalum, R. Klein and L. Leder, J. Chem. Phys. **38,** No. 8, 1963–1866 (Apr. 1963).

Electron impact ionization of atomic hydrogen, S. Geltman, M. R. Rudge and M. J. Seaton, Proc. Phys. Soc. **81,** pt. 2, No. 520, 375–377 (Feb. 1, 1963).

Some free products of cyclic groups, M. Newman, Michigan Math. J. **9,** 369–373 (1962).

Electron energy levels and their relationship to lattice defects in reduced rutile, J. H. Becker and W. R. Hosler (Proc. Intern. Conf. Crystal Lattice Defects), J. Phys. Soc. Japan **18,** Suppl. II, 152–160 (1963).

Addendum: Vibration-rotation spectra of BrCN, A. Maki, J. Chem. Phys. **38,** No. 5, 1261–1262 (May 1963).

Acoustic properties of liquids, M. Greenspan, Am. Inst. Phys. Handb. 2d Ed. sec. 3e, pp. 71–82 (1963).

Reflection mechanisms for sporadic *E*, K. Tao and J. R. Wait, Book, Ionospheric Sporadic *E*, Ed. E. K. Smith and S. Matsushita, ch. 4, pt. II, pp. 13–27 (Pergamon Press, Inc., Oxford, England, 1962).

Review of reviews of atomic spectra, W. Meggers, Appl. Opt. **2,** No. 7, 657–663 (July 1963).

Molecular parameters of ethane, W. J. Lafferty and E. K. Plyler, J. Chem. Phys. **37,** No. 11, 2688–2692 (Nov. 1962).

Multipliers of difference sets, M. Newman, Can. J. Math. 121–124 (Nov. 1961).

New autoionizing atomic energy levels in He, Ne, and A, R. P. Madden and K. Codling, Phys. Rev. Letters **10,** No. 12, 516–518 (June 15, 1963).

The segmental variation of Blaschke products, G. T. Cargo, Duke Math. J. **30,** No. 1, 143–150 (Mar. 1963).

The structure of some subgroups of the modular group, M. Newman, Illinois J. Math. **6,** No. 3, 480–487 (Sept. 1962).

A modification of the Born-Mayer potential function as applied to the crystalline alkali halides, T. B. Douglas, J. Chem. Phys. **38,** No. 10, 2461–2466 (May 15, 1963).

Microbalance techniques for high temperature applications—further developments, N. J. Carrera and R. F. Walker, Book, Vacuum Microbalance Techniques, **3,** 153–177 (Plenum Press, Inc., New York, N.Y., 1963).

Heat capacities, G. T. Furukawa and T. B. Douglas, Am. Inst. Phys. Handb. 2d Ed., sec. 4e, pp. 47–63 (1963).

High resolution spectra in the region from 2 to 6μ, E. K. Plyler and E. D. Tidwell (Proc. Intern. Molecular Conf.), Book, Advances, in Molecular Spectroscopy, pp. 1336–1342 (Pergamon Press Inc., New York, N.Y., 1962).

Impressions of Japan, R. S. Marvin, Japanese J. Kobunshi (High Polymers), Soc. High Polymers **12,** No. 130, 53 (1963).

Theory of the electronic polarizabilities of ions in crystals: Application to the alkali halide crystals, A. R. Ruffa, Phys. Rev. **130,** No. 4, 1412–1423 (May 15, 1963).

Annual report for IAU commission 14, C. E. Moore, Trans. Astronomical Union XIA97–XIB, 208 (1962).

frared spectrum of acetylene-d_1, W. J. Lafferty, E. K. Plyler, and E. D. Tidwell, J. Chem. Phys. **37,** No. 9, 1981–1988 (Nov. 1962).

Nickel and alloys, M. R. Meyerson, Encyclopedia of Engineering Materials and Processes, pp. 439–442 (Reinhold Publ. Corp., New York, N.Y., 1963).

Audiofrequency dispersion effects in lanthanide salts at low temperatures, R. P. Hudson and B. W. Mangum, Book, Magnetic and Electric Resonance and Relaxation, Ed. J. Smidt, pp. 135–146 (North-Holland Publ. Co., Amsterdam, The Netherlands, 1963).

Some problems in temperature measurements from line spectra, J. T. Jefferies, Book, Temperature, Its Measurement and Control in Science and Industry **3,** No. 1, 703–711 (1962).

The invariance of symmetric functions of singular values, Pacific J. Math. **12,** No. 1, 327–332 (1962).

Bounds for cofactors and arithmetic minima of quadratic forms, M. Newman. J. London Math. Soc. **38,** pp. 215–217 (Apr. 1963).

Non-linear effects in spectra of the iron group, R. E. Trees, Phys. Rev. 129, No. 3, 1220–1224 (Feb. 1, 1963).

Nonreciprocity of propagation of VLF radio waves along the magnetic equator, D. D. Crombie, Proc. IEEE **51,** No. 4, 617–618 (Apr. 1963).

Infrared spectrum of carbon tetrafluoride, A. Maki, E. K. Plyler, and R. Thibault, J. Chem. Phys. **37,** No. 8, 1899–1900 (Oct. 1962).

Matrix effects in the gaseous H atom—condensed olefin system; surface reaction—olefin diffusion model, R. Klein and M. D. Scheer, J. Phys. Chem. **66,** No. 12, 2677–2681 (Dec. 1962).

Normal functions, the Montel property, and interpolation in H^∞, G. T. Cargo, Michigan Math. J. **10,** 141–146 (1963).

Stability relations of dravite, a tourmaline, C. R. Robbins and H. S. Yoder, Jr., Geophysical Laboratory Yearbook 1961–62 (Note) (Carnegie Institute of Washington, Feb. 1963).

Critical review of sugar color and turbidity measurements, F. G. Carpenter and V. R. Deitz, Sugar Ind. Tech. **21,** Paper 65, 32–52 (1962).

Molecular vib-rotors. The theory and interpretation of high resolution infrared spectra, H. C. Allen, Jr., and P. C. Cross, Book (John Wiley and Sons, Inc., New York, N.Y., 1963).

Copositive and completely positive quadratic forms, M. Hall, Jr., and M. Newman, Proc. Camb. Phil. Soc. **59,** 329–339 (1963).

On the vacuum ultraviolet refectance of evaporated aluminum before and during oxidation, R. P. Madden, L. R. Canfield, and G. Haas, J. Opt. Soc. Am. **53,** No. 5, 620–625 (May 1963).

Covers and packings in a family of sets, J. Edmonds, Bull. Am. Math. Soc. **LXVIII,** No, 5, 494–499 (Sept. 1962).

An LCAO-MO-SCF study of the structure of HO_2, M. E. Boyd, Program Comm. Intern Symp. on Molecular Structure and Spectroscopy, pp. B404–1—B404–4 (Science Council of Japan, Tokyo, 1962).

On the pedestrian queueing problem, G. Weiss, Bull. Intern. Stat. Inst. **XXXIX,** No. 4, 163–168 (1962).

The kinetics of description II: Ca^+ and Ba^+ from rhenium, M. D. Scheer and J. Fine, J. Chem. Phys. **38,** No. 2, 307 (Jan. 1963).

A computer for the Abel inversion, C. R. Yokley and J. B. Shumaker, Rev. Sci. Instr. **34,** No. 5, 551–557 (May 1963).

Rotation-vibration constants of acetylene, E. K. Plyler, E. D. Tidwell, and T. A. Wiggins, J. Opt. Soc. Am. **53,** No. 5, 589–593 (May 1963).

Calculation of crystallite size distributions from X-ray line broadening, A. Bienenstock, J. Appl. Phys. **34,** No. 5, 1391 (May 1963).

Osmotic and activity coefficients of tetraethylammonium iodide in aqueous solution at 25°, V. E. Bower and R. A. Robinson, Trans. Faraday Soc. **59,** No. 488, 1717–1719 (Aug. 1963).

A connection between Tauberian theorems and normal functions, G. T. Cargo, Bull. Am. Math. Soc. **68,** No. 4, 400–401 (July 1962).

Nuclear moment of Ni^{61} from nuclear resonance studies in steady external magnetic fields, R. L. Streever, Phys. Rev. **128,** No. 4, 1632–1633 (Nov. 15, 1962).

Electromagnetic waves in stratified media, J. R. Wait, Book (Pergamon Press, Inc., New York, N.Y., 1962).

Linear velocity-gradient term in time-dependent pair distribution function, R. E. Nettleton, J. Chem. Phys. **38,** No. 8, 1791–1802 (Apr. 1963).

Absolute magnetic susceptibilities by the Gouy and the Thorpe-Senftle methods, G. A. Candela and R. E. Mundy, IRE Trans. Instr. **I-11,** No. 3–4, 106–109 (Dec. 1962).

Synthesis of perfluorostyrene and (2,2-difluorovinyl) perfluorobenzene (α-hydroheptafluorostyrene). A general method for synthesis of highly fluorinated styrenes, J. M. Antonucci and L. A. Wall, SPE Trans. **3,** No. 3, 225–230 (July 1963).

Radiation transfer problems in the rocket ultra-violet lines, C. Pecker and R. N. Thomas, J. Quant. Spectry. Radiative Transfer **3,** No. 2, 163–165 (June 1963).

Stress-corrosion cracking of type 304 stainless steel at 455 to 615 F, H. L. Logan, M. J. McBee, and M. Romanoff, Mater. Res. Std. **3,** No. 8, 635–639 (Aug. 1963).

Monte Carlo calculations of the penetration and diffusion of fast charged particles, M. J. Berger, Book, Methods in Computational Physics, Ed. B. Alder, S. Fernbach, and M. Rotenberg, I, 135–215 (Academic Press, Inc., New York, N.Y., 1963).

Lines of constant correlated color temperature based on MacAdam's (u,v) uniform chromaticity transformation of the CIE diagram, K. L. Kelly, J. Opt. Soc. Am. **53,** No. 8, 999–1002 (Aug. 1963).

Intrinsic attenuation, R. W. Beatty, IEEE Trans. Microwave Theory Tech. **MTT-11,** No. 3, pp. 179–182 (May 1963).

A note on modular groups, M. Newman, Proc. Am. Math. Soc. **14,** No. 1, 124–125 (Feb. 1963).

Leaf temperature and energy exchange, D. M. Gates, Archiv fur Meteorologie, Geophysik Bioklimatologie, Ser. B, **12,** 321–336 (1963).

Equatorial ionospheric variations during geomagnetic storms, S. Matsushita, J. Geophys. Res. **68,** 2595–2601 (May 1, 1963).

Effects of the nuclear explosion over Johnston Island observed in Peru on July 9, 1962, M. Casaverde, A. Giesecke, and R. Cohen, J. Geophys. Res. **68,** No. 9, 2603–2611 (May 1, 1963).

Derivation of electron density profiles in the lower ionosphere using radio absorption measurements at multiple frequencies, R. Parthasarathy, G. M. Lerfald, and C. G. Little, J. Geophys. Res. **68,** 3581–3588 (June 15, 1963).

Infrared dispersion of some oxide glasses, I. H. Malitson, G. W. Cleek, O. N. Stavroudis, and L. E. Sutton, Appl. Opt. **2,** 741 (July 1963).

Radiolysis of methane, P. J. Ausloos and S. G. Lias, J. Chem. Phys. **38,** and No. 9, 2207–2214 (May 1, 1963).

The structure of hexagonal silver iodide, G. Burley, J. Chem. Phys. **38,** No. 12, 2807–2812 (June 1963).

Radiolysis of propane-d_8 in the presence of organic compounds other than hydrocarbons, I. B. Sandoval and P. J. Ausloos, J. Chem. Phys. **38,** No. 10, 2454–2460 (May 15, 1963).

Thermal conductivity, R. L. Powell, American Institute of Physics Handb. 2d Ed. pp. 4–76–4–101 (McGraw-Hill Book Co. Inc., New York, N.Y., 1963).

Digital pattern recognition by moments, F. L. Alt, Book, Optical Character Recognition, Ed. G. L. Fischer, D. K. Pollack, B. Raddick, and M. E. Stevens pt. II, pp. 153–179 (Spartan Books, Washington D.C., 1962).

D-gluco-L-glycero-3-octulose, a crystalline ketose from D-erythrose, R. Schaffer and A. Cohen, J. Organ. Chem. **28,** 1929–1930 (1963).

A phenomenological theory of overvoltage for metallic particles, J. R. Wait, Book, Overvoltage Research and Geophysical Applications, Ed. J. R. Wait, ch. 3, p. 22 (Pergamon Press, Inc., New York, N.Y., 1959).

Statistics in chemical analysis, W. J. Youden, Handbook of Analytical Chemistry, sec. 14, pp. 14–1–14–9 (McGraw-Hill Book Co., Inc., New York, N.Y., 1963).

Stark energy levels of symmetric-top molecules, J. H. Shirley, J. Chem. Phys. **38,** 2896–2913 (June 15, 1963).

The microwave spectrum of normal propyl chloride, T. N. Sarachman, J. Chem. Phys. **39,** No. 2, 469–473 (July 15, 1963).

Vacuum ultraviolet photochemistry. VI. Photolysis of cyclopropane with the Xenon resonance lines, C. L. Currie, H. Okabe, and J. R. McNesby, J. Phys. Chem. **67,** No. 7, 1494–1497 (July 1963).

Modulary groups of $t \times t$ matrices, M. Newman and J. R. Smart, Duke Math. J. **30,** 253–257 (1963).

An experimental method of estimating F-region collision frequencies (research note), J. K. Hargreaves, J. Atmospheric and Terrest. Phys. **25,** 300–304 (May 1963).

Atomic frequency standards at the National Bureau of Standards, J. M. Richardson, R. E. Beehler, R. C. Mockler, and R. L. Fey, Comite Consultatif, Definition de la Seconde aupres du Comite Intern. des Poids et Mesures, pp. 57–67 (Sept. 1962).

Optical Character Recognition, Ed., G. L. Fischer, D. K. Pollack, B. Raddick, and M. E. Stevens (Spartan Books, Washington, D.C. 1962).

Achievement of measurement agreement among electrical standards laboratories, F. D. Weaver, Instr. Control Systems **36,** 128–131 (July 1963).

Spectroscopic absorption of NO in crystalline and liquid krypton, G. L. Pollack and H. P. Broida, J. Chem. Phys. **38,** No. 8, 2012–2015 (Apr. 15, 1963).

The possibility of guided electromagnetic waves in the earth's crust, J. R. Wait, IEEE Trans. Ant. Prop. **AP-11,** 330–335 (May 1963).

The nature of the compound obtained from aqueous cesium chloride solution and hydrogen chloride, A. G. Maki and R. West, Inorganic Chem. **2,** 657 (1963).

Laboratory investigation of overvoltage, L. S. Collett, A. A. Brant, W. E. Bell, K. A. Ruddock, H. O. Siegel, and J. R. Wait, Book, Overvoltage Research and Geophysical Applications, Ed. J. R. Wait, ch. 5, p. 50 (Pergamon Press, Inc., New York, N.Y., 1959).

1,2,2-trifluorovinyl phenyl ether and 2,3,4,5,6-pentafluorophenyl 1,2,2-trifluorovinyl ether and their polymers, W. J. Pummer and L. A. Wall, SPE Trans. **3,** No. 3, 220–224 (July 1963).

Radiometry, M. M. Reynolds, R. J. Corruccini, M. M. Fulk, and R. M. Burley, American Institute of Physics Handb. 2d edition, pp. 6–153–6–172 (McGraw-Hill Book Co., Inc., New York, N.Y., 1963).

Classification of resonances in the electron scattering cross section of Ne and He, J. A. Simpson and U. Fano, Phys. Rev. Letters **11,** 158 (1963).

Theory of the deep penetration of electrons and charged particles, L. V. Spencer and J. Coyne, Phys. Rev. **128,** No. 5, 2230–2237 (Dec. 1, 1962).

Correlation effects in two- and three-electron systems, J. W. Cooper and J. B. Martin, Phys. Rev. **131,** No. 3, 1183–1186 (Aug. 1, 1963).

Criteria from the transient decay curves, J. R. Wait and L. S. Collett, Book, Overvoltage Research and Geophysical Applications, Ed. J. R. Wait, ch. 6a, p. 71 (Pergamon Press, Inc., New York, N.Y., 1959).

On the interpretation of prominence spectra. VI. Temperature determination and a model for quiescent prominences J. T. Jefferies and F. Q. Orrall, Astrophys. J. **137,** 1232–1241 (May 15, 1963).

The lifetime and movement of artificially produced electron clouds observed with spaced ionosondes, J. W. Wright, J. Geophys. Res. 68, No. 10, 3011–3020 (May 15, 1963).

Isopiestic vapor pressure measurements of the ternary system: Sorbitol-sodium chloride-water at 25°, V. E. Bower and R. A. Robinson, J. Phys. Chem. **67,** 1540–1541 (1963).

The intermediate state of some hard superconductors, V. Arp, R. V. Krospchot, and T. S. Craig, Book, Superconductors, pp. 135–141 (Interscience Publ., New York, N.Y. 1962).

Ferromagnetic resonance and shape dependent effects, L. A. Steinert, J. Appl. Phys. Letter **34,** 2106–2107 (July 1963).

Characteristics of spread F at high geomagnetic latitude, W. K. Klemper, J. Geophys. Res. **68,** No. 10, 3191–3196 (May 15, 1963).

The thermodynamics of the ternary system: Urea-sodium chloride-water at 25°, V. E. Bower and R. A. Robinson, J. Phys. Chem. **67,** 1524–1527 (1963).

Verification of the tenfold assignment of the Baryon resonances, S. Meshkov, C. A. Levinson, and H. J. Lipkin, Phys. Rev. Letters **10,** No. 8, 361–364 (Apr. 15, 1963).

Vapor snakes in solidi argon, G. L. Pollack and H. P. Broida, J. Chem. Phys. **38,** No. 4, 968–969 (Feb. 15, 1963).

The day-to-night ratio of cosmic noise absorption during polar cap absorption events, C. S. Gilmor, J. Atmospheric Terrest. Phys. **25,**, 263–266 (May 1963).

Proposed experiment to measure effects to ground roughness on the dose rate from fallout radiation, C. Eisenhauer, Health Phys. **9,** 503–506 (1963).

Standards for dental radiographic film, G. C. Paffenbarger, Mag. Std. **34,** 148 (May 1963).

The variable-frequency method, J. R. Wait, Book, Overvoltage Research and Geophysical Applications, Ed. J. R. Wait ch. 4, p. 29 (Pergamon Press Inc., New York, N.Y., 1959).

Heat transfer between a cryo-surface and a controlled atmosphere, Suppl. Bull. Intern. Inst. Refrigeration Annexe 1962–1, p. 89 (Aug. 1962).

Mechanical and electrical relaxation in theorium oxide containing calcium oxide, J. B. Wachtman, Jr., Phys. Rev. **131,** 517 (July–Sept. 1963).

Polymers and telomers of 4-chloroperfluoroheptadiene-1, 6, J. E. Fearn and L. A. Wall, SPE Trans. **3,** No. 3, 231–234 (July 1963).

The following papers were published in Ionospheric Sporadic *E*, Ed. E. K. Smith and S. Matsushita (Pergamon Press Inc., New York, N.Y., 1962).

A note on the heights of the different IGY types of E_s, S. C. Gladden, pp. 178–181.

A study of radio wave scattering from sporadic *E* near the magnetic equator, K. L. Bowles and R. Cohen, pp. 51–77.

A theoretical study of sporadic-*E* structure in the light of radio measurements, K. Tao, pp. 235–257.

Lunar tidal variations of sporadic *E*, S. Matsushita, pp. 194–214.

On the width of the equatorial E_s belt, R. W. Knecht and R. E. McDuffie, pp. 215–218.

Recent sporadic-*E* experimental work in the United States, J. F. DeGregorio, J. W. Finney, K. Kildahl, and E. K. Smith, pp. 141–142.

Sporadic-*E* propagation with 3μ sec pulses, G. R. Ochs, R. J. Carpenter, and E. K. Smith, pp. 143–148.

The night-*E* layer, G. A. M. King, pp. 219–231.

The occurrence of sporadic *E*, E. K. Smith, pp. 3–12.

The occurrence of sporadic *E*, during the IGY, H. I. Leighton, A. H. Shapley and E. K. Smith, pp. 166–177.

Variations in frequency of occurrence of sporadic *E*, 1949–1959, W. B. Chadwick, pp. 182–193.

Excitation of pi-electrons in polystyrene and similar polymers by 20 Kev electrons, N. Swanson and C. J. Powell, J. Chem. Phys. **39,** 630–634 (Aug. 1, 1963).

Optical observation of pressure induced transitions in polymers, A. Van Valkenburg and J. Powers, J. Appl. Phys. **34,** No. 8, 2433–2434 (Aug. 1963).

Cane sugar refining. II. Decolorization with adsorbents, V. R. Deitz and F. G. Carpenter, Cane Sugar Handb. Ed, G. P. Meade, 9th edition, pp. 342–385 (John Wiley and Sons Inc., New York, N.Y.,Aug. 1963).

Stable 6300 Å auroral arcs in mid-latitudes, F. E. Roach and J. R. Roach, Planetary Space Sci. **11,** 523–545 (1963).

Some intra-atomic correlation correction studies, M. Krauss and B. J. Ransil, J. Chem. Phys. **33,** 840 (1960).

Parable of the Fisherman, W. J. Youden, Phys. Teacher Editorial **1,** No. 3, 120–121 (Sept. 1963).

Triboluminescence in a mercury bubbler, L. Schoen, Can. J. Phys. **38,** 967–970 (1960).

Deuterium isotope effect on glass transformation temperatures of aqueous inorganic solutions, L. C. Shepley and A. B. Bestul, J. Chem. Phys. **39,** No. 3, 680–687 (Aug. 1, 1963).

Mechanical reading of characters and recognition, M. E. Stevens (Proc. Intern. Patent Office Workshop on Information Retrieval), 125th Anniversary of the U.S. Patent Act of 1836, pt. II, p. 205 (1962).

Band spectrum analysis of mercury hydride, T. L. Porter, J. Opt. Soc. Am. **52,** 1201 (1962).

One year trial for new voltmeter standard, C. Stansbury, Mag. St. **34,** No. 3, 240–241 (Aug. 1963).

Pressure-density-temperature relations of freezing liquid parahydrogen to 350 atmospheres, Cryogenics **3,** No. 1, 12–15 (Mar. 1, 1963).

Status of sugar color and turbidity measurements, F. G. Carpenter and V. R. Deitz, Am. Soc. Sugar Beet Technologists **12,** No. 4, 326–347 (Jan. 1963).

The occurrence of short-duration cosmic noise absorption events inside the southern auroral zone, C. S. Gillmore, Jr., and J. K. Hargreaves, J. Atmospheric and Terrest. Phys. 25, 311–317 (June 1963).

Physical measurements and experiment design, W. J. Youden (Colloq. Intern. Centre Natl. Recherche Sci., Aug.–Sept. 1961), Book, Le Plan d'Experiences, No. 110, p. 115 (Centre National de la Recherche Scientifique, Paris, France, 1963).

Airglow research, F. E. Roach, Trans. Am. Geophys. Union **44,** No. 2, 431–432 (June 1963).

Remarks on coincidence experiments with visible light. Z. Bay and P. S. Farago, Proc. Royal Soc. Edinburgh, Sec. A. Math. and Phys. Sci. **LXVI,** pt. 11, No. 10, 111–115 (Royal Society of Edinburgh, Edinburgh, Scotland, 1963).

Time and frequency broadcasting, A. H. Morgan, ISA J. **10,** No. 6, 49–54 (June 1963).

Precision and accuracy in electromagnetic measurements, R. D. Huntoon (Intern. Conf. Precision Electromagnetic Measurements, Boulder, Colo., Aug. 14–17, 1962), IRE Trans. Instr. **I–11,** Nos. 3 and 4, 84 (Dec. 1962).

Quadrupole coupling constants from the microwave spectrum of hydrazoic acid, R. A. Forman and D. R. Lide, Jr., J. Chem. Phys. **39,** No. 4, 1133–1134 (Aug. 15, 1963).

**Publications for which a price is indicated are available by purchase from the Superintendent of Documents, Government Printing Office, Washington, D.C., 20402 (foreign postage, one-fourth additional). Reprints from outside journals and the NBS Journal of Research may often be obtained directly from the authors.*

U.S. GOVERNMENT PRINTING OFFICE:1964

(Continued from inside front cover)

Troposphere and Space Telecommunications. Data Reduction Instrumentation. Radio Noise. Tropospheric Measurements. Tropospheric Analysis. Spectrum Utilization Research. Radio Meteorology. Lower Atmosphere Physics.

Radio Systems. Applied Electromagnetic Theory. High Frequency and Very High Frequency Research. Frequency Utilization. Modulation Research. Antenna Research. Radiodetermination.

Upper Atmosphere and Space Physics. Upper Atmosphere and Plasma Physics. High Latitude Ionosphere Physics. Ionosphere and Exosphere Scatter. Airglow and Aurora. Ionospheric Radio Astronomy.

RADIO STANDARDS LABORATORY

Radio Standards Physics. Frequency and Time Disseminations. Radio and Microwave Materials. Atomic Frequency and Time-Interval Standards. Radio Plasma. Microwave Physics.

Radio Standards Engineering. High Frequency Electrical Standards. High Frequency Calibration Services. High Frequency Impedance Standards. Microwave Calibration Services. Microwave Circuit Standards. Low Frequency Calibration Services.

JOINT INSTITUTE FOR LABORATORY ASTROPHYSICS-NBS GROUP (UNIVERSITY OF COLORADO)

U.S. DEPARTMENT OF COMMERCE
Luther H. Hodges, Secretary
NATIONAL BUREAU OF STANDARDS
A. V. Astin, Director

Order all publications from the Superintendent of Documents
U.S. Government Printing Office, Washington, D.C., 20402

Use of funds for printing this publication approved by the Director of the Bureau of the Budget (June 19, 1961).

UNIVERSITY MICROFILMS INC
EDITORIAL DEPARTMENT
313 NORTH FIRST ST
ANN ARBOR MICH
S.IR-C JUNE

UNITED STATES
GOVERNMENT PRINTING OFFICE
DIVISION OF PUBLIC DOCUMENTS
WASHINGTON, D.C. 20402

OFFICIAL BUSINESS

PENALTY FOR PRIVATE USE TO AVOID
PAYMENT OF POSTAGE, $300
(GPO)

JOURNAL OF RESEARCH of the National Bureau of Standards Vol. 68C, No. 1 January–March 1964
C. Engineering and Instrumentation

Contents

	Page
A Fabry-Perot spectrometer for high-resolution spectroscopy and laser work. Klaus D. Mielenz, Robert B. Stephens, and Karl F. Nefflen.	1
A variable impedance power meter, and adjustable reflection coefficient standard. Glenn F. Engen.	7
A laser with a multihole diaphragm. Tadashi Morokuma.	25
Principles of cryometric impurity determination as applied to samples of small sizes. Charles P. Saylor and Gaylon S. Ross.	35
Reference tables for thermocouples of iridium-rhodium alloys versus iridium. G. F. Blackburn and F. R. Caldwell.	41
Publications of the National Bureau of Standards.	61

Library of Congress Catalog Card Number: 62–3900

For sale by the Superintendent of Documents, U.S. Government Printing Office, Washington, D.C., 20402. Price 75 cents (single copy). Subscription price: $2.25 a year; 50 cents additional for foreign mailing.
UNITED STATES GOVERNMENT PRINTING OFFICE, WASHINGTON : 1964